**Department of Civil Engineering**

# Behaviour of Fly Ash Geopolymer Containing Fillers and Fibres at Elevated Temperatures and its Application as Fire Resistant Coating for Timber

**Sharany Haque**

**This thesis is presented for the Degree of**
**Doctor of Philosophy**
**of**
**Curtin University**

**May 2017**

# DECLARATION

To the best of my knowledge and belief this thesis contains no material previously published by any other person except where due acknowledgment has been made.

This thesis contains no material which has been accepted for the award of any other degree or diploma in any university.

Signature: সুরবী হক

Date: 19/05/2017.

# ABSTRACT

The fly ash based geopolymer has emerged as an attractive alternative to ordinary Portland cement due to its lower carbon footprint and superior mechanical, durability and fire resistance properties. Timber structures experience significant risk to damage due to fire during its service life. Various fire retardant coating materials are used to reduce the flame spread and the damage of timber against fire. However, they exhibit limited success in terms of adverse effects on wood properties and their durability. This research evaluated the effectiveness of fly ash based geopolymer coating to protect the damage of timber against fire. This study is completed in three phases.

In the first phase, the effect of sodium and potassium based activators with different ratios of silicate to hydroxide of both types on mechanical and physical properties of fly ash geopolymer is evaluated at various elevated temperature of $200^0$C, $400^0$C, $600^0$C and $800^0$C. Results show significant improvement is compressive strength in the case of $Na_2SiO_3$/NaOH ratio of 3 than 2 and 2.5, where the residual compressive strengths are increased up to 600°C. Better results on the geopolymer synthesized with potassium based activators are obtained where the residual compressive strength up to 600 °C are much higher than their sodium based counterparts. It is also found that the fly ash geopolymer synthesized with potassium based activators is more stable at elevated temperatures than its sodium based counterparts in terms of higher residual compressive strengths, lower mass loss, lower volumetric shrinkage and lower cracking damage. X-ray diffraction (XRD) and thermogravimetric analysis (TGA) results of sodium and potassium activator synthesized fly ash geopolymer also corresponds to the measured residual compressive strengths.

The effects of different fillers and fibres on the mechanical and physical properties of sodium and potassium based activators synthetised fly ash geopolymers are evaluated at various elevated temperature of $200^0$C, $400^0$C, $600^0$C and $800^0$C in the second phase of this study. Nano silica powder and very fine sand are used as filler and carbon fibre and basalt fibre at various amounts are used to reinforce the geopolymers in this study. Results show that the 2% nano silica by wt. exhibited the highest compressive strength at all temperatures in both sodium and potassium based activators synthetised geopolymer. The measured mass loss and volumetric shrinkage are also lowest in both geopolymers containing 2% nano silica among all nano silica contents. However, in the case of geopolymer containing fine sand, an opposite phenomenon is observed and 10% fine sand by wt. is found to the optimum content with some deviations. Quantitative X-ray diffraction analysis also shows higher amorphous content in both geopolymers containing nano silica at elevated temperatures than those containing fine sand. The result also shows that the geopolymer containing 1wt.% basalt and 1wt.% carbon fibre exhibited better compressive strength, lower volumetric shrinkage and mass loss than other fibre contents. Among two fibres composites, the carbon fibre geopolymer exhibited better performance than its basalt fibre counterpart at all elevated temperatures and ambient temperature. The microstructure of carbon fibre reinforced geopolymer composite also exhibited better in terms of lower pores/voids and more compact

microstructure than its basalt based counterpart at elevated temperatures. The results also support the fact that carbon fibre is better than basalt fibre at elevated temperature and showed better bonding with geopolymer at elevated temperature.

An innovative application of fly ash geopolymer as fire resistant coating of timber is evaluated in the third phase of this study. In a trial fire test, the effects of sodium and potassium based activators synthetised fly ash geopolymer pastes, two coating thicknesses of 2 mm and 4 mm of above geopolymers and the carbon fibre and basalt fibre reinforced geopolymer coatings on fire resistant of pine timber plate are evaluated in this phase. Results show that both sodium and potassium based fly ash geopolymers coated timber having 2 mm coating thickness exhibited comparable fire resistant in terms of char depth under direct fire where an elevated temperature of about 1100$^{o}$C is maintained for 12 minutes. The char depth is significantly reduced by about 35-45% by doubling the geopolymer coating thickness from about 2 to 4 mm under the same fire condition for 20 minutes. The damage of potassium based geopolymer coating exhibited less damage in terms of fewer cracks after exposure to fire than its sodium based counterpart, which can be explained by the measured lower linear contraction and smaller thermal conductivity of the former than the latter. The addition of both carbon fibre and basalt fibre in potassium based geopolymer coated timber exhibited better fire damage resistant in terms of smaller char depth than the non-fibrous geopolymer coating. The addition of 1.5% carbon fibre in 4 mm thick potassium based geopolymer coating exhibited about 79% and 67% reduction in char depth than 2 mm and 4 mm thick non-fibrous potassium based geopolymer coating, respectively. The surface cracking of carbon fibre reinforced potassium based geopolymer coating after exposure to fire is also lower than non-fibrous geopolymer coating due to bridging of cracks by carbon fibre. A finite element based numerical model using ANSYS is also proposed to simulate the temperature development behind the geopolymer coating of the coated timber specimen subjected to the same temperature on coating side in the fire test.

**Keywords:** Geopolymer, Fly ash, Timber coating, Fire test, Sodium and Potassium activator, elevated temperature, nano silica, carbon fibre, basalt fibre, char depth, fine sand.

# ACKNOWLEDGEMENT

It is a blessing from The Almighty that I got the opportunity to do this research comfortably with sound health.

I am thankful to a lot of people who helped me during the path to PhD. I was surrounded by and guided by so many nice people to pursue my study comfortably. The research would not be possible without the help and direct or indirect contribution of them.

I would like to thank Dr. Faiz Uddin Ahmed Shaikh, Associate Professor, Department of Civil Engineering of Curtin University for his continuous guidance, excellent support and extra ordinary supervision during this study. I am grateful for his enthusiastic supervision and direction that leads an effective outcome of this research.

I also extend my thanks to all the staff members in the Concrete Laboratory of Curtin University; Dr. Arne Bredin, Mr Mick Ellis, Mr. Ashley Hughes, Mr. Luke English, Mr. Craig Gwyther and Mr. Rob Walker for their support during my experimental works in the laboratory. Their cooperation and help facilitated my work to accomplish successfully.

Thanks a lot to all the staff members of Microscopy & Microanalysis Department specially Ms Elaine Miller and Ms Veronica Avery for helping me to pursue the micro-structural analysis of the samples.

I thankfully acknowledge Dr. Les Vickers and Dr. William Rickard of department of Physics at Curtin University to facilitate the fire testing, thermal conductivity and dilatometer tests of this study.

Last but not least I would like to thank my Parents, my Husband and my Kids for their continuous inspiration and encouragement through this journey.

# TABLE OF CONTENTS

# LIST OF ACRONYMS

AS Australian Standard

ASTM American Society of Testing Materials

$CO_2$ Carbon Dioxide

FA Fly Ash

$K_2SiO_3$ Potassium Silicate

KOH Potassium Hydroxide

$Na_2SiO_3$ Sodium Silicate

NaOH Sodium Hydroxide

TGA Thermogravimetric Analysis

XRD X-Ray Diffraction

XRF X-Ray Fluorescence

# LIST OF TABLES

# LIST OF FIGURES

# LIST OF PUBLICATIONS

1. Anwar Hosan, Sharany Haque, Faiz Shaikh, “Compressive behaviour of sodium and potassium activators synthetized fly ash geopolymer at elevated temperatures: a comparative study”, Journal of Building Engineering, Volume 8, December 2016, Pages 123-130.

2. Faiz Shaikh, Sharany Haque, Jay Sanjayan, “Behaviour of fly ash geopolymer coated timber in Fire” Paper under Review in Journal of Construction and Building Materials.

3. Faiz Shaikh, Sharany Haque, "Effect of nano silica and fine sand on compressive strength of sodium and potassium activators synthesized fly ash geopolymer at elevated temperatures", Paper under review, Journal of Fire Sciences, Sage Journals.

4. Faiz Shaikh, Sharany Haque, "Behaviour of carbon and basalt fibres reinforced fly ash geopolymer at elevated temperatures", Paper under Review in Fire Technology, Springer Journals.

5. Anwar Hosan, Sharany Haque, Faiz Shaikh, “Comparative study of sodium and potassium based fly ash geopolymer at elevated temperatures”, Second International Conference on Performance-based and Lifecycle Structural Engineering (PLSE 2015), Brisbane, Australia, 9-11, December 2015.

6. Faiz Shaikh, Sharany Haque, “Comparative study of sodium and potassium based fly ash Geopolymer at elevated temperatures”, School of Civil and Mechanical Engineering Colloquium 2015, Curtin University, 2nd September 2015.

# CHAPTER I

# INTRODUCTION

## 1.1. BACKGROUND

Timber is used as building structural material in many countries including Australia. The main advantage of timber is its environmental friendliness, e.g. it absorbs carbon-di-oxide and produces oxygen. The absorbed carbon-di-oxide remains locked inside until it rots or is burnt; as a result its carbon-footprint is extremely low. Other benefit of timber as building material include availability, light weight, faster construction and deconstruction, easy recycling, cost effectiveness, etc.

However, timber is highly combustible material, which limits its wide spread application in building industry. Various fire retardant coating materials are used to reduce the flame spread and the damage of timber against fire. However, most of them exhibit limited success in terms of adverse effects on wood properties and their durability. Fire retardant treated timber become moisture and UV sensitive, discoloured and corrosive (Ostman et al., 2001). The mechanical strength of wood is reduced and most of the treatments are not durable in exterior applications (Ostman et al., 2001). Moulds growth has also been reported on fire retardant coating containing phosphorous and nitrogen as both are fertilizers and nutrition for microorganisms (Ostman et al., 2001). Swelling and shrinkage have also been reported in some fire retardant treated timbers. Most of the fire retardant coatings for timber provide resistant against flame spread, however, for protection against fire, fire resistance is the required property of timber which delay the onset of thermal degradation leading to char formation (Richardson and Cornelissen, 1987). Experimental results also show that cement based coating performs well in terms of smaller char thickness and lower temperature under coating than other chemical based fire retardant coatings (Richardson and Cornelissen, 1987).

Geopolymer has recently been emerged as an excellent alternative to cement in construction industry due to its superior mechanical and durability properties than conventional cement. Extensive researches have been conducted to study various mechanical and durability properties of geopolymer. Significant efforts have also been made by many researchers to study the effect of elevated temperatures on mechanical properties of geopolymer. Davidovits (1994) noted that by increasing the Si:Al ratio, the fire and heat resistant characteristics of geopolymer can be improved. Most of the studies evaluated different geopolymers which were made by different types of source materials and alkali activators, e.g. fly ash activated by sodium based alkali activators (Rickard et. al., 2012; Omar et. al., 2014; Ranjbar et. al., 2014; Shaikh and Vimonsatit, 2015) fly ash activated by combined sodium and potassium based activators (Kong and Sanjayan, 2008; Kong and Sanjayan, 2010; Bakharev, 2006) combined fly ash and slag activated by sodium based activator (Guerrieri and Sanjayan, 2010) metakaolin activated by combined sodium and potassium based activators (Kong and Sanjayan, 2008), etc. Among all above source materials the class F fly ash is rich in silica and alumina and low in calcium oxide, which enables its higher stability at elevated temperature in fire than others. Moreover, it is cheaper, easily and widely available than other source materials.

Fillers and fibres can be added to geopolymers to reduce the thermal expansion/shrinkage of the composite and extend the usable temperature range. Various additives are used in geopolymer matrix to improve its fire resistance e.g. quartz and granite aggregates (Subaer et. al. 2007; Kamseu et. al. 2010), alumina particles (Bell et. al. 2005; Lin et. al. 2009), wollastonite (Silva et. al. 1999), etc. Various organic and inorganic fibres are also added to reinforce geopolymers to improve its fire resistance. Masi et al. (2015) reported a study where poly vinyl alcohol (PVA) and basalt short fibres are added to fly ash based geopolymer activated by sodium hydroxide and sodium aluminate solutions. Results show better mechanical properties of basalt fibre reinforced geopolymer at elevated temperatures than its PVA fibre reinforced counterpart. In another study the effect of elevated temperatures on fibre-matrix interaction of continuous basalt fibre reinforced dehydroxylated halloysite geopolymer is evaluated by Welter et. al. (2015). Zhang et

al. (2014) reported effects of various short carbon fibre contents on the compressive and bending strength of metakaolin-fly ash geopolymers at evaluated temperatures. Results show that 2% carbon fibre reinforced geopolymer containing 50% fly ash and 50% metakaolin exhibited excellent behaviour at 500$^{o}$C. The only reported study on the effect of nano silica on the microstructure of geopolymer at elevated temperatures is by Estrada-Arreola et al. (2014), where X-ray diffraction, atomic-force microscopy and optical profilometry techniques were used to identify the changes in microstructure of nano silica modified geopolymer at elevated temperatures. No significant changes in micro-structure of geopolymer containing nano silica at elevated temperature of 1000$^{o}$C are noticed in their study. Bastami et al. (2014) reported a study on the effect of nano silica on the compressive behaviour of high strength concrete at elevated temperatures. Their results show that the addition of nano silica improved the mechanical properties of high strength concrete at elevated temperatures and better than concrete containing silica fume.

In a number of studies cementitious and geopolymer coating to protect concrete and steel structures against fire are evaluated. Cheng and Chiu (2003) fabricated a granulated blast furnace slag based geopolymer panel for fire resistant application. A 10mm thick geopolymer panel was exposed to 1100$^{o}$C flame, with the measured reverse-side temperature reaching less than 350$^{o}$C after 35 minutes. In another study, Kim et al. (2010) studied the fire resistance of bottom ash – cement blended coating containing polypropylene fibre. Reinforced concrete slab was coated with above cementitious coating having three different thickness of 20, 30 and 40mm. In that experiment the coating side was exposed to 1200$^{o}$C temperature and the measured temperatures behind the coating were about 600$^{o}$C, 470$^{o}$C and 280$^{o}$C for 20, 30 and 40mm thickness coating, respectively. In another study, Barnes and Fidell (2006) studied the effectiveness of cementitious coating of 20mm thick to protect fibre reinforced polymer (FRP) in strengthened beams subjected to a temperature of about 950$^{o}$C and reported that a maximum temperature of 310$^{0}$C is reached in the interface between the fire protection coating and the FRP plate.

Based on above it can be seen that the effectiveness of geopolymer and cementitious coating ranging from 20 to 40mm in thickness for fire resistance of concrete is evaluated. However, only one study evaluated the effectiveness of cement coating to prevent the damage of timber against fire. A cement coating thickness of 25-50mm is used in the study by Richardson and Cornelissen (1987). In any timber structure or even in concrete or steel structures the use of very thick coating of about 20-50mm increases the dead weight of the structure which require bigger cross-section of structural members and the foundations. Being an excellent fire resistance characteristics, the geopolymer can be an ideal candidate to coat timber against high temperature and fire resistance. Due to higher fire resistant characteristics than the cement matrix, thinner geopolymer coating can also be applied on timber to achieve the similar level of fire resistant behaviour. This will result in less additional dead weight to the structure and hence, smaller footing sizes and cost savings. The fly ash geopolymer based fire resistant coating for timber will also be cheaper than other fire retardant coatings because fly ash is by-product of coal fired power stations. Moreover, its adhesion with timber is also expected to be higher than the cement matrix due to its lower water content. Better adhesion of geopolymer with concrete and steel is reported by several researchers (Zanotti et al., 2016; Sarker, 2011).

## 1.2. RESEARCH SIGNIFICANCE

Now-a-days with lots of environmental concerns, geopolymer has been proved as a green material with an impressive fire resistance property, durability, less hazardous as well as inexpensive. In geopolymer most widely used aluminosilicate materials are metakaolin, fly ash and slag. In consideration of cost effectiveness the fly ash is cheaper than metakaolin (skvara, 2007). In recent years, the use of nano materials has received particular attention in the application of construction materials especially in cement mortar and concrete. The effect of nano silica on the properties of concrete and geopolymer at elevated temperatures has received very limited attention despite its positive influence on mechanical and durability properties of cement and geopolymer based binder. High temperature resistant fibres e.g. carbon fibre and basalt fibres showed excellent thermal stability at elevated temperatures. However, not enough studies present the behaviour of nano silica, carbon and basalt

fibre filled/reinforced fly ash based geopolymer at elevated temperatures. Nor the effectiveness of geopolymer synthetised using above materials as fire resistant coating for pine timber as it is the most widely used timber in building industry in Australia and in many countries due to its availability and low cost. This research studied the effects of sodium and potassium based activators on the compressive strength and damage behaviour of fly ash geopolymer exposed to elevated temperature up to 800°C. The effects of nano silica, ultra-fine sand, carbon fibre and basalt fibres as fillers/reinforcements of geopolymer on the compressive strengths and physical changes e.g. the mass loss, volumetric shrinkage, cracking behaviour of fly ash geopolymer at above elevated temperatures are also evaluated. X-ray diffraction (XRD) and thermogravimetric analysis (TGA) are also used to support the observed physical behaviour and strength properties. This research also presents preliminary results on a pilot study on the effectiveness of reducing the damage of fly ash geopolymer coated timber against direct fire exposure. The effectiveness of two different coating thickness, two types of alkali activators, effect of carbon and basalt fibre as filler/reinforcement of geopolymer coating on reduction of char thickness of timber and the temperature behind the coating are evaluated. The research flow of the thesis is added in the Appendix E-1.

## 1.3. SCOPE AND OBJECTIVES

The aim of this study was to evaluate the effectiveness of geopolymer as fire resistant coating of timber. To achieve the above aim the following objectives were considered to:

1. Study the effect of sodium and potassium based alkali activators and their silicate to hydroxide ratios on the residual compressive strength, mass loss, volumetric shrinkage and cracking behaviour of fly ash geopolymer subjected to elevated temperatures up to $800^0$C.
2. Study the effect of nano silica and ultra-fine sand as fillers of fly ash geopolymer synthetised using the activator type which exhibited better residual properties in above study under same elevated temperature exposure.

3. Study the effect of carbon fibre and basalt fibre as reinforcements of fly ash geopolymer synthetised using the activator type which exhibited better residual properties in above study under same elevated temperature exposure.
4. Study the microstructural and changes of various polymer phases of both sodium and potassium activators synthetised fly ash geopolymer after exposure to elevated temperatures and the thermal expansion and thermal conductivity of above geopolymers.
5. Study the adhesion bond behaviour of both sodium and potassium based geopolymer coating with timber.
6. Study the effectiveness of two different coating thickness, two types of alkali activators, and effect of quantities of carbon and basalt fibres as filler/reinforcements of geopolymer coating on fire resistance of timber under direct fire exposure.

This research is conducted in three phases. In the first phase sodium hydroxide and sodium silicate and potassium hydroxide and potassium silicate activators are used to synthetized the fly ash geopolymer paste. The ratios of sodium silicate to sodium hydroxide and potassium silicate to potassium hydroxide were 2, 2.5 and 3. Class F fly ash was used as the source material for geopolymer in this research. The activator to fly ash ratio is kept constant at 0.35. A total of six samples are cast for each ratio and activator type and heated at elevated temperature of $200^0$C, $400^0$C, $600^0$C and $800^0$C. In the second phase, nano silica and ultra-fine sand are used as partial replacement of fly ash at 1%, 2% and 4% by weight of fly ash and 5%, 10% and 15%, by weight of fly ash, respectively. Carbon fibre and basalt fibres at 0.5%, 1% and 1.5% by weight of fly ash are also used in the geopolymer in this phase. The alkali activator to binder ratio in this phase is 0.4 to provide the desired workability. Similar to above, a total of six samples are also cast for each filler/fibres type and quantity and heated at elevated temperature of $200^0$C, $400^0$C, $600^0$C and $800^0$C.

The fire resistance behaviour of geopolymer coated pine timber plate subjected to direct fire exposure of about 12-20 minutes is evaluated in the third phase. Two geopolymer coating thickness of about 2mm and 4mm for both sodium and potassium based geopolymers are used for coating of timber subjected to fire test.

The effect of carbon and basalt fibres at 0.5%, 1% and 1.5% by weight of fly ash are also used to reinforce the 4mm thick potassium based geopolymer coating.

## 1.4. STRUCTURE OF THE THESIS

The thesis comprises in eight chapters, which is described as followed:

Chapter I: This chapter describes the background of the study, the significance, objectives and scope of this work.

Chapter II: This chapter describes the previous research regarding geopolymer and its application at elevated temperature. The previous research of geopolymer for different coating purpose on timber and other materials are also summarized in this chapter.

Chapter III: This chapter states the methodology followed in the research. The material used, its proportions, instruments used for the analysis are all elaborately illustrated in this chapter.

Chapter IV: This chapter explained about geopolymer with varying activators with different ratios at elevated temperature. Fly ash based geopolymer with sodium and potassium based activator was used.

Chapter V: This chapter describes about geopolymer with nano silica and fine sand at elevated temperature. The samples were prepared with fly ash based geopolymer with sodium and potassium based activator.

Chapter VI: This chapter describes about fly ash based geopolymer with addition of basalt and carbon fiber at elevated temperature. As basalt and carbon fibre has a good thermal endurance property so the geopolymer stated in chapter 4 was used with replacement of fly ash by carbon and basalt fibre of 1%, 2% and 4%.

Chapter VII: This chapter describes about geopolymer coating on timber plates at elevated temperature and also the samples were kept at direct fire. The behaviour of coating on timber plates at elevated temperature including the bond between geopolymer and timber are illustrated in this chapter. Modelling of the coating on the timber plates was done using ANSYS and illustrated also in this chapter.

Chapter VIII: The conclusions of this experimental work and recommendation for further studies are written in this chapter.

# CHAPTER II

# LITERATURE REVIEW

## 2.1. GEOPOLYMER

Geopolymer is an inorganic alumino silicate polymer that is synthesised from mainly aluminium and silicon material from geological origin or a by-product ingredients like fly ash (Davidovits, 1991). Geopolymers can be obtained from metakaolinite or kaolinite by combining sodium silicate, potassium silicate, potassium hydroxide or sodium hydroxide as activators (Kriven, 2010). Geopolymers generally are produced by activation of a source material. The basic materials used for the geopolymerisation process is mostly a mixture of different types of materials but also may be from a single source of material.

Materials such as fly ash or metakaolin can be activated by the combination of alkaline activators. The chemical structure and microstructure of the geopolymer is mostly amorphous in nature (Kriven, 2010).

Researches on geopolymer have been carried out for several decades due to two major advantages: low energy consumption and low $CO_2$ emission in the preparation process (Wang et al. 2010). Geopolymer materials have an extensive range of applications as a substitute for traditional cements due to their unique properties, such as the ability to withstand elevated temperatures and fire, along with acid and salt resistance compared to those of Portland cement. Geopolymer is prepared by combining supplementary cementitious materials (SCMs) such as metakaolin (produced by calcining kaolin at 650–800 °C). The main components are amorphous $Al_2O_3$ and $SiO_2$ with high pozzolanic activity. Besides the filling effect, metakaolin reacts with calcium hydroxide, which is one of the hydration products of Portland cement, to form calcium silicate hydrate gels) or industrial by-products with strong alkali solutions such as sodium hydroxide (NaOH) and sodium silicate (in most cases) to form a three-dimensional amorphous aluminosilicate network with properties similar to or better than cement (Luo et al., 2014) and (Part et al., 2015)

## 2.2. GEOPOLYMERIZAITON PROCESS

Geopolymers comprise mostly a polymeric Si-O-Al framework where $SiO_4$ and $AlO_4$ are connected consecutively by the share of the O atoms. According to Davidovits Al is 4 co-ordinated with respect to O creates a negative charge inequity, so the existence of cations such as K+, Na+, and $Ca_2$+ is important to keep up an electrical neutral stance at matrix form (Davidovits, 1993). The polymerisation procedure includes a compound reaction with a high alkaline situations of Al Si minerals that yield polymeric bond of Si-O-Al-O. According to Kriven (2010), Geopolymerisation is mainly an exothermic reaction. As a construction material, one of the most important properties of geopolymers is the strength which is influenced by the type of source material as well as heat treatment (Davidovits, 1993).

Geopolymer that is attained from calcined basic material like fly ash, metakaolinite (calcined kaolinite), and showed better compressive strength than those with non calcined materials like kaolinite clay. The properties of geopolymer mostly dependent on the behaviour of raw materials, activator liquid to material ratio, curing temperature as well as curing time. Curing at elevated temperature accelerate the reaction process so geopolymerization is mostly carried at elevated temperature and special caution should be taken for the minimization of the loss of water.

Geopolymer, as stated before is a type of amorphous and alkali aluminosilicate material that has various terms of use like inorganic polymer, alkali activated cement, geo-cement, alkali bonded ceramics etc. A diversity of aluminosilicate material like feldspar, kaolinite and some industrial deposits like fly ash, slag, etc. are the raw material in the total geopolymerization. The source material of the geopolymer are amorphous with low water requirement and with sufficient reactive glassy content and have the property to release aluminium easily. Among the activators, potassium hydroxide has more alkalinity comparing to sodium hydroxide yet previous research confirmed that sodium hydroxide possess greater capacity to liberate aluminate and silicate monomers (Duxon et al., 2007). The properties of geopolymer varies with raw material and mix design so choice of mix design is crucial for a particular application (Duxon et al., 2007).

Barbosa et al. (2000) stated that polymerization is almost same as the gel effect which is occurred by radical polymerization by working on the alteration in the viscosity of the polymerization of geopolymer mixture. According to Xu and Van Deventer (2000) with the setting process the dissolution of Si and Al from aluminosilicate starting material in alkaline solution gives hydrated reaction product in the form of $[Mx(AlO_2)y(SiO_2)z.nMOH.mH_2O]$ gel. This gel development is mostly dependent on the degree of dissolution of the aluminosilicate material. Coating of gel is made on the external part of the starting material when it gives reaction with the alkaline solutions. This gel then proceeds from the surface of the particle to larger interstitial spaces between neighbouring particles with precipitation of gel and the simultaneous dissolution of the neighbouring particles. As this gel harden, the neighbouring particle is firmly bound together (Xu & Van Deventer 2000).

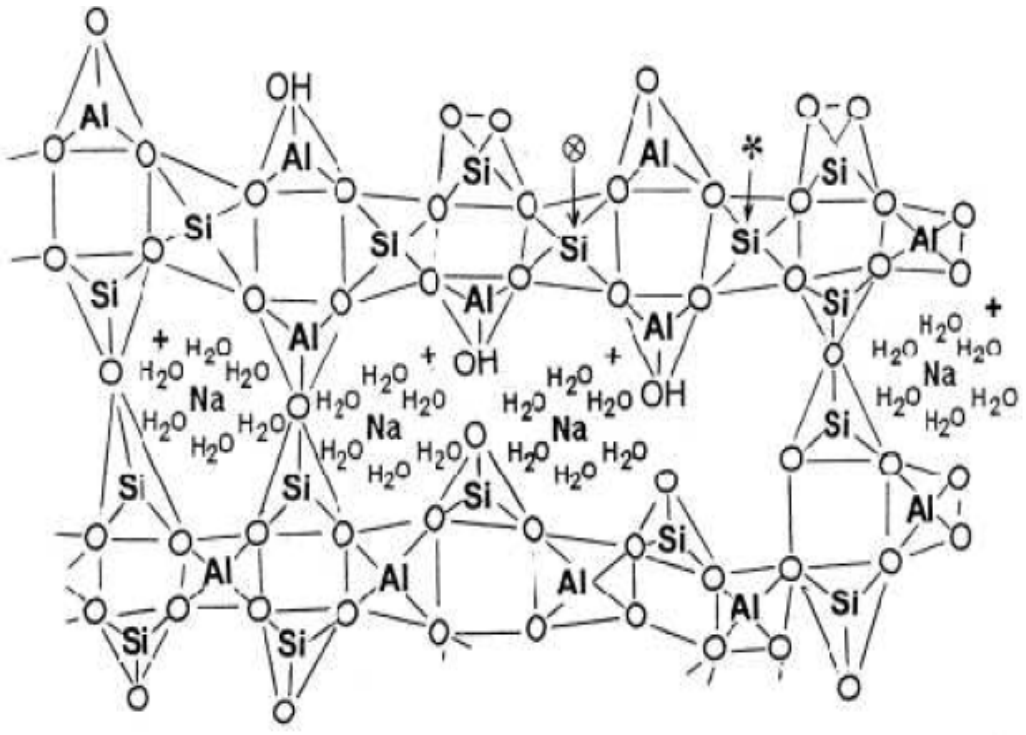


**Figure 2. 1: Proposed semi-schematic structure for Na-polysialate polymer (Barbosa et al. 2000)**

NMR studies of geopolymer identified a lack of long-range atomic order which is confirmed by x-ray diffraction (XRD) results (Barbosa et al. 2000). This indicates that geopolymers show structural characteristics similar to glasses or hydrated

silicate minerals in having a range of Si environments but predominantly those of framework structures saturated in Al (Figure 2.1).

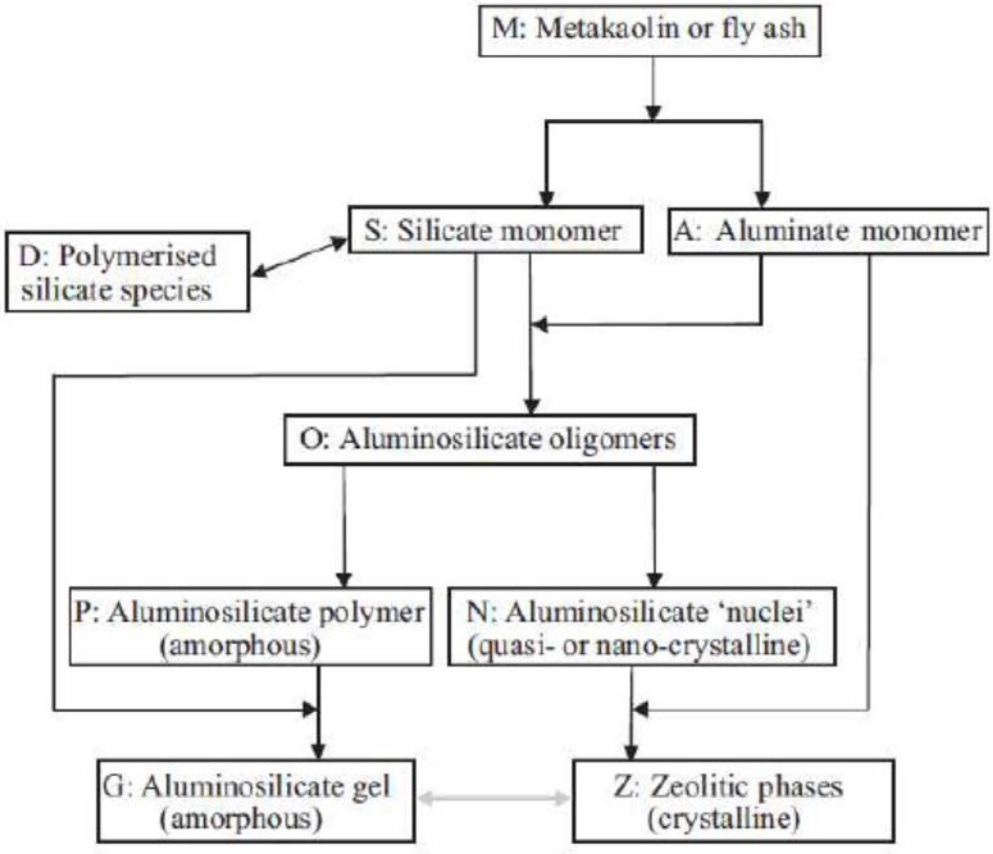


**Figure 2. 2: Reaction process by Provis and van Deventer (2007b).**

Provis and Van Deventer (2007a, 2007b) worked on modelling and experimental research on the kinetics of geopolymerisation. The research anticipated the formation process to consist of the dissolution of starting aluminosilicate source material with the alkaline activating solution, followed by the formation of an initial amorphous gel phases followed by its transformation into the final amorphous gel phase.

The proposed reaction sequence of geopolymerisation by Provis and van Deventer (2007b) (Figure 2.2) showed an aluminosilicate 'nuclei' element that suggests the formation of zeolitic phases as in the next step.

## 2.3. GEOPOLYMER AT ELEVATED TEMPERATURE

Davidovits (1994) describes higher Si:Al ratio improves heat and fire resistant properties of geopolymer. Cheng and Chiu (2003) fabricate a granulated blast furnace slag based geopolymer for fire resistant application. The geopolymer panel was exposed to $1100^0$C flame, with the measured reverse-side temperature reaching less than $350^0$C after 35 minutes.

Therefore, geopolymer is good for elevated temperature as well as for fire protection. In order to analyse the fire resistant behaviour of engineered geopolymer composites, the most important parameter among many is the determination of its residual strength (compressive strengths) (Lyon et al., 1996, 1997) after fire exposure for structure applications.

Tippayasam et al. (2016) reported about metakaolin based geopolymers that is made by using potassium hydroxide and potassium silicate as an activator. The paper describes the influence of the concentration of potassium hydroxide, temperature of curing as well as heat treatment on geopolymer. The potassium hydroxide (KOH) concentration was varied at 6, 8, 10, 20, 30 and 40 M. The potassium silicate to potassium hydroxide ($K_2SiO_3$/KOH) ratios were 1 and 1.5 and curing temperatures of 40 °C and 60 °C for 24 h. According to the result geopolymer made with 10M potassium hydroxide with a curing temperature $40^0$C for 24 hour and then heat treated at $550^0$C showed the maximum compressive strength. Analysing further showed that heat treated geopolymer has denser micro-structure than that of non heat treated samples which leads to a high compressive strength.

Omar et. al. (2013) demonstrates the influence of elevated temperature of geopolymer paste, mortar and lightweight aggregate geopolymer concrete (LWAGC). The thermo-physical, mechanical properties were investigated for elevated temperature at $400^0$C, $600^0$C and $800^0$C. The changes of the structures of the geopolymeric gel after elevated temperature exposure were explored and described. According to the study, though the lightweight aggregate geopolymer concrete (LWAGC) have lower water absorption as well as density than the geopolymer mortar and paste yet introduction of light weight aggregate improves the microstructural and mechanical properties of the geopolymers at elevated

temperature due to the low thermal conductivity properties of light weight aggregate which hinders the heat transmission in the samples.

Some other research also states that the geopolymer has low permeability, high strength and also great protection to chemical attack (Li et. al, 2004; Wallah, Rangan, 2006; Gourley J, 2005).

Though sodium based activators are mostly used as they are easily available and low cost as well as highly reactive (Provis, 2014) but potassium hydroxide (KOH) and potassium silicate ($K_2SiO_3$) are better for elevated temperature applications (Barbosa et al. 2003, Kamseu et al. 2010, Kamseu et al. 2009, Lizcano et al. 2012).

Hardjito et al. (2004) states that age does not have any effect of the strength of the geopolymer samples after the heat curing of the samples at elevated temperature. The paper concludes that higher the concentration of the sodium hydroxide solution gives higher compressive strength. The paper also added that by increasing the sodium silicate to sodium hydroxide ratio by mass increases the compressive strength of the geopolymer. The paper concludes that addition of admixture upto 2% of fly ash by mass has shown an improvement in the workability but has a very little effect on the compressive strength of the hardened concrete.

According to Kong and Sanjayan J. (2010) the use of superplasticizers is not useful in geopolymer at elevated temperature. The research describes that the conventional superplasticizers that is very common to use with ordinary Portland cement does not have much effect on the overall workability of the mix when used as additive.

Several research (Rovnanik, P. 2010) have been done to analyse the effect of different curing conditions on the of geopolymer pastes properties. Different research reports curing temperature in a range that is from $40^0$C to $85^0$C to complete the total geoplymerisation process.

After that Kamseu et al. (2010) analysed about of metakaolin geopolymers, with ambient curing ($21^0$C–$23^0$C) and heat curing conditions ($40^0$C– $60^0$C) using a maintained relative humidity (RH) for a total of 24 h and states that curing with 30% relative humidity is preferable than that of 70% relative humidity (RH).

Heah et al., (2011) analysed with metakaolin based geopolymers and described that curing at ambient temperature did not give reasonable result while higher temperature like 40, 60, 80 and $100^0$C showed strength gain within one to three days. Though curing for longer time with a higher temperature was not suggested.

Kani et. Al. (2009) described long procuring at ambient temperature is useful before the application of elevated temperature for curing for better development of strength. They prepared three mixes with different ratios with different curing temperatures like $45^0$C, $65^0$C and $85^0$C for the time of 5h to 20h with one and seven days of procuring.

In the research of Kiatsuda et. al. (2011) they also supports the above findings that sufficient curing is beneficial to achieve better mechanical strength and durability properties.

According to Swanepoel and Strydom (2002) the curing time and the curing temperature has an effect on the compressive strength. Also the optimum strength found when the specimen was cured at $60^0$C for a 48 hours. The geopolymer samples were casted using sodium hydroxide and sodium silicate solution with an addition of fly ash and kaolinite.

Van Jaarsveld et al. (1999) studied the geopolymer paste prepared by the alkali activator and five different fly ash obtain from difference source in South Africa and Australia. The 50 mm cubical sample were prepared and cured at $30^0$C for 24 hours in oven before testing after 7 day curing for compressive strength. They used XRD and FTIR technique to illustrate the fly ash from various places for studying the dissolution behaviors, reactivity as well as mechanical property of fly ash Geopolymer. The experiment result also revealed the fact that the physical property of Geopolymer (fly ash based) depends on the various parameters including water content, calcium percentage, alkali-metal percentage as well as size of the particle, thermal history, and crystalline and amorphous degree of fly ash.

Hardijito et al. (2004) researched on the influence of various synthesizing parameter on fly ash based Geopolymer concrete prepared by low calcium class F fly ash with sodium hydroxide and sodium silicate activated solution. Four type of local available aggregate of size 20 and 14 and 7 mm and fine sand. Mixture was casted using 100

x200 mm steel cylinder mould with 30-60 min rest period. The compressive strength test specimen was performed to find the influence of various Geopolymer synthesizing parameters such as (a) Concentration of sodium hydroxide (b) Sodium silicate to sodium hydroxide liquid ratio (c) Curing time and curing temperature, (d) adding of High range water reducing admixture (e) Handling time (f) Water content in the mixture. Results revealed that the higher concentration of sodium hydroxide solution result in a higher strength of Geopolymer concrete. Higher ratio of sodium silicate to sodium silicate by mass increases the compressive strength. Curing temperature in the range of 30 to $90^0$C and Curing time 6 to 96 Hours produce large amount of compressive strength. Fresh Geopolymer concrete easily handle up to 120 min without any setting. It was also observed that a little drying shrinkage and low creep with high resistance against sodium sulphate.

Hardjito et al (2008) researched on the effect of various parameters of low-calcium fly ash-based Geopolymer mortar. 50 $mm^3$ cubic moulds was used to cast the geopolymer. According to this paper curing temperature is a vital factor for the total geopolymerization. The specimens get maximum compressive strength when those are cured at ambient temperature before the elevated temperature curing at oven for 24 hours. With the rise in the water ratio of the geopolymer mortar the compressive strength decreases. The result reported that sodium hydroxide with higher concentration gives higher compressive strength for the geopolymer. According to the paper when the activator/fly ash ratio is 0.40 (by mass) that gives highest compressive strength. After that the compressive strength decreases with an increase in the ratio that may be due to an excess amount in the OH concentration.

Dimitrios (2007) researched on the influence of sodium hydroxide and sodium silicate contents in the reaction of fly ash based geopolymer. The compressive strength was measured along with X-ray diffractograms and Fourier-transform infrared (FTIR) spectroscopy. According to the paper the compressive strength is improved with lower water content and also with increase in the sodium silicate solution for dissolution of geopolymers. Sodium hydroxide content is also one of the prime factor to affect considerably on the compressive strength of the geopolymer. Fourier Transform Infrared (FTIR) spectroscopy analysis showed essential fly ash phase transformations in geopolymer that affect their strength.

Hardjito (2003) worked on Geopolymer concrete. In Geopolymer concrete the inorganic alumino-silicate polymer gel synthesized from source materials rich in silicon and aluminium, such as low calcium (class F) fly ash, binds the loose course and fine aggregates, and other un-reacted material in the mix. The test results shows, the effect of sodium silicate to sodium hydroxide ratio and sodium hydroxide concentration effect the strength of the mix. Higher curing temperature and longer curing time resulted in larger compressive strength, curing temperature $60^0$C and 48 hours was the optimum value for increasing the strength. The freshly casted concrete was kept at room temperature for 60 minutes. With the decrease of water to geopolymer ratio the compressive strength of the concrete increases. Test results reveal the fact that Geopolymer concrete show less drying shrinkage and possesses good sulphate attack resistance.

Chindaprasirt et. al (2009) conducted the research for Geopolymers made from three concentrations of NaOH (5, 10, and 15 M) and from ground bottom ash and fly ash. The Geopolymer was cured at 65 °C for 48 h. Result show that both fly ash and bottom ash can be utilized as source materials for the production of Geopolymers. The FT-IR, DSC thermo gram, SEM, and XRD analysis reveal the fact that bottom ash is less reactive than fly ash and gives a lesser degree of geopolymerization. The dissolution of fly ash in the NaOH solution would be higher than that of the bottom ash. The strength of a Geopolymeric also depends on NaOH concentration. The optimum concentration of 10M is suitable for both bottom and Fly Ash materials.

Songpiriyakij S. (2006) studied fly ash based Geopolymer concrete and mortar. Sodium hydroxide (NaOH) and Sodium Silicate ($Na_2SiO_3$) solution was taken as alkaline activator in seven difference mix proportion. Specimen was cured at two difference temperature, at $25^0$C and also at $60^0$C for 24 hour. Result suggested that high curing temperature is beneficial for the development of strength in the concrete.

Sofi et al. (2007) used class F fly ash from three different sources like Port Augusta (PA), Tarong and Gladstone. This study determines poisson's ratio, compressive strength, splitting tensile strength, flexural strength and modulus of elasticity of Inorganic polymer concrete. This study compares various parameters of Inorganic Portland Concrete (IPC) with ordinary Portland cement (OPC).

Pavel (2010) analysed alkali activated metakaolin material with a curing temperature of $10^0$C, $20^0$C, $40^0$C, $60^0$C and $80^0$C and also with different time and analysed its effect on compressive strength and the microstructure of geopolymer material.

Songpiriyakij (2010) showed that curing time affects the compressive strength development in mortar. The paper concluded that mixing temperature and curing temperature effects the compressive strength and higher curing temperature promotes and improves early compressive strength of geopolymer mortars.

Ghosh et al. (2009) researched with geopolymer from class F fly ash from India. The paper studied the effect of alkali and silica content, water content, sand content by casting six series of paste and mortar samples with varying curing time and temperature. The mortal and pastes were also analysed with XRD and SEM and suggested that increase in alkali content increases the compressive strength. SEM result suggested that an increase of alkali content from 0.46 to 0.62 decreases unreacted fly ash particle and thus increases aluminosilicate gel which gives better compressive strength. The paper suggested that decreasing the water content increases the compressive strength, with maintaining the required workability. Results also concluded that fine aggregate addition to 50% does not improve the compressive strength but adding more decreases the compressive strength.

Olivia et al. (2008) studied on water penetrability properties of geopolymer concrete and states that water to binder ratio is an important factor for low calcium fly ash geopolymer.

Pan Zhu et al. (2009) studied on the ductility of the geopolymer mortar and stated that it has a relation on the behaviour of the strain gain or loss. The paper state that geopolymer mortar sometimes can increase in strength and other time decrease in strength after elevated temperature exposure to $800^0$C.

Valeria et al. (2003) reports in their research on thermal behaviour of the samples like high temperature endurance property, the reaction phase, and thermal expansion properties of sodium polysialate.

## 2.4. FLY ASH BASED GEOPOLYMER AT ELEVATED TEMEPRATURE

Geopolymer matrix and its thermal and chemical properties are mostly dependent on it key ingredients, mix ratio, curing temperature and also on the casting precautions. Material from different source and the activator types also effect the property of the geopolymer. As it has different mineral and also different reaction rate with each other. So according to Van Jaarsveld et al. (2003) source of fly ash and the properties of fly ash is very important to understand its reactivity. According to Diaz et al. (2010) fly ash with finer particles or finely grind can increase the reaction rate and can increase the degree of geopolymerization process. The fly ash with high content of glass phase can also speed up the process and can add a positive effect to the compressive strength of the samples.

Fernandez and Palomo (2003) stated that to achieve high strength the class F fly ash is most suitable one. The properties and ingredients of the fly ash is also important; like mullite percentage should be below 5% in the fly ash. They suggested a higher glass content for the fly ash is better and also size of the particle if in the range of 10 to 40 μm gives a higher compressive strength geopolymer. This study also suggested some properties of the fly ash. These are:

- the percentage of unburned material < 5%;
- $Fe_2O_3$ content ≤ 10%;
- CaO content (≤ 10%);
- content of reactive silica between 40–50%;
- percentage of particles with size lower than 45 μm between 80–90%
- high content of vitreous phase (>50%)
- [$SiO_2$] reactive/[$Al_2O_3$] reactive ratio > 1.5

According to Chen Tan et al (2009) the amorphous iron oxide has no important role in the geopolymerization process. The paper suggested that high calcium fly ash or class C fly ash in not suitable for the geopolymerization process as the excess calcium content can increase the rate of reaction which is responsible of the flash setting of the samples.

According to Ranjbar et al. (2014) geopolymer specimens prepared with fly ash (FA) or palm oil fuel ash (POFA) lost strength when exposed to temperature more than $500^0$C. The research measured the compressive strength of geopolymer with sodium based activator (sodium hydroxide and sodium silicate) at an elevated temperature. The samples prepared with fly ash as well as palm oil fly ash gained its strength upto $500^0$C.

Thakur et al. (2009) investigated on mechanical and microstructure characteristic of Geopolymer with fly ash composite expose to elevated temperature exposure. Bulk density apparent porosity, compressive strength and the Microstructure of fly ash based Geopolymer paste and mortar Specimen was studied at an elevated temperature exposure up to $900^0$C.The apparent porosity and bulk density of the Geopolymer matrix increase corresponding with Si: Al Ratio and decrease with increase with expose temperature. The thermo gravimetric analysis was done and revealed the fact that samples loss its weight due to dehydration after elevated temperature exposure. Dehydroxylation and densification process takes place through transient heating from room temperature up to $900^0$C.

Kong et al. (2008) researched on geopolymer and geopolymer matrix at elevated temperature exposure. This study focussed on the thermal change and damage of class F fly ash geopolymer. The samples were heated up to $800^0$C for evaluation. Compressive strength were measured for analysis. The paper concluded that fly as to activator ratio is a crucial factor for the achievement of better strength and for gaining fire resistant property. The study used sodium silicate and potassium hydroxide as an activator. According to the study the optimum sodium silicate to potassium hydroxide ratio was 2.5 and activator to fly ash ratio was 0.33. The author stated that fly ash based geopolymer with this ratio showed an increase in strength after exposure to elevated temperature. The paper supports the fact that this increase in strength is due to the improvement in the combination of the reaction polymerization at higher temperature. After adding aggregates, the strength of the geopolymer decreased after elevated temperature exposure in the study. The paper suggests that this might be due to different thermal expansion property of the geopolymer materials. The microstructures of the samples were also analysed in the study.

Thokchom et al. (2009) studied on fly ash based geopolymer mortar and analyse the porosity, durability, and water absorption property. The geopolymer mortar specimens were kept in the sulphuric acid solution. The activator to fly ash ratio was kept to 0.33 and Low calcium (class F) fly ash was used in this research. The samples was exposed to ten percent sulphuric acid solution for 24 week. This experiment showed that geopolymer mix activated with lower alkali content gives higher water absorption and porosity. This research also showed the effect on residual compressive strength on sulphuric acid exposure. The samples with lower alkali content had lower compressive strength also the samples that has lower porosity, water absorption and sorptivity gives higher residual compressive strength after 24 week sulphuric acid exposure.

Skvara et al. (2007) investigated the effect of temperatures from 20°C to 1000°C on aluminosilicate polymers (ASP) materials based on brown coal fly ash. Brown coal fly ash from Czech Republic was used for investigation with a specific surface area 210 $m^2$/kg. More than 60 % of $H_2O$ were lost on heating at temperatures below 200°C. The residual water was lost, or OH groups were split off after heating at temperatures above 600°C.The strength values of ASP increase after the heating to 200°C decreases afterwards. The porosity of the samples drops on heating at a temperature below 1000°C and the material density increases.

Rattanasak et al. (2009) researched on fly ash based sodium hydroxide geopolymer. The research was conducted with curing at $65^0$C for a total period of 48 hour. Leaching of Si, Al and other minor ions begins after fly ash was mixed with NaOH and the total leaching process was dependent of sodium hydroxide concentrations. The result concluded that the mixing process should be done for 10 min with 10M sodium hydroxide solution.

Palomo et al. (1999) analysed the effect of alkali activated class F fly ash with high concentration of alkali activator NaOH and KOH. The Geopolymer specimen were cast with 1x1x6 cm mould and cured in an oven at $65^0$C and $85^0$C for 2, 5 and 24 hours. The specimen was tested for compressive strength after taking out of the oven. The Samples were also studied by X-ray diffraction (XRD), Fourier transforms infrared spectroscopy (FTIR) and scanning electron microscopy / Energy dispersion

X11 Ray spectroscopy (SEM/EDX). The Samples studied through SEM/EDX had different microstructure for different activator composition. It was observed that the average compressive strength increases with the curing time.

Daniel et al (2008) demonstrates their work for fly ash and metakaolin based geopolymer after elevated temperature exposure. Potassium hydroxide and sodium silicate solution was used for casting purpose. According to the paper fly ash geopolymer performs better than metakaolin geopolymer at elevated temperature. According to the paper metakaolin based geopolymer had a drop of strength by 34% while fly ash based geopolymer had a strength increase by 6% after elevated temperature exposure.

Shaikh et al., (2015) worked with fly ash based geopolymer with sodium based activator. The compressive strength was measured after keeping the samples at elevated temperature from 200ºC, 400ºC, 600ºC and 800ºC. The study reports that the fly-ash-based geopolymer concretes showed steady loss of its original compressive strength at all elevated temperatures up to 400 °C irrespective to the molarities and aggregate size. At 600°C the geopolymer concretes increase its strength than that of $400^0$C. But the strength decreases at $800^0$C. At $800^0$C the strength was less than that of ambient temperature.

Temuujin et al. (2010) detected around 10% mass loss from fly ash geopolymer and it occurred before 200°C and started to stabilize at temperature around 500°C .

Bakharev (2005) illustrates the influence of elevated temperature on development of strength and microstructure analysis in Geopolymer materials. Class F fly ash was added to sodium hydroxide with sodium silicate solution, providing up to 10% Na in mixture and water to binder ratio of 0.3. The paste were cast in plastic mould of size (25x50) mm cylinder, compressive strength was measured at 1, 2, 7, 14, 28, 60, and 120 days. Three types of curing were used. First mixture was cured for 2 hour at room and then ramped to $75^0$C for one month. In second case mixture were cured for 24h for room temperature and ramped to $75^0$C and $95^0$C for 24 hours. In third case mixture ware cured for 24h and then ramped to $75^0$C for 6 hours. The experiment result showed that long procuring at room temperature was benefit for strength development all type of samples. The investigation explains that the first 6 hours heat

curing give major change in geopolymer material. Long pre-curing at room temperature made significant dissolution of fly ash, this was beneficial because it increase the homogeneity in the Geopolymer material.

## 2.5. EFFECT OF VARIOUS FIBRES/FILLERS ON ELEVATED TEMPERATURE BEHAVIOUR OF FLY ASH GEOPOLYMER

Fillers and aggregates can be added to geopolymers to reduce the thermal expansion/shrinkage of the composite and extend the usable temperature range. Various additives are used in geopolymer matrix to improve its fire resistance e.g. quartz and granite aggregates (Subaer, 2007; Kamseu, 2010), alumina particles (Bell, 2005; Lin, 2009), wollastonite (Silva, 1999), etc. Various organic and inorganic fibres are also added to reinforce geopolymers to improve its fire resistance. Alomayri et al (2014) researched on carbon and cotton fibres reinforced geopolymer composites at elevated temperatures.

Dylmar and Clelio, (2005) investigated the influence of the volumetric fraction of the fibers on the fracture toughness of geopolymeric cement concretes reinforced with basalt fibers. The values of fracture toughness, critical stress intensity factor and critical crack mouth opening displacement were measured on 18 notched beams tested by three-point bending. The $a_0/h$ (notch height/beam height) ratio was equal to 0.2 and the $L_0/h$ (distance between the supports/beam height) ratio was equal to 3. According to the experimental results, geopolymeric concretes have better fracture properties than conventional Portland cement. They are also less sensitive to the presence of cracks.

Masi et al. (2015) reported a study where poly vinyl alcohol (PVA) and basalt short fibres are added to fly ash based geopolymer activated by sodium hydroxide and sodium aluminate solutions. Results show better mechanical properties of basalt fibre reinforced geopolymer at elevated temperatures than its PVA fibre reinforced counterpart. In another study the effect of elevated temperatures on fibre-matrix interaction of continuous basalt fibre reinforced dehydroxylated halloysite geopolymer is evaluated (Welter, 2015).

Zhang et al. (2014) reported effects of various short carbon fibre contents on the compressive and bending strength of metakaolin-fly ash geopolymers at evaluated temperatures. Results show that 2% carbon fibre reinforced geopolymer containing 50% fly ash and 50% metakaolin exhibited excellent behaviour at 500$^{o}$C. While both basalt and carbon fibres show excellent thermal stability at elevated temperatures and class F fly ash is commonly used as source material for geopolymer not enough research studied the behaviour of carbon and basalt fibre reinforced fly ash based geopolymer at elevated temperatures.

Recently, nano materials and its use gathered specific attention in the use of construction material. Among various manufactured nano particles and nano silica (NS) recently has been applied and introduced as advanced pozzolan to develop a better microstructure and properties of geopolymer and also in concrete. As a result significant improvements in various mechanical property as well as durability of concretes and concretes containing industrial by products e.g. fly ash are reported in a number of studies (Shaikh and Supit, 2014; Shaikh et. al., 2014; Supit and Shaikh, 2014; Shaikh and Hosan, 2016). In geopolymers, the incorporation of nano materials is relatively new. In a recent study, Deb (2015) analysed and described nano silica effect on the development of strength of ambient cured geopolymer. The results show that the early age compressive strength is increase due to the addition of nano silica, which was evidenced by dense microstructure. Low calcium fly ash was mixed with Portland cement or blast furnace slag which helped with the ambient temperature curing. The research concluded that compressive strength was increased with replacement or adding of nano silica up to 2%.

Adak et. al. (2014) researched on geopolymer with nano silica of (0%, 4%, 6%, 8% and 10% ) in replacement of fly ash and concluded that with addition of 6% nano silica gives better result with 28 days ambient curing in the strength properties.

Phoo-nhernkham et. al. (2014) worked with high calcium fly ash with an addition of nano silica as well as nano alumina. This study used ambient temperature curing. The geopolymer were casted using 10M sodium hydroxide solution. The sodium silicate to sodium hydroxide ratio was (by mass) 2.0 and also activator to binder ratio kept at

0.6. The result supports the face that one to two percent nano silica have a positive effect on the compressive strength, flexural strength and elastic modulus of paste due to additional gel formation.

Improvement of compressive strength of geopolymer due to addition of nano kaolin is also reported by Hassaan et. al. (2015). The effect of addition of calcined nano-clay (Cloisite 30B) on the mechanical and thermal properties of geopolymer composites was researched by Assaedi and Shaikh (2015). The nanoclay particles improved the physical structure of geopolymer matrices, produced geopolymer with superior mechanical performance. The geopolymer containing nano clay also exhibited better thermal stability than pure geopolymer. In another study, it has been reported by Nazari (2015) that the silica and alumina nano-particles have the ability to reduce the porosity and water absorption of geopolymer matrices.

The effect of nano silica on the properties of concrete and geopolymer at elevated temperatures has received very limited attention despite its positive influence on mechanical and durability properties of cement and geopolymer based binder. Bastami et al. (2014) reported a study on the effect of nano silica on the compressive behaviour of high strength concrete at elevated temperatures. Their results show that the addition of nano silica improved the mechanical properties of high strength concrete at elevated temperatures and better than concrete containing silica fume. The only reported study on the effect of nano silica on the microstructure of geopolymer at elevated temperatures is by Estrada-Arreola et al. (2014), where X-ray diffraction, atomic-force microscopy and optical profilometry techniques were used to identify the changes in microstructure of nano silica modified geopolymer at elevated temperatures. No significant changes in micro-structure of geopolymer containing nano silica at elevated temperature of 1000$^{o}$C are noticed in their study.

## 2.6. DAMAGE OF TIMBER IN FIRE

Timber is one of the earliest used building materials for construction. Most building materials requires large amount of energy for the processing purpose, for construction purpose as well as for the ultimate demolition purpose. But as a building material timber require less energy is environment and ecological friendly. For this

reason though a lot of building materials are invented, timber is still one of the most favourable choice among the users as well as the builders.

Using timber as a construction material is an excellent option. Timber structures are very common in Australia and also in other parts of the world. As it is less expensive and easy to build so this option is very much popular worldwide. Especially in earthquake prone or in aggressive weather region, in household structures as well as in small construction timbers and different types of wooden frames are a very popular option as a building material.

The benefits of the timber structures are:

*Close to nature*

Timber is a widely used construction material which has a lot of benefits than other building materials. It does not have any toxic vapour, harmless to the builder. With the aging of the timber, it is a biological procedure and it does not give any unsafe by-product which may harm the human being.

*Great availability*

Timber is one of the oldest construction material which has a very good availability everywhere even in the most remote areas. Timber is available even locally and can be used for the building purpose after some processing.

*Less energy Consumption*

Some processing is necessary to use the timber for construction. Processing of timber as a construction material is energy efficient than most other building materials.

*Carbon efficient*

Timber is one of the most carbon efficient building material which does not cause any harm to the environment.

*An excellent insulation property*

Timber is a good insulator to sound and heat. It is widely used in the door, floor as well as in the window.

*Easy to recycle*

Timber is easy to recycle. Can be used again even in a smaller construction or can be recycled to use in other aspects.

*Easy to work*

Timber is very easy to construct and also easy to install. Being light in weight this can be installed with very simple equipment.

Though the type of timber structures are very much safe in earthquake but greatly vulnerable to fire and at elevated temperature. Due to the global warming and other issues bushfires are getting more common and more frequent in Australia as well as in other parts of the world. Australia's worst ever recorded natural disaster was the Victorian Black Saturday bushfires of 2009, where over 450,000 hectares of land was destroyed with a total of 414 person were injured and the number of total fatality was 173. (https://en.wikipedia.org/wiki/Bushfires_in_Australia).

In the Victorian Black Saturday bushfire, more than 3500 buildings were destroyed among them more than 2000 buildings were dwelling houses. This types of natural calamities effect the timber structures the most. So regarding the fire safety issue timbers used in those wooden structures or wooden frames can be treated or coated for its better action.

In the last decades, the need for fire safety of timber structures pushed the scientific community to conduct extensive research on this topic. Among possible applications of engineered geopolymer composite, its use as protection layer in timber structure could be highly beneficial. According to Australian Code (www.woodpanels.org.au) fire resistance of timber structure is the capacity of a building material to protect fire, but still have its structural purpose. Fire resistance levels (FRL) are given as performance property, in minutes, for structural adequacy, integrity and insulation. This factor is expressed as, e.g. 30/30/30 for which the:

- first number relates to structural stability, i.e. the time to elapse before collapse;

- second number is an integrity requirement, i.e. flames must not pass through the component for this number of minutes;
- third number is an insulation value, i.e. limits heat transfer through the component.

## 2.7. GEOPOLYMER CEMENTITIOUS COATING AT ELEVATED TEMPERATURE

Using geopolymer as a coating material is a new option and a new research idea to protect materials from negative impact like chemical or fire.

Ramasamy et. al. (2016) studied the bond behaviour of Kaolin based geopolymer coating with lumber wood substrate. The paper concluded that the coating with 0.9 solid to liquid ratio and 0.45 sodium silicate to sodium chloride ratio with a mole of 6M gives the best adhesive strength.

Pavel et. al. (2013) summarizes the protection of timber with alkali aluminosilicate protective coating to protect timber fire or elevated temperature. The study used alkali alumina silicate and fillers like microspheres, limestone for the coating purpose and studied the mass loss and degree of burning of the samples. Pine wood with 35x50x150 mm were used for the coating purpose with 2 and 19 mm thickness respectively.

Jang-Ho et. al. (2010) evaluate the behaviour of cementitious coated tunnel exposed to fire. The application of the coating is used in construction purpose and can be used for fire resistance purpose also. The coating proposed was in low cost and high in strength and are mostly composed of cement, bottom ash and polypropylene fibers. The paper suggest that fire protection property is mostly dependent on the aggregate type than on the cement type so ordinary Portland cement is used for the coating material. Accelerated setting agent was used to increase the bond strength during shotcreting. Coating thickness used was 20mm, 30mm and 40mm to compare the thickness effect on the fire protection performance. The paper suggest that thickness between 30 mm and 40 mm can be considered optimal for the fire protection coating of the tunnel lining.

Vit Petranek et. al. (2014) researched on geocement based thermal insulator with ground limestone and aluminosilicate pallet. The thickness used in this study was 3 mm to 4.5mm that swells after exposure to heat flow. The paper suggest that this material can be used as an insulator on wood, metal and concrete surfaces from and one sided heat source.

Richardson and Cornelissen (1987) worked with a flame retardant paint and coating on timber that can reduce the formation of char by as much as 70% after 30 minutes exposure to fire conditions. 460 mm x390 mm and 530 mm x 530 mm timber panels were used for coating purpose and two cementitious coating and two fibrous coating was used for comparison purpose. 50 mm cementitious coating and 25 mm fibrous coating with glass fibre was used for the coating purpose.

Temuujin et al (2010) worked with fly ash based geopolymer composite and analysed geopolymer coating on steel. The geopolymer composition used with molar ratio of Si:Al was 3.5. The research showed strong adhesion of geopolymer to steel and showed that it is very much promising for fire protection. Class F fly ash with sodium based activator was used as a coating material. The research proceeds with varying Si:Al (molar ratio). The bond strength of the coating was measured and conclusion was drawn that this strength was dependent largely in the chemical composition of the geopolymer. The workability of the geopolymer, the thickness of the coating was largely dependent on the consistency of the mix which is dependent on the water content in the mix. Microstructure analysis was also done and fire test proves the fact that geopolymer 1.5 mm coating on steel is an excellent idea for fire protection.

## 2.8. CONCLUSION

Review of the geopolymer along its key ingredients are summarized in this chapter. The proportion of its key ingredients and use of different additives are also discussed in this chapter. The knowledge gathered from the previous research helps to proceed the research and give some direction about how the geopolymer behave and how its property changes at elevated temperature. As timber structures are vulnerable to fire

so this geopolymer can be used as a coating on the timber to protect the timber from fire.

# CHAPTER III

# METHODOLOGY

## 3.1. INTRODUCTION

Previous chapter summarizes some of the previous research done on geopolymer with different varying ingredients and its application as well as effectiveness of the application at elevated temperature. This chapter describes about the current research and methodology of the work done to study the fly ash based geopolymer which can endure elevated temperature heat up to $800^0$C. The description about the ingredients and materials used and the research methodology is described in this chapter.

## 3.2. MATERIALS

Different materials are used to synthetise geopolymer that exhibits superior fire resistance property. The only source material for geopolymer in this research is class F fly ash activated with sodium and potassium based activators like sodium hydroxide (NaOH), sodium silicate ($Na_2SiO_3$) and potassium hydroxide (KOH) and potassium silicate ($K_2SiO_3$). Different fillers e.g. nano silica and ultra-fine sand and fibres e.g. carbon and basalt fibres are used as partial replacement of fly ash to reinforce the geopolymer matrix.

### 3.2.1 Fly Ash

Fly ash is by-product of coal fired power stations which is produced every day of about millions of tonnes in many countries in the world and only about 20-25% of the total is properly utilised. Compared to meakaolin, which is naturally occurring, it is cheaper and protect the environmental in terms of dumping and contamination of ground water. Though it contain significant amount of impurities like iron oxide in the form of hametite and magnetite and unburn carbon, it is also less reactive to metakaolin. Previous work by Krivenko and Kovalchuk (2002) investigated heat resistant geopolymer materials manufactured using class F fly ash, which had good thermal resistance properties upto $800^0$C. Class F fly ash supplied by Gladstone

power station of Queensland, Australia was used as source material to prepare the geopolymer pastes. Table 3.1 shows the chemical compositions of the fly ash.

**Table 3. 1 : Chemical Composition of Fly Ash (mass %)**

| **Compounds** | **Fly Ash** |
|---|---|
| $SiO_2$ | 51.11 |
| $Al_2O_3$ | 25.56 |
| $Fe_2O_3$ | 12.48 |
| CaO | 4.3 |
| $Na_2O$ | 0.77 |
| $K_2O$ | 0.7 |
| MgO | 1.45 |
| $P_2O_5$ | 0.885 |
| $SO_3$ | 0.24 |
| $TiO_2$ | 1.32 |
| MnO | 0.15 |
| LOI | 0.57 |

### 3.3.1. Alkali activators

The activating alkali liquids consisted of $Na_2SiO_3$ and NaOH solutions as well as $K_2SiO_3$ and KOH solutions. The Na-based activator was composed of 8.0 M sodium hydroxide (NaOH) and D Grade sodium silicate ($Na_2SiO_3$) solutions. NaOH solution was prepared with a concentration of 8.0 M using NaOH beads of 97% purity and tap water. The D Grade $Na_2SiO_3$ solution was supplied by PQ Australia with a specific gravity of 1.51 and a modulus ratio (Ms) equal to 2.0 (where Ms = $SiO_2$/ $Na_2O$, $Na_2O$ = 14.7%, $SiO_2$ = 29.4% and water-55.9%). The NaOH and $Na_2SiO_3$ solutions were mixed together with $Na_2SiO_3$/NaOH mass ratio of 2, 2.5 and 3 to prepare the Na-based activators. The K-based activator was composed of 8.0 M potassium hydroxide (KOH) and potassium silicate ($K_2SiO_3$) solutions. KOH solution was prepared with a concentration of 8.0 M using KOH flakes of 90% purity

supplied by Perth Scientific, Australia and tap water. The $K_2SiO_3$ (KASIL 2236 Grade) solution was supplied by PQ Australia with a specific gravity of 1.32 and a modulus ratio (Ms) equal to 2.23 (where Ms = $SiO_2/K_2O$, $K_2O$ = 11.2%, $SiO_2$ = 24.8% and water=64%). KOH and $K_2SiO_3$ solutions were mixed together with $K_2SiO_3$/KOH mass ratio of 2, 2.5 and 3 to prepare the K-based activators.

### 3.3.2. Water

Tap water was used in this study. The main use of water is mostly for the preparation of sodium hydroxide or potassium hydroxide solution.

### 3.3.3. Nano Silica and fine sand

The powder nano silica (NS) was obtained from Nanostructured and Amorphous Materials, Inc. of USA with average particle diameter of 25 nm and specific surface area of 160$m^2$/g. The purity of NS is 99% $SiO_2$ according to chemical analysis. The fine silica sand (FS) used in this study was supplied by Rocla, Australia with particle sizes ranging from 150-300 microns.

### 3.3.4. Basalt Fibre and Carbon Fibre

The chopped basalt fibres were 13 micron in diameter and 12.7mm in length while the chopped carbon fibres were 11 microns in diameter and 6 mm in length.

## 3.3. PREPARATION OF ALKALINE ACTIVATOR SOLUTION

Sodium hydroxide and potassium hydroxide solutions were prepared one day before the casting and stored in a sealed container when it was cooled. The mixing process was done in the fume hood. On the day of casting the final mixing of sodium silicate solution with sodium hydroxide solution was done. Similarly in the case of potassium series the potassium hydroxide solution was mixed with the potassium silicate solution on the day of casting. The mixing was also done in the fume hood. The reaction done by the mixture creates heat and so it was necessary to cool it before adding to other ingredients.

## 3.4. MIX PROPORTIONS

The experimental program is consisted of three phases. The first phase consisted of two parts. The first part is geopolymer paste containing sodium based activators combinations, where three different sodium silicate to sodium hydroxide ratios of 2, 2.5 and 3 are considered and for each ratio the geopolymers are heated at 200, 400, 600 and $800^0$C temperatures as well as at ambient temperature. Thus fifteen series of pastes are casted and tested at elevated temperatures in the first part. The second part is similar to the first part in every aspect except the alkali activators where potassium silicate and potassium hydroxide are used. For each series, in both parts, six 50 mm cube specimens are cast and tested and the average value is shown in the results. In all geopolymer pastes a constant activator/fly ash ratio of 0.35 is considered.

In the second phase the effects of nano silica and fine sand as fillers and carbon fibre and basalt fibres as reinforcement of the geopolymer which exhibited highest residual compressive strength, lowest mass loss the volumetric shrinkage in the first phase is considered. The nano silica is used as partial replacement of fly ash at 1%, 2% and 4% by wt. of fly ash, while fine sand is used as partial replacement of fly ash at 5%, 10% and 20% by wt. of fly ash. The carbon fibre and basalt fibres are added at 0.5%, 1% and 1.5% by wt. of fly ash in geopolymer. Potassium based activators synthetised geopolymer having silicate to hydroxide ratio of 3 exhibited best workability and residual mechanical properties compared to its sodium based counterpart and other silicate to hydroxide ratios in the first phase. Hence, geopolymer synthetised by potassium silicate and potassium hydroxide ratio of 3 is used in the second phase of this research with a slightly higher activator solution to fly ash ratio of 0.4 to maintain the similar workability because total surface areas of particles are increased due to addition of ultra-fine fillers. In the case of carbon fibre and basalt fibre reinforced potassium based activators synthetised geopolymer the initial activator to fly ash ratio of 0.35 is also used. The mix proportions are added in the Appendix.

## 3.5. MIXING METHODS

All pastes were prepared in a Hobart mixer (Figure 3.1). To prepare the Na- and K-based geopolymer paste the alkaline activators in the form of solution were added to the fly ash and mixed for about 4 min. The fresh geopolymer pastes were cast into standard 50 mm plastic cube (according to ASTM C 109, 2012) moulds and compacted using a vibrating table. The specimens were subjected to heat curing. All moulds were sealed with plastic wrap to minimize the moisture loss and placed in an oven at 70ºC for 24 h.

At the end of heat curing period, the specimens were removed from the oven and kept undisturbed until being cooled and then removed from the moulds and left in the laboratory at controlled atmosphere (Figure 3.2) until the day of elevated temperature exposure.


**Figure 3. 1: Hobart mixer**

## 3.6. ELEVATED TEMPERATURE EXPOSURE

A locally manufactured kiln was used to heat the geopolymer specimens, where the specimens were heated from 200ºC to 800°C. After $800^0$C the strength of the sample is very poor so the heating temperature is limited to $800^0$C. The specimens were positioned inside the kiln where two thermocouples were touched the specimens one in the top surface and the other at side of a specimen, and two more thermocouples were also inserted inside the kiln to monitor the kiln air temperature. The thermocouples were connected to the data logger and were used to monitor the temperature on the mortar surface and the kiln air as shown in Figure 3.3 and Figure 3.5. A heating rate of 5°C per minute was selected, which is very close to the RILEM

**Figure3.2:Geopolymer Samples**

recommended heating rate (RILEM TC 129-MHT (2000). During heating process the temperatures of four thermocouples were monitored. Once the specimen's surface reached the target temperature, the temperature inside the kiln was hold for one hour. The rate of temperature increase in the kiln and in the specimen is shown in Figure 3.4. As can be seen in the figure, there is a significant lag between the surface temperature of cubes and air temperature inside the kiln, particularly for the 200 and 400°C temperature profiles. This is due to the heat capacity of the specimens and the rate at which they are able to absorb heat. However, the difference in temperature

between the kiln and the cubes at $600^0$ and 800°C is less. As the sample size is small 50x50x50 $mm^3$ so effect of any small difference of temperature among the faces of the cube is also negligible.

**Figure 3. 2 : Geopolymer specimens inside the kiln**

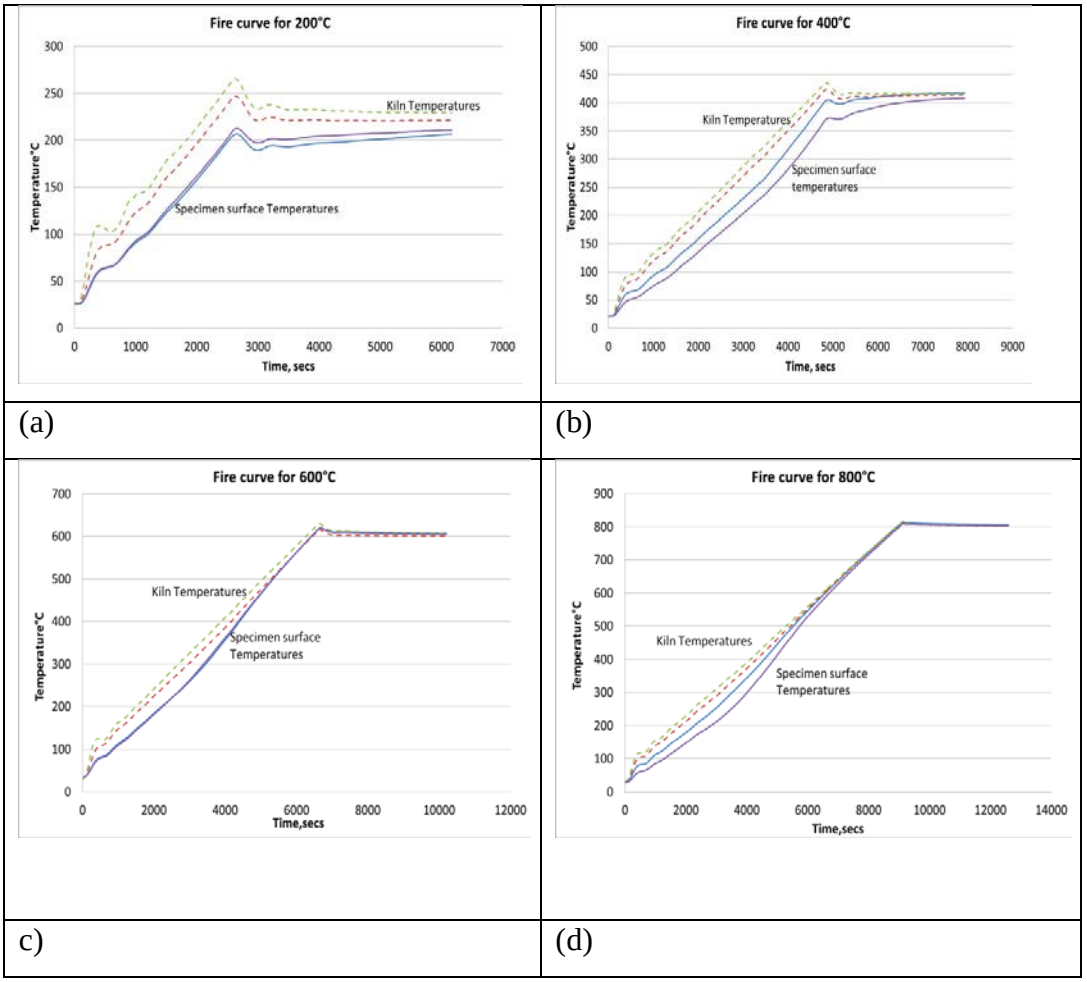


**Figure 3. 3 : Fire curves for different elevated temperatures in the kiln during heating.**

Even though the difference in temperature between the kiln and the cubes existed, the target test temperatures in all cubes were maintained for one hour, which can be seen in the thermocouples readings in Figure 3.4.


**Figure 3. 4 : Oven Setup and data logging**

## 3.7. COMPRESSIVE STRENGTH, MASS LOSS AND VOLUME CHANGES

Compressive strength of all specimens was measured according to AS 1012.9 (2014). For each mix, at least three to six specimens were tested (Figure 3.6) in order to check the variability of performance under compression. The volumetric shrinkage of pastes was determined by measuring the length of three sides of the cubes before and after heating at respective elevated temperatures. The difference in volume changes indicates the volumetric shrinkage and six specimens were used to measure the volumetric shrinkage for each series. Similar method was also used to determine the mass loss of geopolymer pastes after exposed to respective elevated temperatures.


**Figure 3. 5: Compressive strength test setup**

## 3.8. SAMPLE PREPARATION FOR TGA AND XRD ANALYSIS

The thermal stability of samples was studied by thermogravimetric analysis (TGA). A Mettler Toledo TGA one star system analyser was used for all these measurements. Samples of 25 mg were placed in an alumina crucible and tests were carried out in Argon atmosphere with a heating rate of 10ºC/min from 25 to 1000ºC. In the case of XRD analysis, the samples were measured on a D8 Advance Diffractometer (Bruker-AXS) using copper radiation and a Lynx Eye position sensitive detector. The diffractometer were scanned from 7º to 70º in steps of 0.015º using a scanning rate of 0.5º/min. XRD patterns were obtained by using Cu Ka lines (k = 1.5406 Å). A knife edge collimator was fitted to reduce air scatter. The sample preparation for the TGA and XRD test are showed in Figure 3.7.

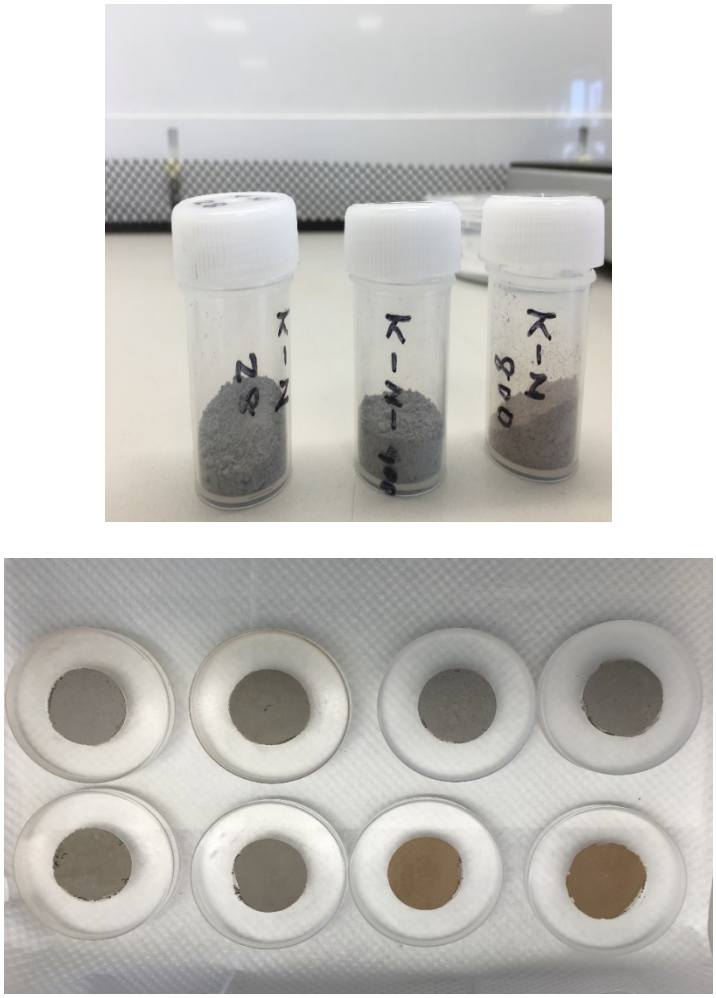

**Figure 3. 6 : Sample preparation for XRD and TGA analysis**

## 3.9. COATING OF TIMBER PLATE USING GEOPOLYMER

Pine wood is most commonly used timber in the construction in Australia. Commercial pine timber plates are sourced from local hardware store. Small timber plate of approximately 200x80x20mm is cut and is used to coat one side of the timber plate with both types of geopolymer pastes. Geopolymer paste is prepared by mixing class F fly ash, sodium silicate and 8M sodium hydroxide solutions (and potassium silicate and potassium hydroxide solutions) in a Hobart mixer. Alkali activator to fly ash ratio of 0.35 is used to achieve good workability of the paste. The paste is poured on top of the timber plate and spread using rectangular trowel. Sufficient care is taken to maintain uniform thickness of the coating. Fig. 3.8 shows the geopolymer coated

timber. The coated timber plates are covered with clean plastic sheet and then placed in oven at a temperature of 70$^{o}$C for 6 hrs. After 6 hrs of curing the samples were removed from the oven very carefully and kept at room temperature for another 24 hours. After 24 hours the samples were unwrapped and kept in the lab till the day of testing. Before the testing day a 2 mm diameter hole is made in the timber very carefully just under the geopolymer coating layer in the cross section to insert the thermocouple during testing.

The heat cured specimens are then left in open air until testing. In the same manner the potassium based activator coated timber plate specimens are also prepared. Two different coating thickness of about 2mm and 4mm are used for both geopolymers. At least 3 geopolymer coated timber plates are prepared for each thickness and geopolymer type. One specimen is used to measure the adhesion bond strength of geopolymer coating with timber, while the other two are used to perform the fire test. Chopped carbon fibre (CF) and basalt fibre (BF) are used to reinforce the K-based geopolymer paste in this study.

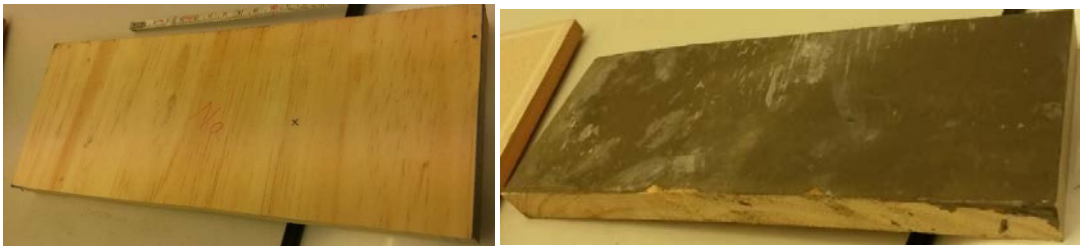

**Figure 3. 7: Timber plate (left) and geopolymer coated timber plate (right)**

**Figure 3. 8: Na-based geopolymer coated timber**

**Figure 3. 9: K-based geopolymer coated timber**

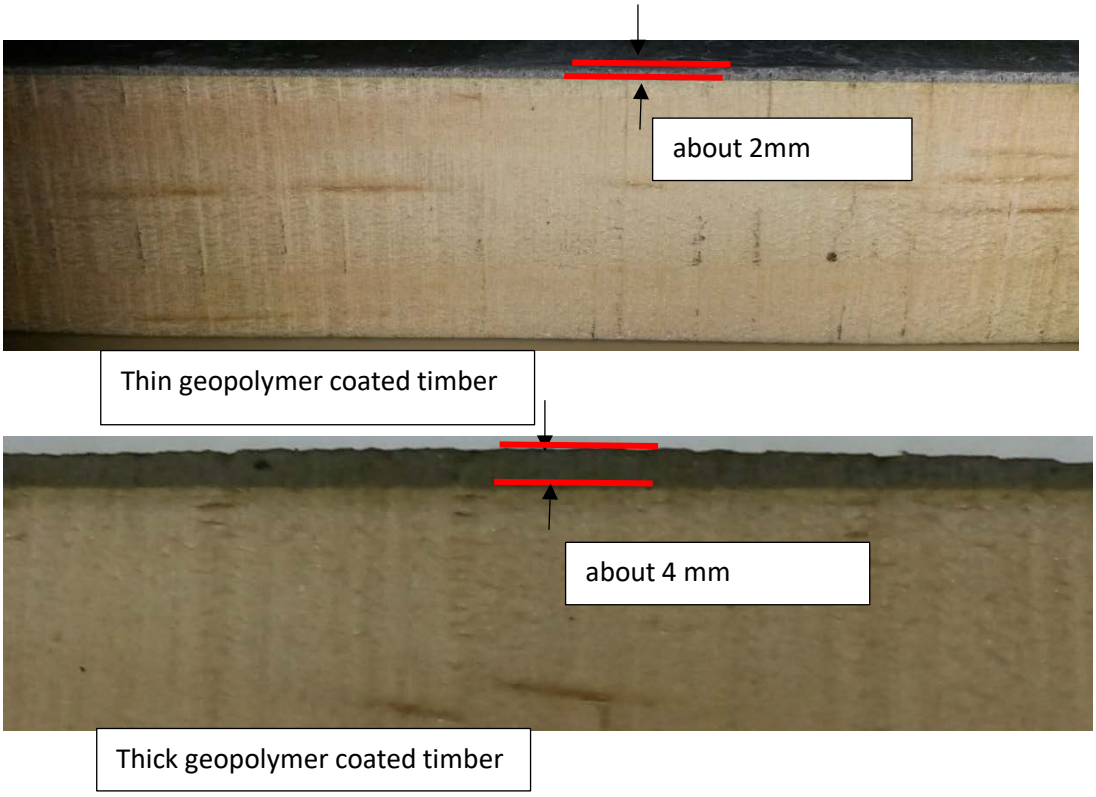


**Figure 3. 10: Geopolymer coating on timber plate**

## 3.10. ADHESION BOND TEST OF THE GEOPOLYMER COATING WITH THE TIMBER PLATE

The adhesion bond strength of both Na-based and K-based geopolymer coatings with timber was measured using a portable adhesion tester as shown in Figure 3.12 according to American society for testing and materials (ASTM) standard (ASTM D4541-09). In this test a small dolly is glued (Figure 3.13) to the geopolymer coating using a special two parts epoxy and was left 24 hrs to harden according the manufacturer's instruction. Prior to testing the detaching assembly (portable tester) was engaged with dolly and fluid was pumped using a loading fixture where the applied pull-out pressure is displayed (Figure 3.14). The pullout pressure at which the dolly detached from the geopolymer coating is considered as the adhesion bond strength of geopolymer coating with timber.


**Figure 3. 11: Portable adhesion tester.**

**Figure 3. 12 : Dolly glued to the geopolymer coating (left) Detaching assembly engaged with dolly (Right)**


**Figure 3. 13 : Display of pull out pressure in the loading fixture.**

## 3.11. FIRE TEST OF THE TIMBER PLATE

The geopolymer coated timber plates are subjected to direct fire test shown in Fig. 3.15. The schematic of the fire testing is shown in Fig. 3.16. As can be seen a portable Butane gas torch is used to apply the fire continuously on geopolymer coating side for 12 minutes. A temperature of about $1100^0$C is developed on the geopolymer

coating very quickly which is measured using a thermocouple as shown in Fig. 3.17. In addition, two thermocouples are also used to measure the temperature on un-coated side of the timber plate and approximately 2 mm behind the geopolymer coating by drilling a hole, detail of which is illustrated in actual test setup in Fig. 3.17. A commercial heat conducting paste is inserted into the drilled hole to facilitate the heat transfer from geopolymer coating to the thermocouple.

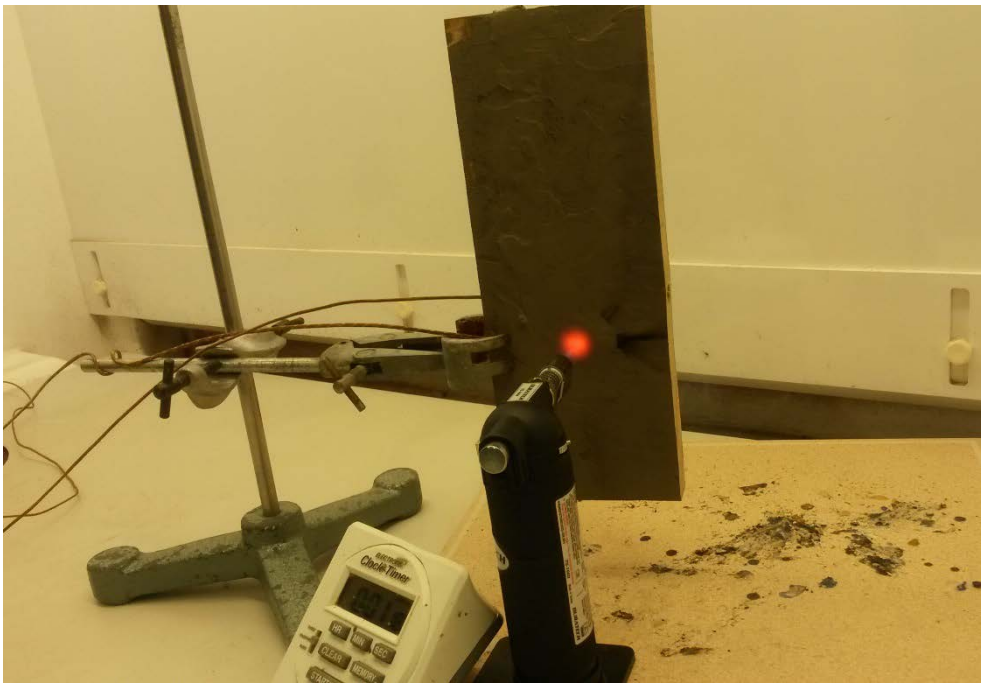

**Figure 3. 14: Geopolymer coated timber plate subjected to direct fire test.**

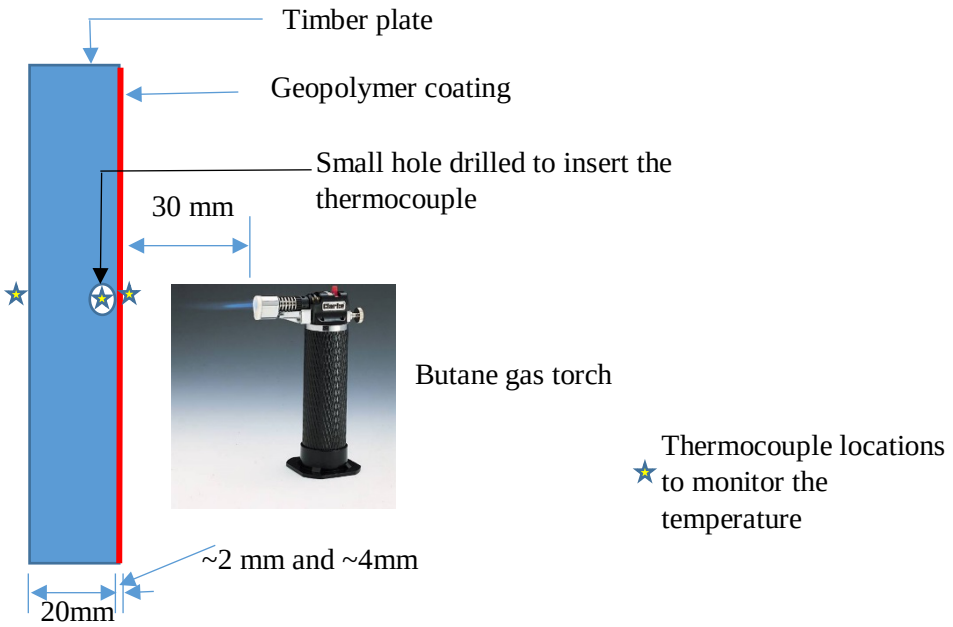


**Figure 3. 15: Schematic of the fire test.**

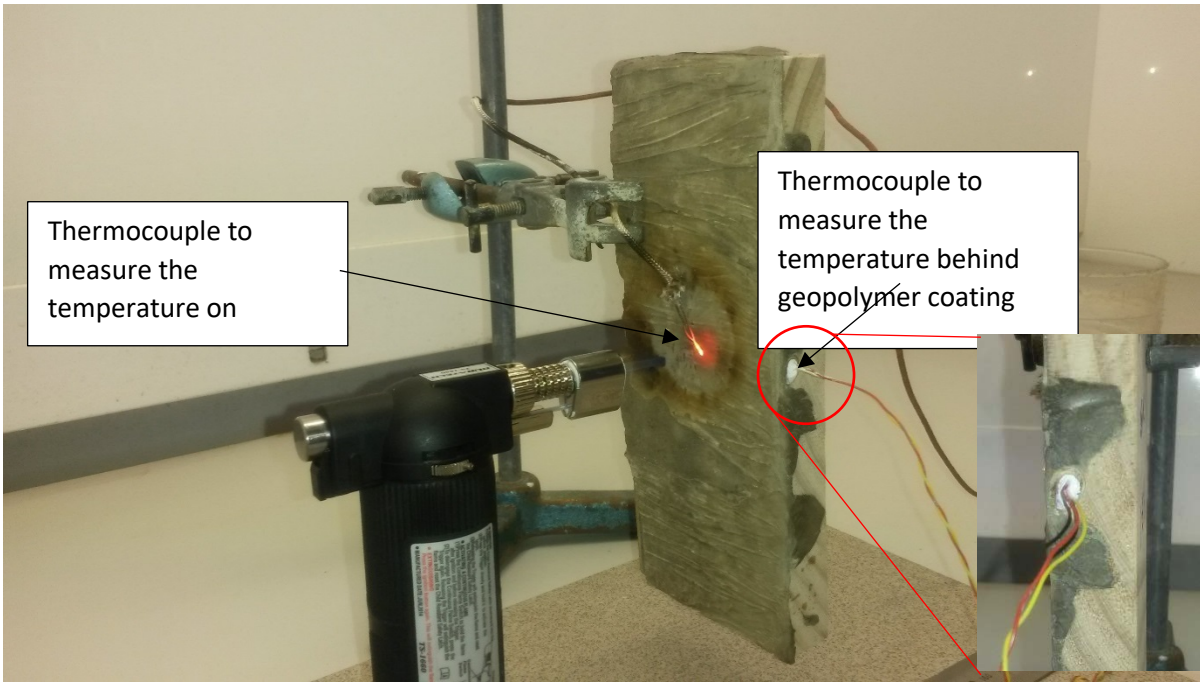


**Figure 3. 16: Position of thermocouples to measure the temperature on geopolymer coating and behind the coating. (Note: Insert shows the close-up position of thermocouple few millimetres behind the geopolymer coating)**

## 3.12. THERMAL CONDUCTIVITY SAMPLE PREPARATION AND TEST

Thermal conductivity is a measurement of the rate at which heat is transferred through a material. Thermal conductivity determination for both Na- and K-based geopolymers is required to access the geopolymer coating's stability as potential thermal barrier in fire. Heat flux plate and heat flux sensor assembly shown in Fig. 3.19 is used to measure the heat flow rate and the temperature difference to calculate the thermal conductivity of geopolymers according to the following equation (Askeland et al., 2010). The samples were circular plate having 20 mm thick and 70 mm diameter (Figure 3.18). A circular shape plastic mould was used to cast the samples. After casting the geopolymer samples were wrapped carefully to minimize any moisture loss during oven curing. The samples were kept in the oven at 70oC for 24 hours and after cooling the samples were demoulded and kept in the curing room till the day of casting. After 28 days both flat sides of the samples were polished.

$$k = Q\frac{\Delta x}{A\Delta T} \quad (1)$$

Where k=thermal conductivity ($Wm^{-1}K^{-1}$)

Q=heat flow rate ($Js^{-1}$)

$\Delta$x=thickness of sample (m)

A=Exposed surface area ($m^2$)

$\Delta$T= Temperature difference (K)

**Figure 3. 17: Thermal Conductivity Sample**

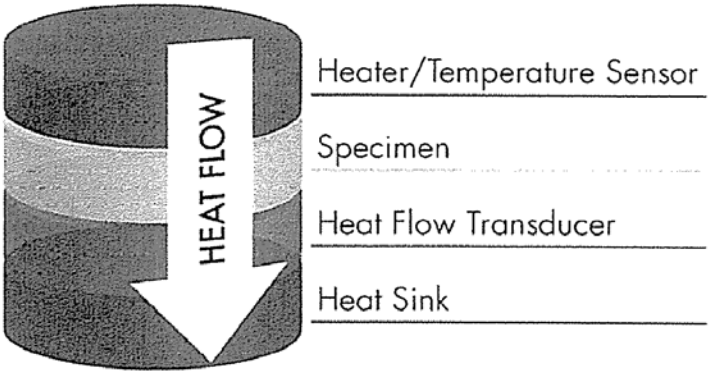


**Figure 3. 18: A schematic of thermal conductivity test setup**

## 3.13. LINEAR THERMAL EXPANSION OF GEOPOLYMER

Dilatometer was used to measure Linear Thermal Expansion of geopolymer samples. The samples were casted at a size of 2mm diameter and 4 cm long cylindrical shape. The heating rate was $5^0$C per minute. The test was done following ASTM E 37 (2011, 2012) code.

## 3.14. MERCURY INTRUSION POROSIMETRY (MIP) ANALYSIS

This measurement was performed with a Pore Master series – Quantachrome instruments, with a pressure ranged between 0.0083 and 207 MPa, and the pore diameter and intrusion mercury volume were recorded at each pressure point. Small broken pieces of approximately 10mm in sides are collected from the crushed geopolymer cubes containing 1 wt.% carbon and basalt fibres at ambient, 400 and 800$^{o}$C temperatures. The pressures were converted to equivalent pore diameter using the Washburn equation, (Washburn, 1921) as expressed in Eq. (1):

$$d = \frac{-4\gamma cos\theta}{p} \qquad (2)$$

Where d is the pore diameter (μm), c is the surface tension (mN/m), h is the contact angle between mercury and the pore wall ($^{o}$), and P is the net pressure across the mercury meniscus at the time of the cumulative intrusion measurement (MPa).

# CHAPTER IV

# ELEVATED TEMPERATURE BEHAVIOR OF GEOPOLYMER WITH VARYING ACTIVATORS

## 4.1. INTRODUCTION

This chapter presents the effects of sodium and potassium based activators on compressive strengths and physical changes of class F fly ash geopolymer exposed to elevated temperatures. Samples were heated at $200^0$C, $400^0$C, $600^0$C and $800^0$C to evaluate the residual compressive strength after 28 days of curing. The fly ash geopolymer were synthesized with combined sodium silicate and sodium hydroxide solutions and potassium silicate and potassium hydroxide solutions by varying mass ratios of $Na_2SiO_3$/NaOH and $K_2SiO_3$/KOH of 2, 2.5 and 3. X-ray diffraction (XRD) and thermogravimetric analysis (TGA) of sodium and potassium activator synthesized fly ash geopolymer at ambient and elevated temperature are also performed to evaluate the changes in geopolymerization.

## 4.2. RESIDUAL COMPRESSIVE STRENGTHS

The measured compressive strengths of geopolymer pastes containing different $Na_2SiO_3$/NaOH ratios of 2, 2.5 and 3 after exposed to 200, 400, 600 and 800$^o$C temperatures are shown in Figure 4.1. It can be seen that the residual compressive strengths of geopolymer paste containing $Na_2SiO_3$/NaOH ratio of 2 and 2.5 are increased by about 9-11% at 200$^o$C compared to ambient temperature strength. However, with further heating at 400, 600 and 800$^o$C temperatures the residual compressive strengths of above geopolymer pastes are decreased below the ambient condition (see Figure 4.2). On the other hand, the same geopolymer paste containing $Na_2SiO_3$/NaOH ratio of 3 showed significant increase in residual compressive strength by about 25-35% up to 600$^o$C with exception at 800$^o$C, where the residual compressive strength is decreased by more than 30% (See Figure 4.2).

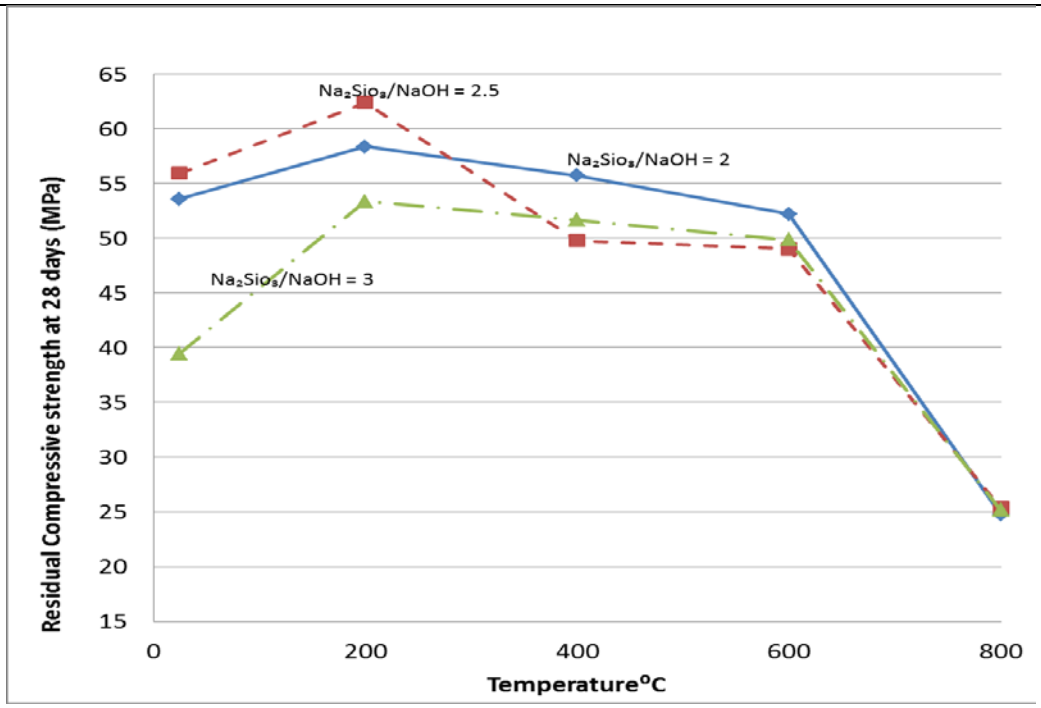


**Figure 4. 1: Residual compressive strength of geopolymer pastes containing Na-based activators at various elevated temperatures**

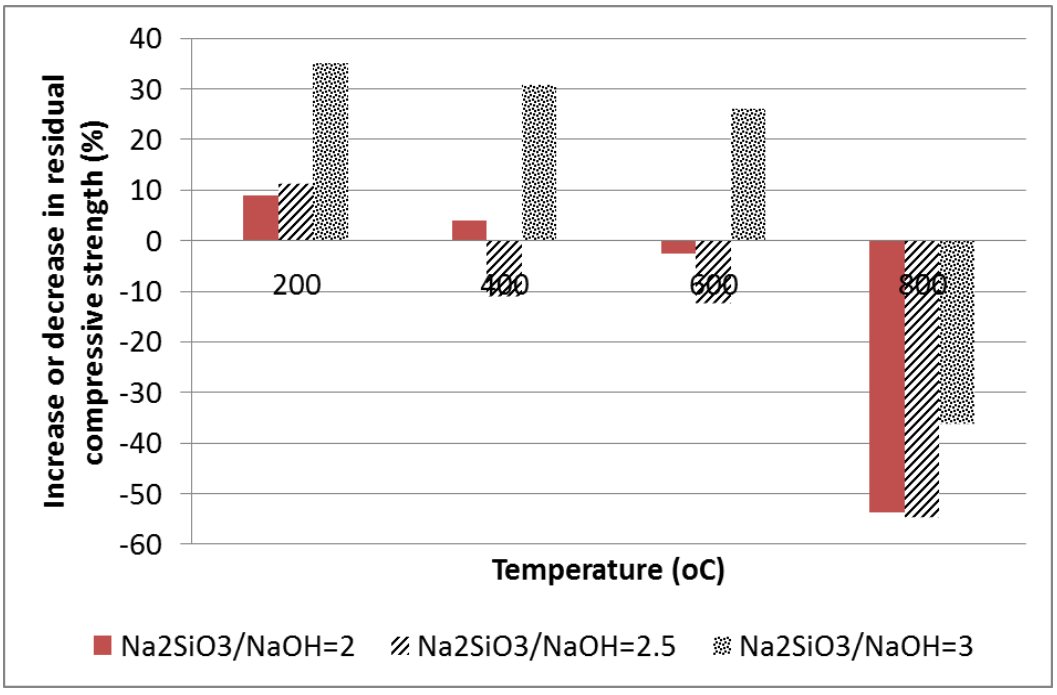


**Figure 4. 2: Relative increase or decrease in residual compressive strength of geopolymer pastes containing Na-based activators at various elevated temperatures compared to ambient temperature.**

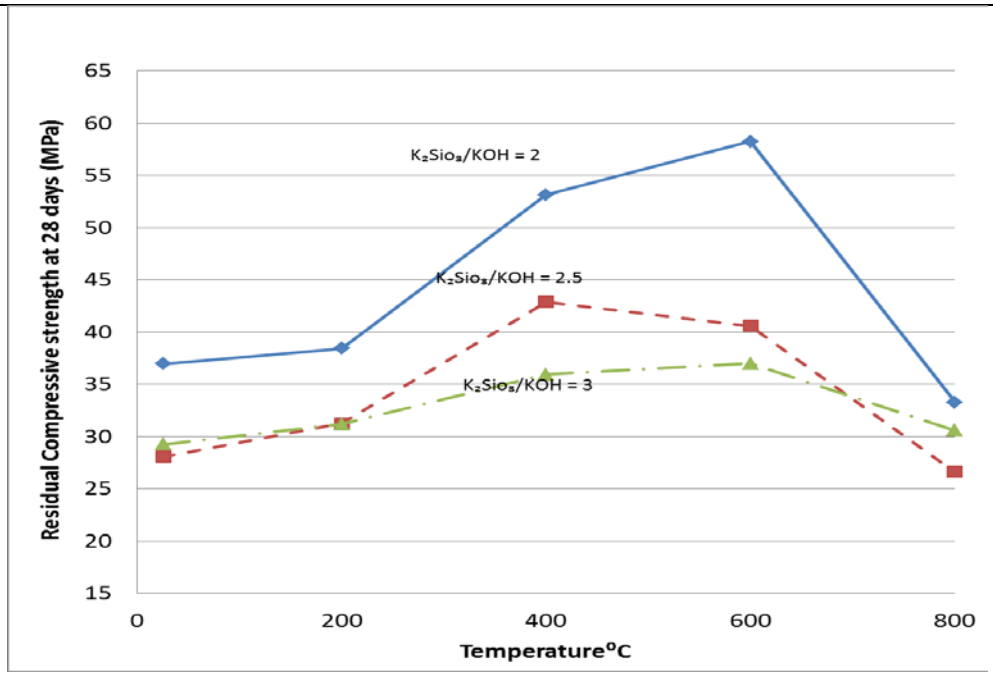


**Figure 4. 3: Residual compressive strength of geopolymer pastes containing K-based activators at various elevated temperatures**

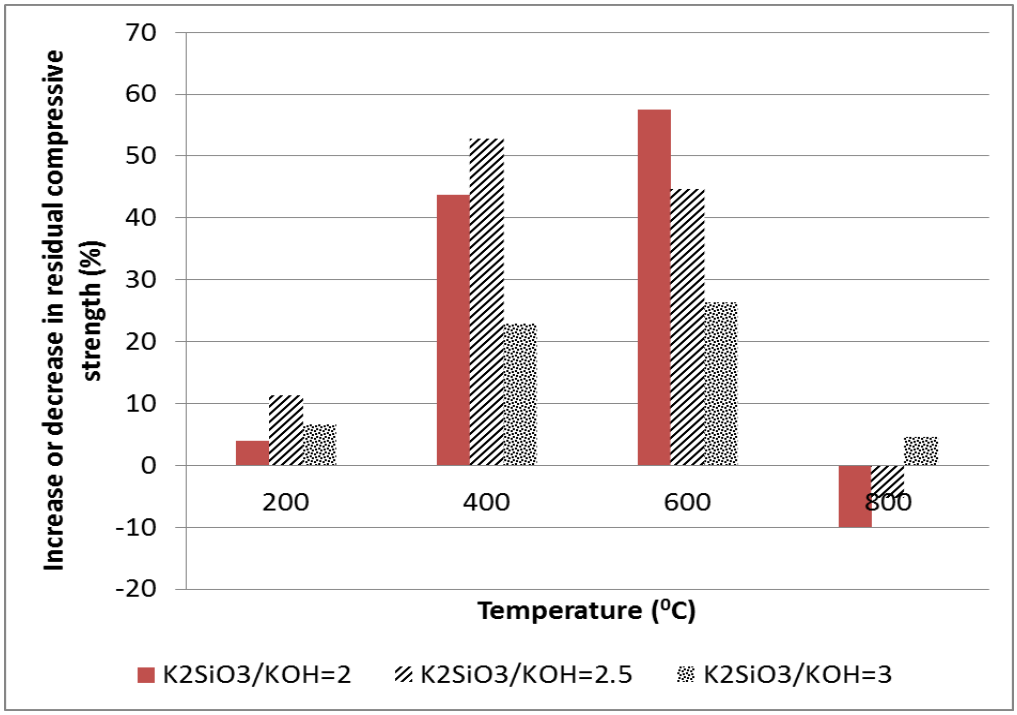


**Figure 4. 4: Relative increase or decrease in residual compressive strength of geopolymer pastes containing K-based activators at various elevated temperatures compared to ambient temperature.**

The effect of K-based activators on the compressive strength of geopolymer paste at elevated temperatures is also evaluated in this study and is shown in Figures 4.3-4.4. Figure 4.3 shows the measured compressive strengths of geopolymer pastes containing different $K_2SiO_3$/KOH ratios of 2, 2.5 and 3 after exposing to 200, 400, 600 and 800$^oC$ temperatures. It can be seen in the figure that for all three $K_2SiO_3$/KOH ratios the residual compressive strengths of geopolymer pastes are much higher than the ambient temperature strength and the residual compressive strengths are increased with increase in elevated temperatures until 600$^oC$. It is also interesting to see that at 400 and 600$^oC$ the geopolymer paste containing $K_2SiO_3$/KOH ratios of 2 and 2.5 show about 40-55% increase in compressive strength compared to ambient condition. Although the increase in compressive strength of paste containing $K_2SiO_3$/KOH ratios of 3 is slightly lower (about 22-26%) at those temperatures, the compressive strength is increased by about 5% at 800$^oC$ temperature, which is not observed in the case of $K_2SiO_3$/KOH ratios of 2 and 2.5 (see Figure 4.4).

By comparing both Na and K based geopolymer series in Figure 4.5 it can be clearly seen that the K-based activators show higher compressive strength retention capacity for geopolymer pastes than its counterpart Na-based series compared to ambient temperature strength. It can also be seen that in both geopolymer the ambient strength decreases with increase in silicate/hydroxide ratios for both Na- and K-based activators. This is attributed to the low water evaporation and less geopolymer structure formation due to excessive sodium silicate and potassium silicate (Chew, 1993). Interestingly the geopolymer with $K_2SiO_3$/KOH=3 exhibited higher compressive strength at all elevated temperatures than ambient temperature, which is also true for Na-based counterpart, however up to 600$^oC$. The increase in compressive strength in the former can be attributed to the lower diffusion coefficient of $K^+$ at elevated temperatures, which results in higher melting temperature (Bakharev, 2006).

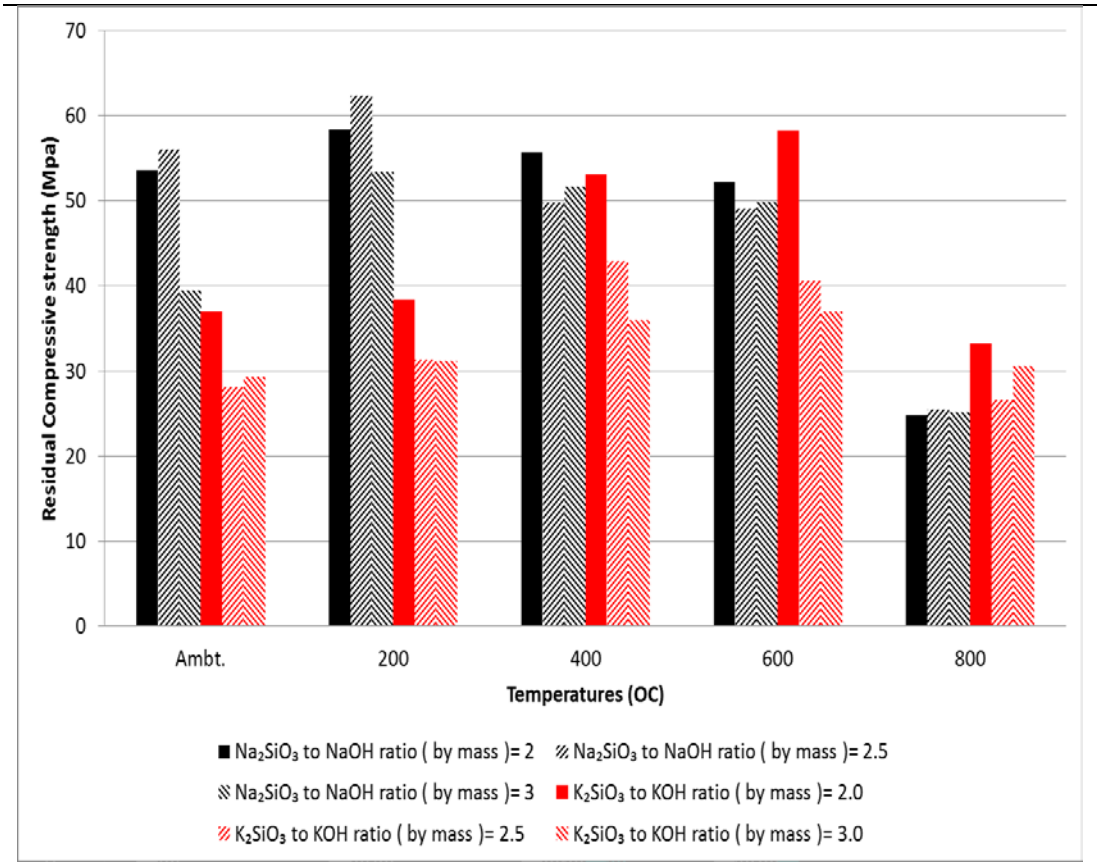


**Figure 4. 5: Comparison of compressive strengths of Na- and K-based geopolymer pastes.**

## 4.3. POST-HEATING PHYSICAL BEHAVIOUR

The effects of elevated temperatures on physical behaviour of both Na- and K-based activator synthetized fly ash geopolymers are shown in Figures 4.6-4.8. Figure 4.6 shows the formation of cracks on specimens' surface in both geopolymers. It can be seen that up to 400$^{o}$C no cracks are formed in both geopolymers. However, Na-based geopolymer showed signs of cracks at 600$^{o}$C and it becomes worst at 800$^{o}$C, where many wide cracks on the surface are formed. The geopolymer containing K-based activator, however, survived from surface cracking up to 600$^{o}$C, but fine cracks are formed at 800$^{o}$C. Figure 4.7 shows the reduction of mass of both geopolymers at various elevated temperatures.

| | Na-based | K-based |
|---|---|---|
| 200ºC | 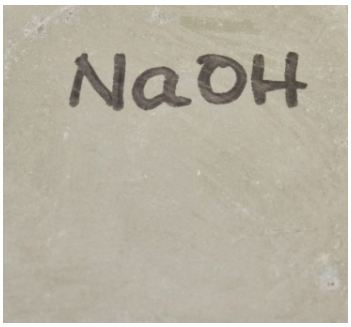  |   |
| 400ºC | 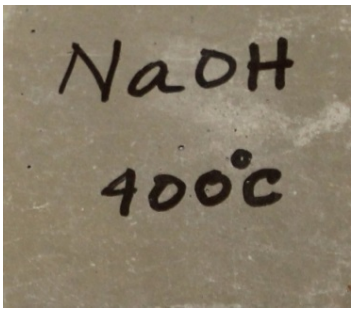  |  |
| 600ºC |  |  |
| 800ºC |  |  |

**Figure 4. 6: Cracking behaviour of fly ash geopolymers containing Na- and K-based activators at elevated temperatures.**

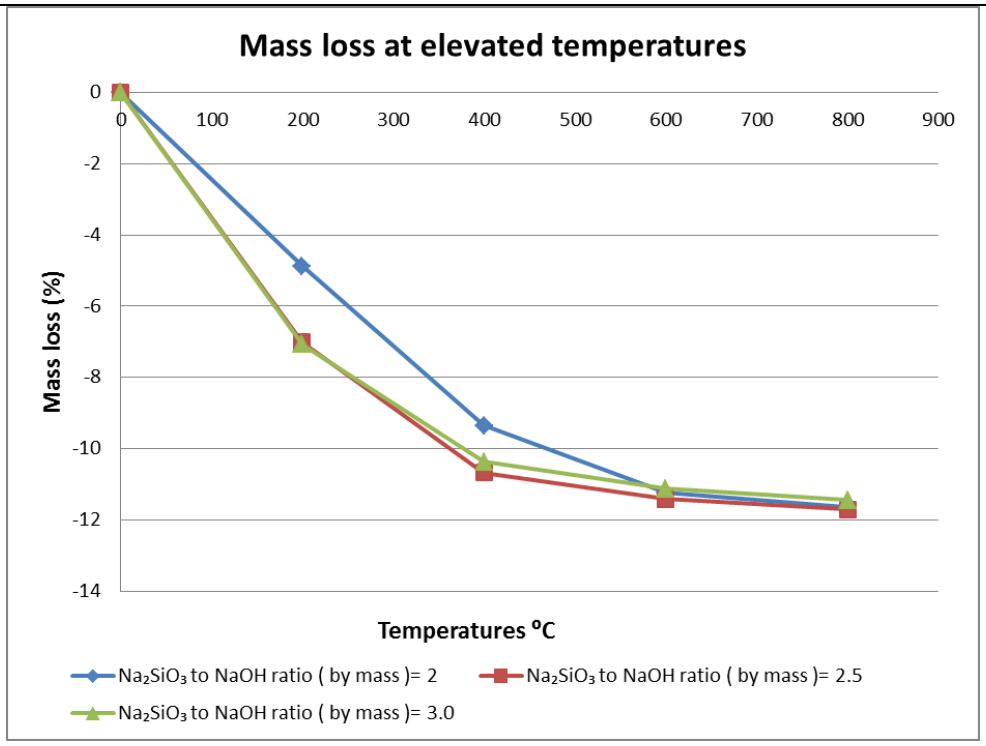


a)

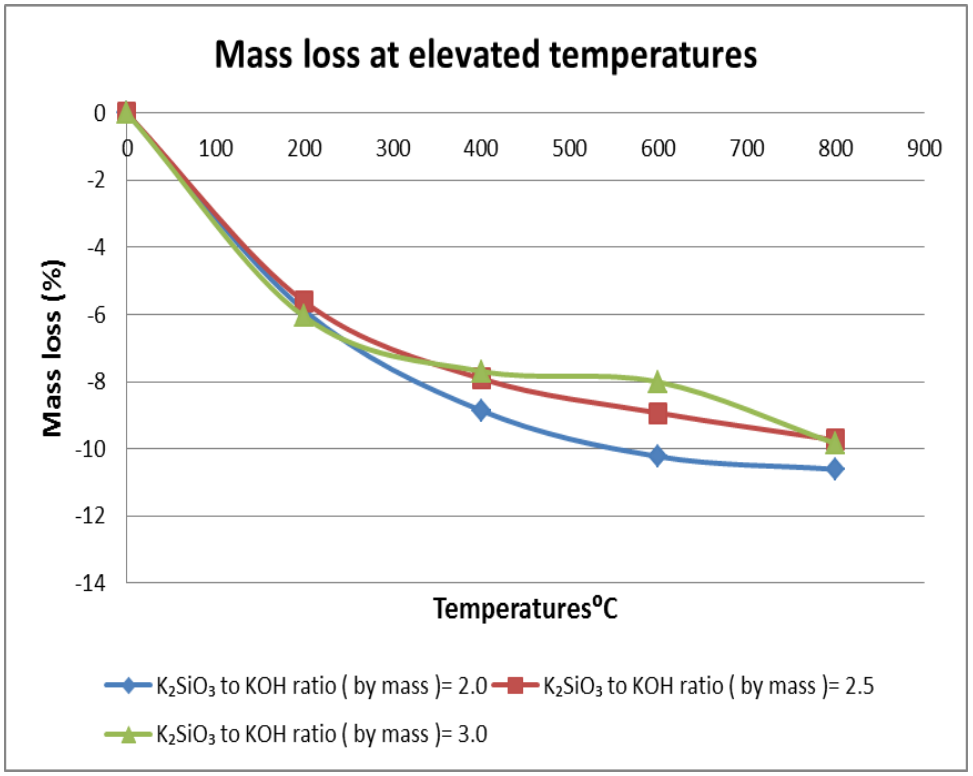


b)

**Figure 4. 7 (a-b): Comparison of mass loss of Na- and K-based geopolymer pastes at elevated temperatures.**

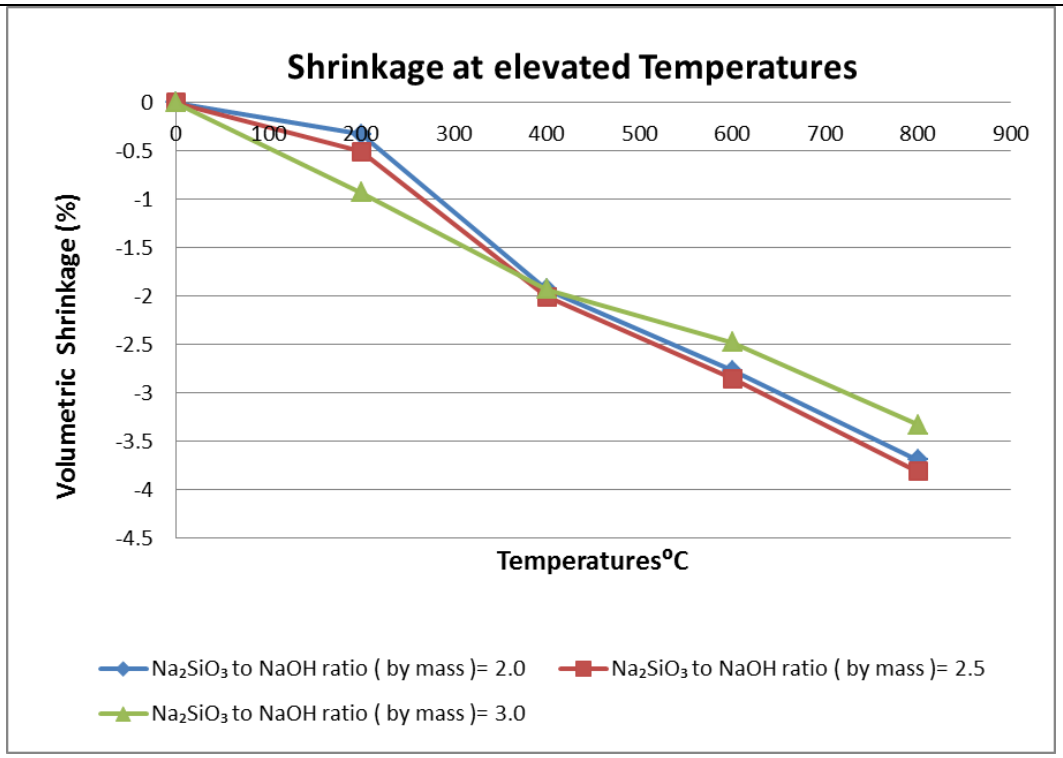


a)

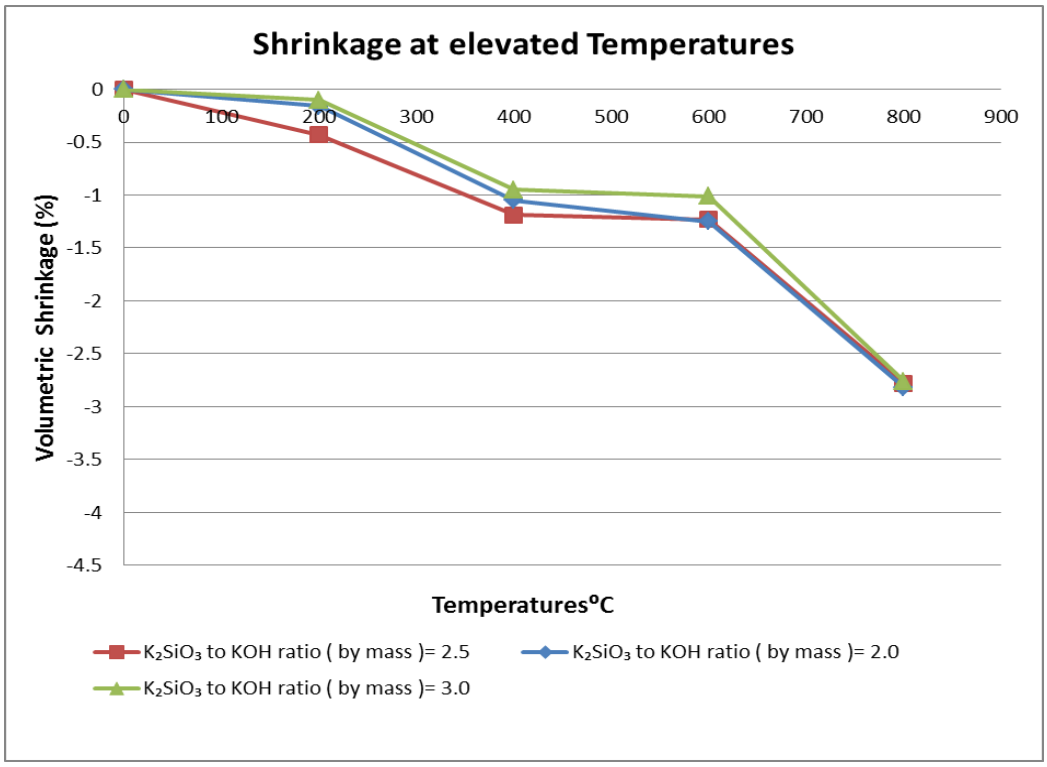


b)

**Figure 4. 8 (a-b): Comparison of volumetric shrinkage of Na- and K-based geopolymer pastes at elevated temperatures.**

It can be seen that the mass loss of Na-based geopolymer is slightly higher than that of K-based counterpart. An interesting observation is also noted that by increasing the $Na_2SiO_3$/NaOH ratios the mass loss is slightly increased, which is opposite in the K-based system. It can also be seen that up to 400$^oC$ significant reduction in mass loss of about 8-10% is observed in both geopolymers and the mass loss becomes stable afterword.

In the case of volumetric shrinkage of both geopolymers at elevated temperatures similar results to those of mass loss are also observed, where the K-based geopolymer showed lower shrinkage than its Na-based counterpart at all elevated temperatures. The observed less cracks in the K-based activator synthetized geopolymer is due to its lower mass loss and lower volumetric shrinkage than Na-based system. The higher residual compressive strength of K-based activator synthetized geopolymer than its counterpart Na-based system is also due the less cracking in the former than the latter, as pre-existing cracks cause stress concentration in the specimen under compression and hence failure at lower loads.

## 4.4. FURTHER DISCUSSION CONSIDERING XRD AND TGA/DTA RESULTS

Among three different ratios of silicate-to-hydroxide of both Na and K-based activators the ratio 3 exhibited the best in terms of highest residual compressive strengths after elevated temperatures exposure. Even among Na and K-based activators the K-based activator showed the best performance. In order to get more insight on the above difference in behaviour powder samples were collected from tested specimens at ambient condition, 400$^oC$ and 800$^oC$ for both activators for silicate-to-hydroxide ratio of 3. X-ray diffraction (XRD), thermogravimetric analysis (TGA) and differential thermal analysis (DTA) of above powder samples were conducted to identify the change in geopolymer reaction phases due to exposure to elevated temperatures for both activators.

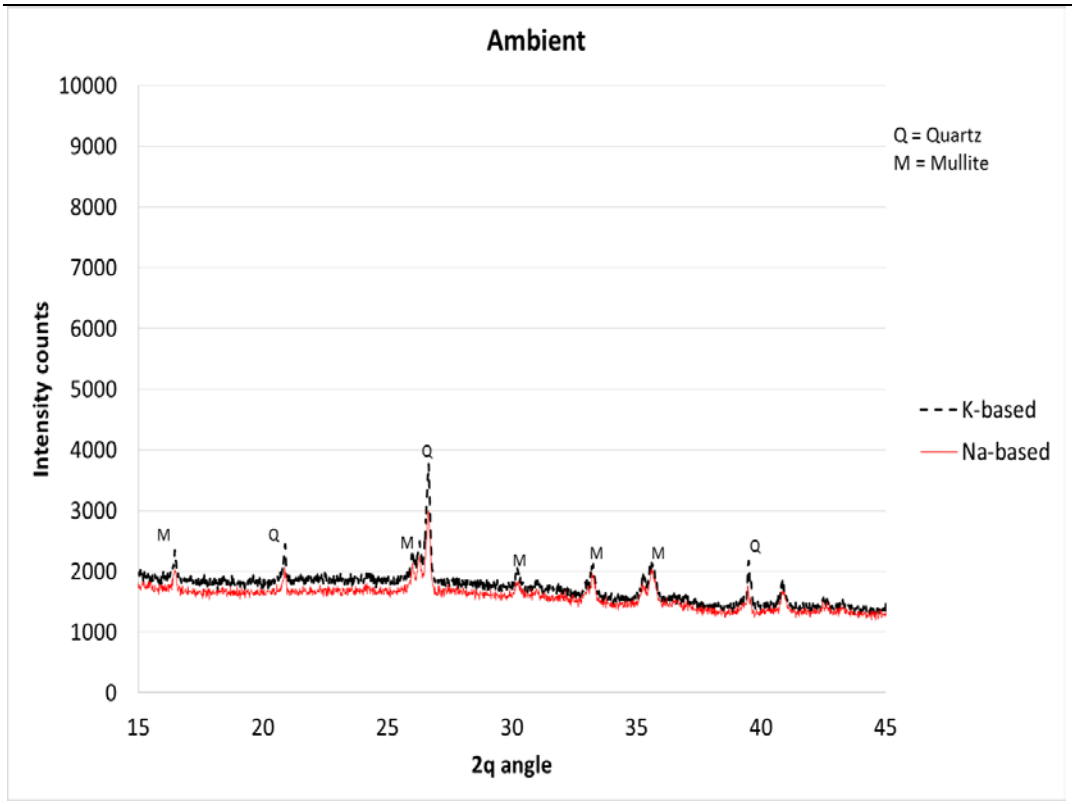
Ambient
Intensity counts
2q angle
Q = Quartz
M = Mullite
K-based
Na-based

(a)

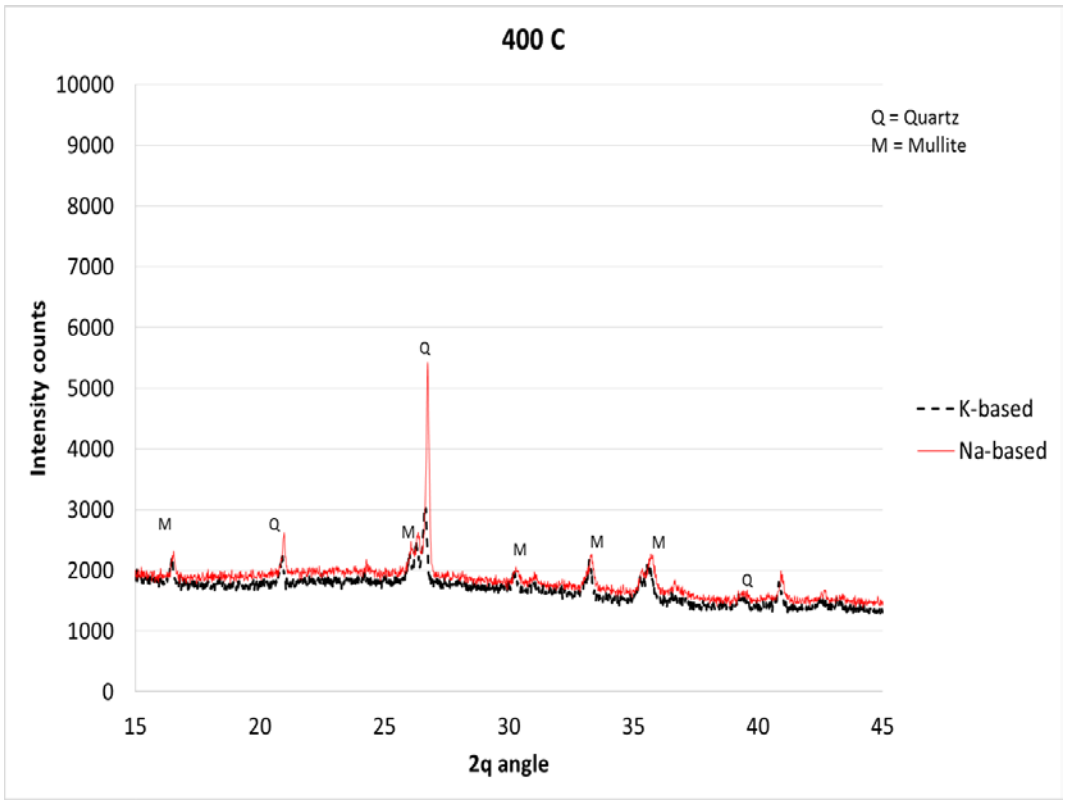
400 C
Intensity counts
2q angle
Q = Quartz
M = Mullite
K-based
Na-based

(b)

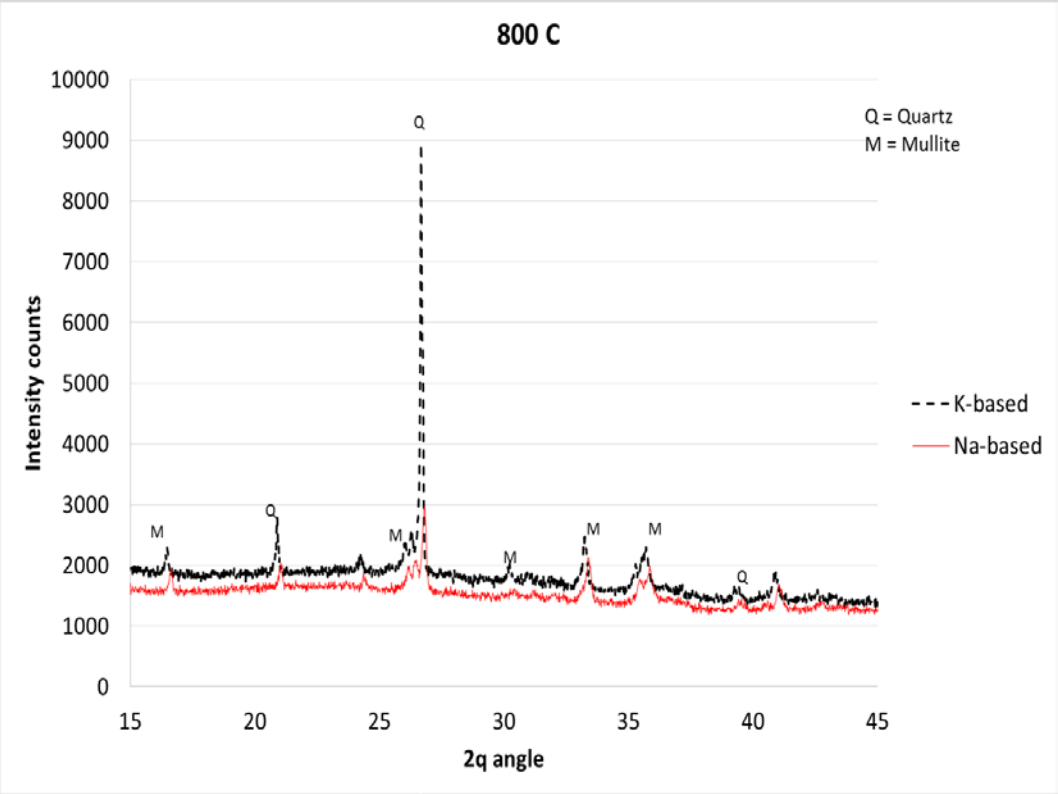


( c )

**Figure 4. 9 : XRD analysis results of Na- and K-based fly ash geopolymer at (a) ambient, (b) at 400°C and (c) at 800°C temperatures.**

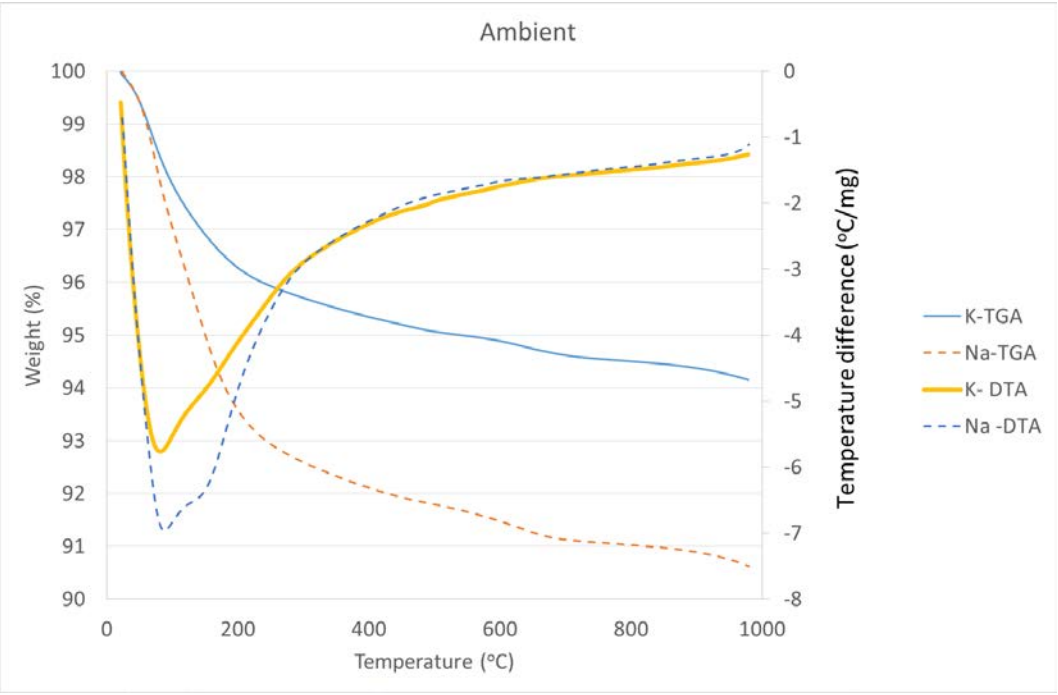


(a)

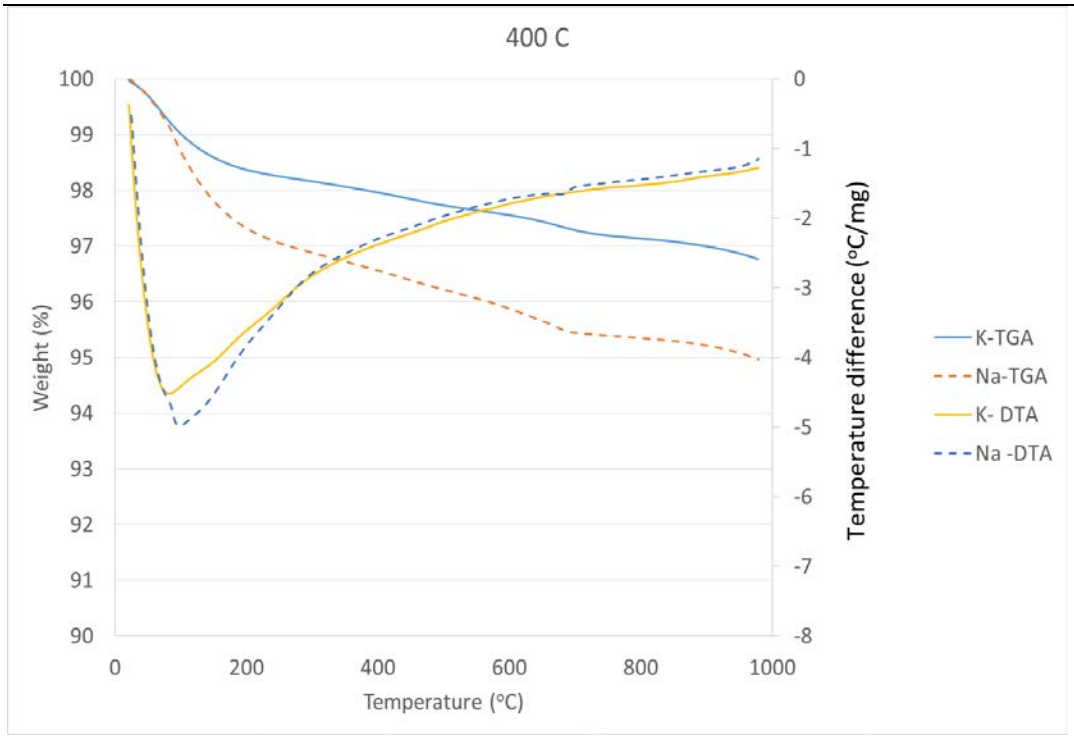


(b)

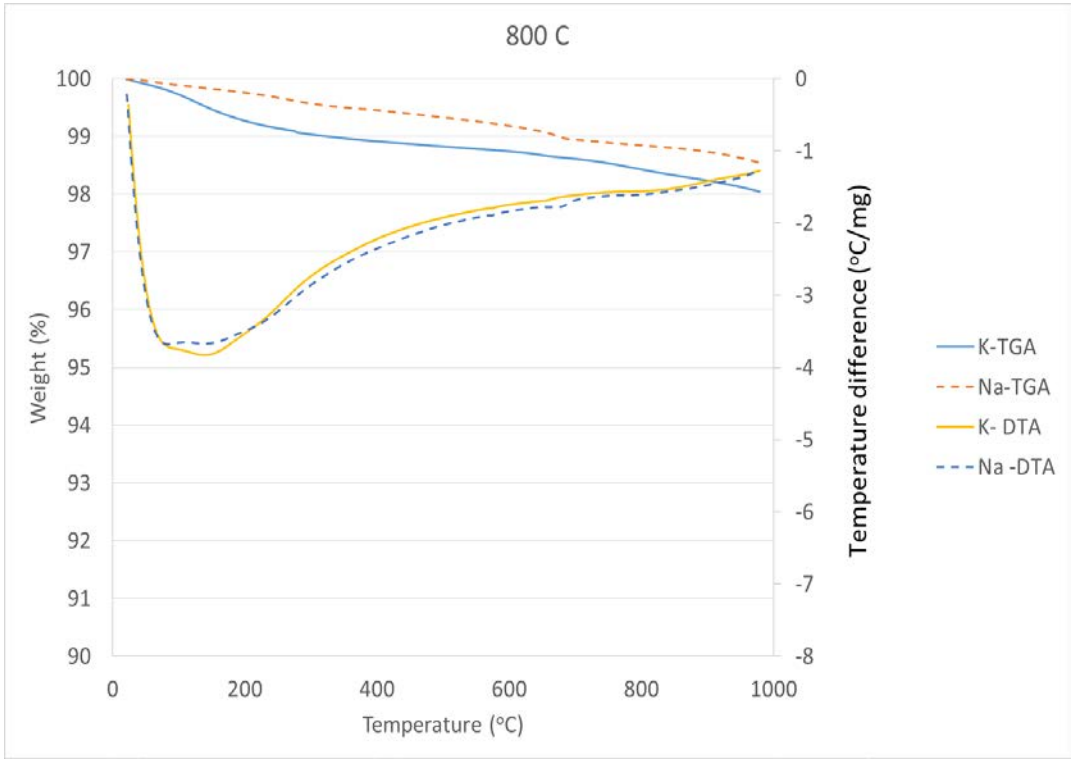


(c)

**Figure 4. 10 : TGA/DTA analysis results of Na- and K-based fly ash geopolymer at (a) ambient, (b) at 400ºC and (c) at 800ºC temperatures.**

Figures 4.9 a-c show the XRD patterns of both Na and K-based geopolymers at ambient and after exposure to 400ºC and 800ºC temperatures. The strong peaks in the fly ash geopolymers mainly identify the presence of quartz and mullite at ambient temperature. Mullite is the stable crystalline phase of the $Al_2O_3$-$SiO_2$ system under atmospheric condition and is a refractory. Mullite retains its room temperature strength at elevated temperatures and has high temperature stability up to 1840ºC (Rickard et. al., 2012) with low thermal expansion and oxidation resistance. In Both Na- and K-based fly ash geopolymers at room temperature several quartz peaks at 2ɵ angles of 20.83º, 26.65º and 39.51º and several mullite peaks at 2ɵ angles of 16.46º, 26.53º, 30.26º, 33.20º and 35.66º are observed (Figure 4.9a). However, in K-based geopolymer the quartz and mullite peaks are more prevalent than the Na-based system. Both geopolymers after exposure to 400ºC also show the presence of quartz and mullite peaks, with slightly stronger quartz and mullite peaks in Na-based geopolymer than the K-based geopolymer. After 800ºC an opposite trend is observed with stronger quartz and mullite peaks in K-based geopolymer than the Na-based geopolymer.

Thermogravimetric analysis (TGA) and differential thermal analysis (DTA) were used to assess the weight loss during controlled heating of both Na- and K-based fly ash geopolymers before and after exposure to elevated temperatures in order to identify the present of phases. Figures 4.10a-c show the TGA and DTA curves of both geopolymers at ambient condition and after heating to 400 and 800ºC temperatures. It can be seen in Figure 4.10a that the weight loss of Na-based fly ash geopolymer is much higher than its K-based counterpart. In DTA curves a peak is located at approximately 90ºC and is caused by loss of absorbed and combined water in the N-A-S-H gels (Rashad, 2011). It can also be seen that the DTA peak is greater for Na-based fly ash geopolymer than its K-based counterpart, meaning more geopolymerization has occurred with Na-based activator (Rashad, 2011). And this can be reflected by comparing the compressive strength values in Figures 4.3 and 4.5 at ambient temperature for both geopolymers. On the other hand, the weight loss in both geopolymer in TGA decreased after their exposure to 400ºC and 800ºC and the difference in weight loss between the Na- and K-based systems decreased gradually at 400ºC and 800ºC exposures. This is also reflected in the reduction in the difference

in peaks in DTA cures in both geopolymers at both 400 and 800°C temperatures. This lower weight loss in both geopolymers can be attributed to the loss of absorbed water in the geopolymer matrix due to heating at 400°C and the combined water in geopolymer gels at 800°C. No weight loss or DTA peak at approximately 450°C is observed which is usually for $Ca(OH)_2$. It is also interesting to note that the weight loss and the DTA peak at approximately 100°C is higher in Na-based geopolymer than its K-based counterpart at 400°C exposure. On the other hand, the K-based geopolymer showed slightly higher weight loss and DTA peak than Na-based geopolymer at 800°C. These results are consistence with XRD and compressive strength results, where the XRD peaks of quartz and mullite phases are higher in Na-based fly ash geopolymer than the K-based at 400°C compared to 800°C. The residual compressive strength of Na-based fly ash geopolymer is also higher than the K-based geopolymer at 400°C.

## 4.5. CONCLUSION

Sodium and potassium based activator geopolymer is analysed for elevated temperature exposure and volumetric shrinkage, mass loss, residual compressive strength were evaluated.

Though the geopolymer with sodium based activator showed higher compressive strength at ambient temperature but after heating beyond $600^0$ C the compressive strength of potassium based geopolymer was slightly higher than its sodium based counterpart. Mostly potassium based geopolymer behaves better and give higher strength than sodium based geopolymer at elevated temperature. Among all the activator proportion the potassium silicate to potassium hydroxide ratio of 3 proves better regarding residual compressive strength at $200^0$C, $400^0$C, $600^0$C $800^0$C compared to ambient temperature. The surface crack also supports this fact and less crack is found in the samples with potassium based activator. In the XRD analysis the existence of quartz and mullite peaks were found which might be responsible to maintain the residual compressive strength by both geopolymers at elevated temperature. The Na-based fly ash geopolymer exhibited higher weight loss in TGA and higher DTA peak at about 100°C than its K-based counterpart after exposure to 400°C. The higher weight loss and DTA peak is associated with the loss of absorbed and combined water in geopolymer gels, which indicate that higher geopolymer gels

are remained in Na based geopolymer after 400$^{o}$C exposure than K-based system, which agrees well with the observed compressive strength results. An opposite trend is observed after exposure to 800$^{o}$C.

The next chapter continues with the research of geopolymer with some addition of nano silica and fine sand with replacement of fly ash. Sodium hydroxide with sodium silicate and potassium hydroxide with potassium silicate were used as an activator in the next phase of the research.

# CHAPTER V

# BEHAVIOUR OF GEOPOLYMER CONTAINING NANO SILICA AND FINE SAND AT ELEVATED TEMPERATURE

## 5.1. INTRODUCTION

Environment friendly geopolymer is a new binder which gained increased popularity due to its better mechanical properties, durability, chemical resistance and fire resistance. This chapter presents the effect of nano silica (NS) and fine sand (FS) on residual compressive strength of sodium and potassium based activators synthesized fly ash geopolymer at elevated temperatures. Six different series of both sodium and potassium activators synthesized geopolymer were cast using replacement of fly ash with 1%, 2% and 4% NS and 5%, 10% and 20% FS. The samples were heated at 200$^{o}$C, 400$^{o}$C, 600$^{o}$C and 800$^{o}$C at a heating rate 5$^{o}$C per minute and the residual compressive strength, volumetric shrinkage, mass loss and cracking behaviour of each series of samples are also measured in this study.

## 5.2. EXPERIMENTAL PROGRAM

The experimental program is divided in to two parts. In both the parts the fly ash geopolymer paste is prepared with sodium and potassium based activators, with sodium silicate to sodium hydroxide and potassium silicate to potassium hydroxide ratios of 3 as it was found as the optimum content for fire resistant based on authors previous research (Hosan, 2016). Control geopolymers pastes synthetised by sodium and potassium based activators without any NS and FS are also cast. In the first part fly ash was replaced with 0%, 1%, 2% and 4% of nano silica (NS) and in the second part fly ash was replaced with 0%, 5%, 10% and 20% of fine sand (FS). A constant activator/fly ash ratio of 0.4 is considered in all the series in both parts.

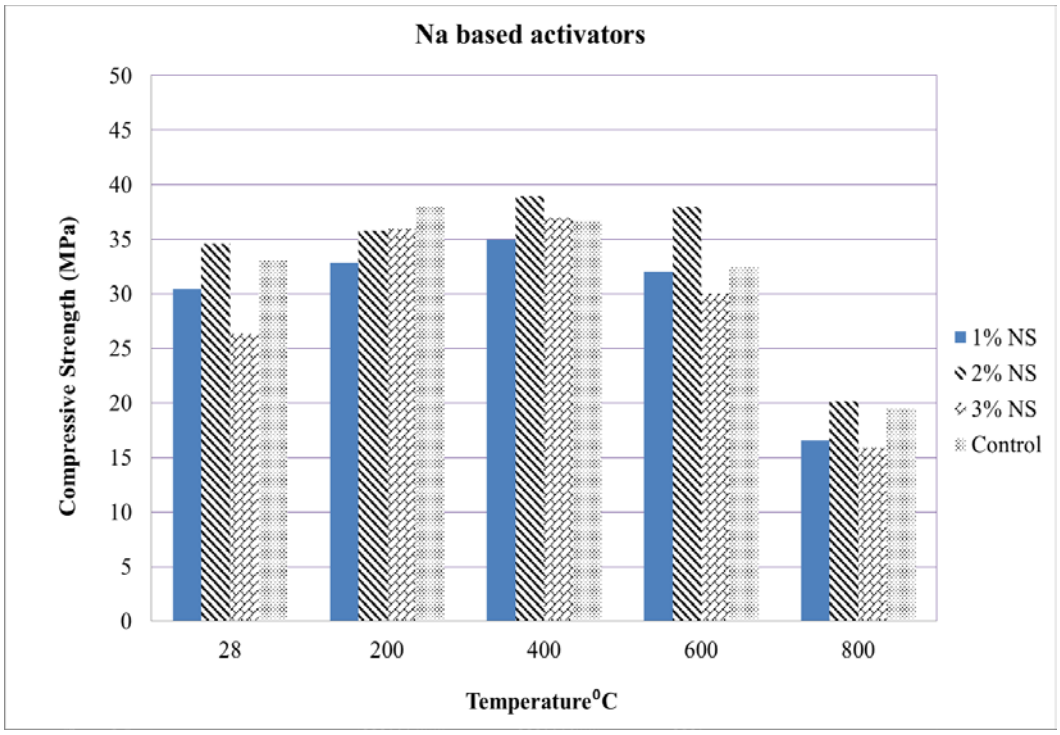


3(a)

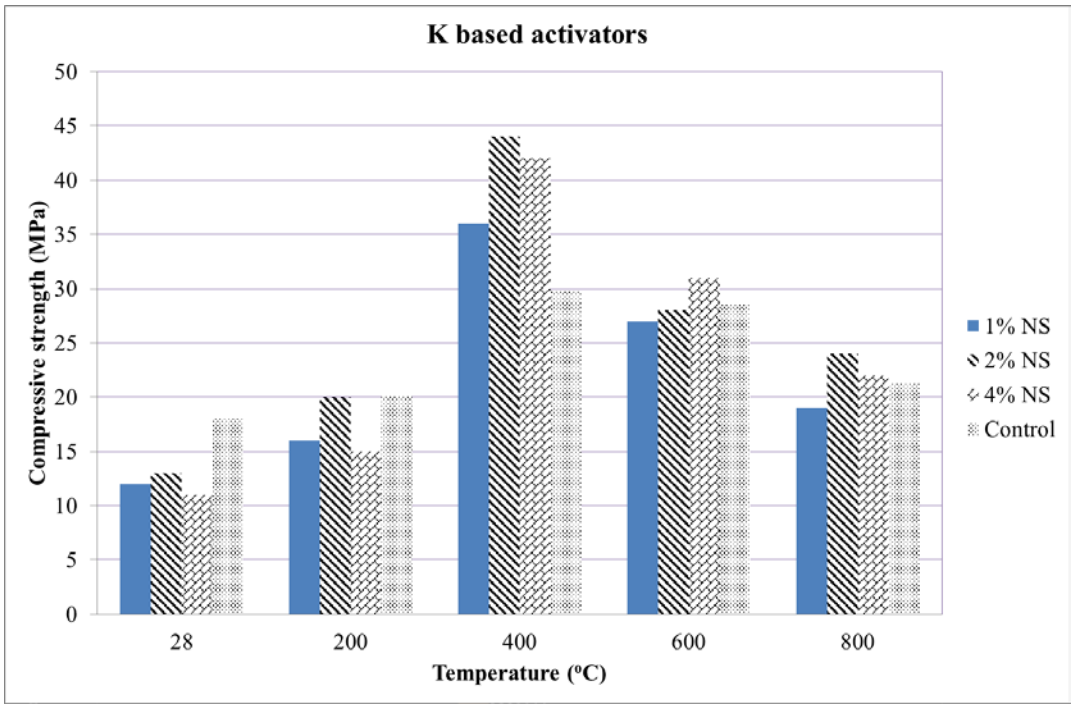


3(b)

**Figure 5. 1: Effects of various nano silica contents on the residual compressive strength of (a) sodium and (b) potassium activators synthetized geopolymer at various elevated temperatures**

For each NS and FS content for both sodium and potassium activators synthetised geopolymers, six 50mm cube specimens are cast and are heated at 200, 400, 600 and 800$^{o}$C temperatures. This 16 series of specimens are cast to test at ambient and above four elevated temperatures.

## 5.3. RESULTS AND DISCUSSION

### 5.3.1. Effect of nano silica on residual compressive strengths

The measured compressive strengths of sodium and potassium based activators synthetised geopolymer pastes containing different wt.% of nano silica as partial replacement of fly ash after exposed to 200, 400, 600 and 800$^{o}$C temperatures are shown in Figure 5.1. It can be seen in Figure 5.1a that the residual compressive strength of sodium activator synthetised geopolymer pastes containing all nano silica contents increases with increase in elevated temperature up to 600$^{o}$C, with a significant drop at 800$^{o}$C. It can also be seen that the sodium activator synthetised geopolymer containing 2% nano silica exhibited the highest residual compressive strength at all elevated temperatures among all nano silica contents.

The effect of different nano silica contents on the residual compressive strength of potassium based activators synthetised geopolymer pastes at various elevated temperatures is shown in Figure 5.1b.

Unlike sodium based series, significant improvement in residual compressive strength from 400$^{o}$C can be seen in potassium based series for all nano silica contents. The most significant improvement is observed at 400$^{o}$C where the residual compressive strength is increased from 13 MPa to 44 MPa about 330% increase at 2% nano silica content. Even at 800$^{o}$C, the improvement was about 180% at 2% nano silica content. It is also interesting to note that at ambient temperature the potassium based activator synthetised geopolymer exhibited much lower compressive strength then its sodium based counterpart. In a study reported by Fernandez-Jimenez et al. (2006) shows that the potassium based activators synthetised geopolymer exhibits lower crystallization speed of zeolites and slower development of prezeolitic gel due to larger size of K+ compared to its sodium based counterpart, which affects the formation of more porous gel in potassium based activators synthetised geopolymer than sodium based system

and hence affects the mechanical strength. The above can explain the observed lower compressive strength of potassium based series at ambient temperature than sodium based series.

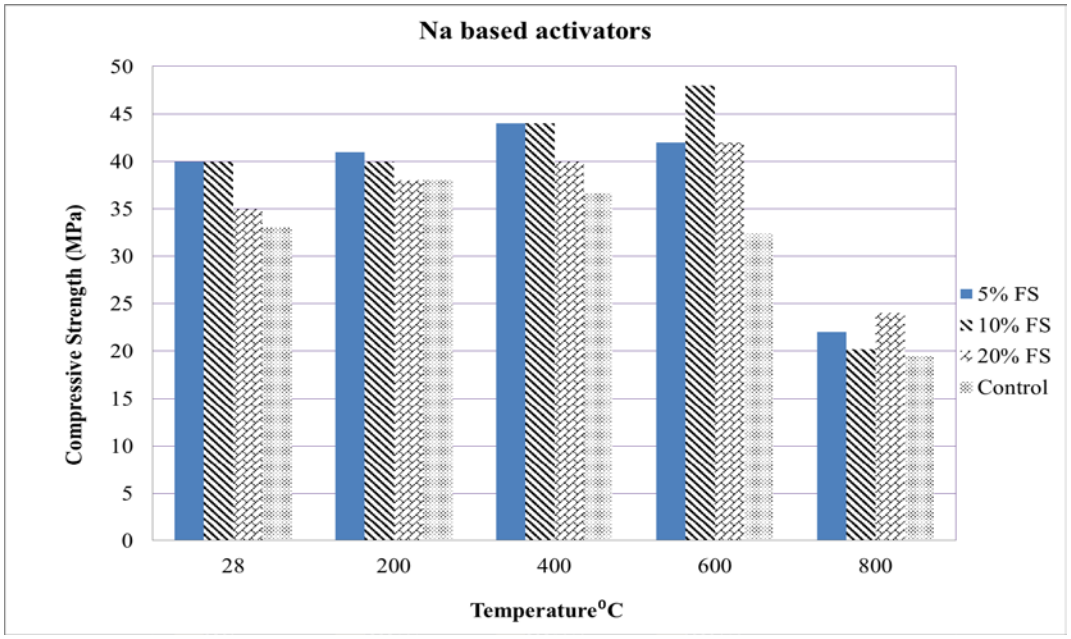


(a)

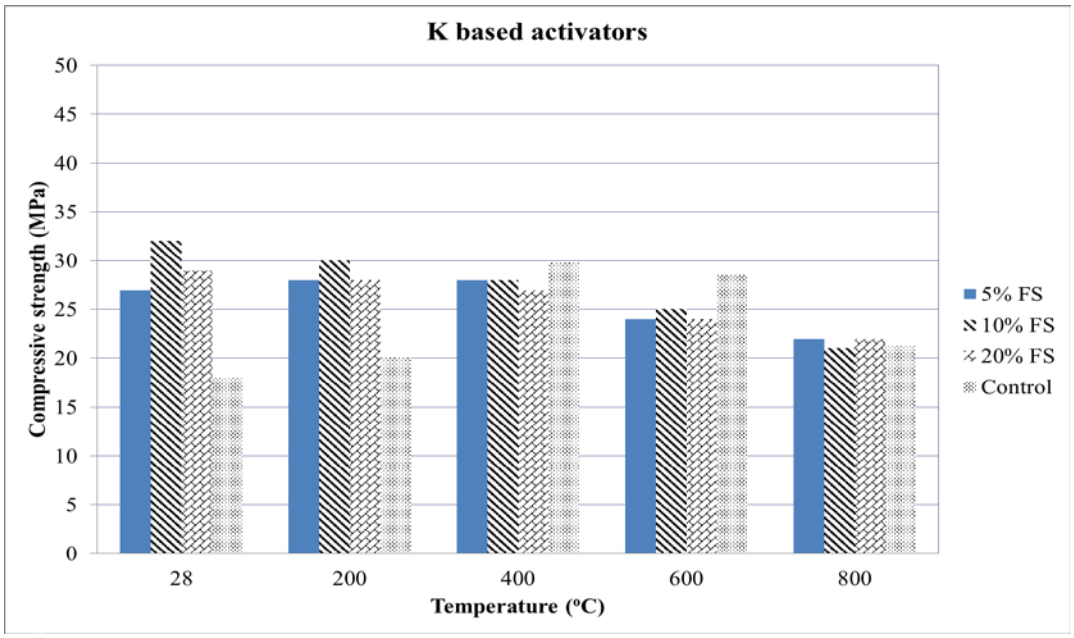


(b)

**Figure 5. 2 : Effects of various fine sand contents on the residual compressive strength of (a) sodium and (b) potassium activators synthetized geopolymer at various elevated temperatures**

### 5.3.2. Effect of fine sand on residual compressive strengths

The effect of fine sand on the residual compressive strengths of sodium and potassium activators synthetised fly ash geopolymer at various elevated temperatures is shown in Figure 5.2. It can be seen in Figure 5.2a that the residual compressive strengths of sodium activators synthetised geopolymer increased at elevated temperatures up to 600$^{o}$C followed by drop in compressive strength at 800$^{o}$C, similar to those observed in same geopolymer containing nano silica.

However, in the case of fine sand the residual compressive strengths of geopolymer containing fine sand is higher than those containing nano silica at all elevated temperatures.

It can also be seen that among three fine sand contents the 5 and 10% fine sand exhibited higher residual compressive strengths than 15% fine sand at all elevated temperatures. The effect of fine sand on the residual compressive strengths of potassium activators synthetised geopolymer at various elevated temperatures is shown in Figure 5.2b.

It can be seen, by comparing Figures 5.1b and 5.2b, that the residual compressive strength of potassium activators synthetised geopolymer containing fine sand is higher than those containing nano silica in elevated temperatures except at 400 and 600$^{o}$C. The reason is not clear, however, lower amount of Mullite and amorphous detected in potassium activators synthetised geopolymer containing 10% fine sand than that containing 2% nano silica in quantitive XRD analysis might be responsible for this which will be discussed in following section. It is also interesting to see that the addition of fine sand significantly increased the compressive strength of both sodium and potassium activator synthetised geopolymer at ambient temperature than those containing nano silica. One of the reason could be the contribution of fine sand as filler in the geopolymer matrix which reduced the volume of pores and improved the compressive strength.

### 5.3.3. Physical behaviour at elevated temperature

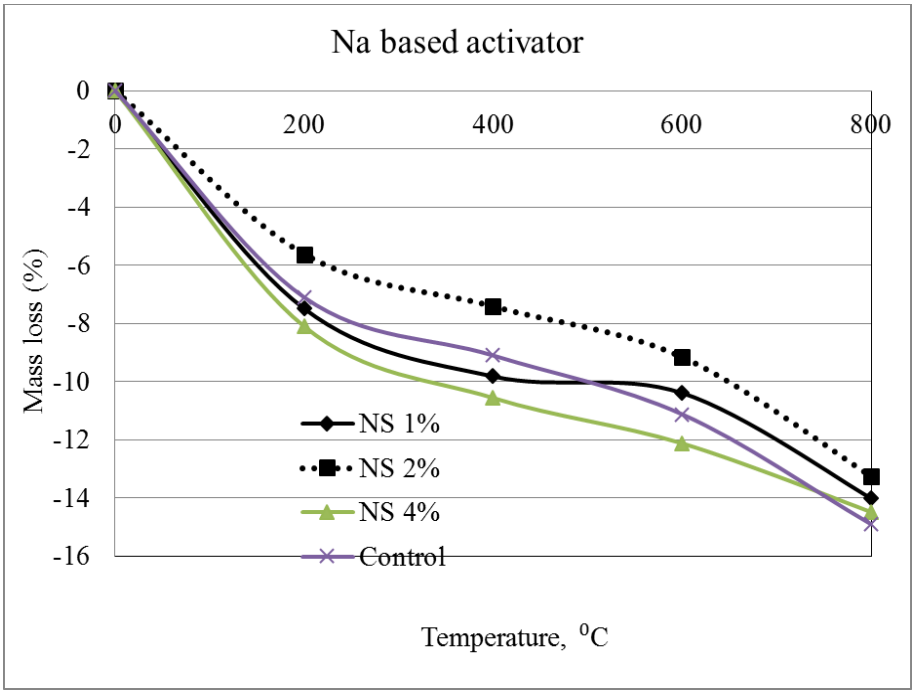


(a)

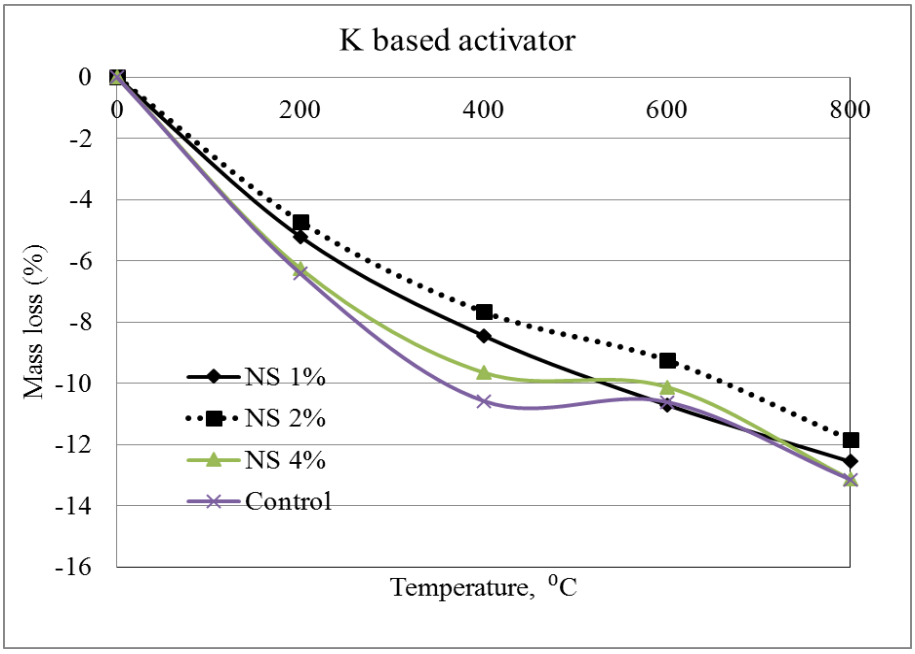


(b)

**Figure 5. 3: Effects of various nano silica contents on the mass loss of sodium and potassium activators synthetized geopolymer at various elevated temperatures.**

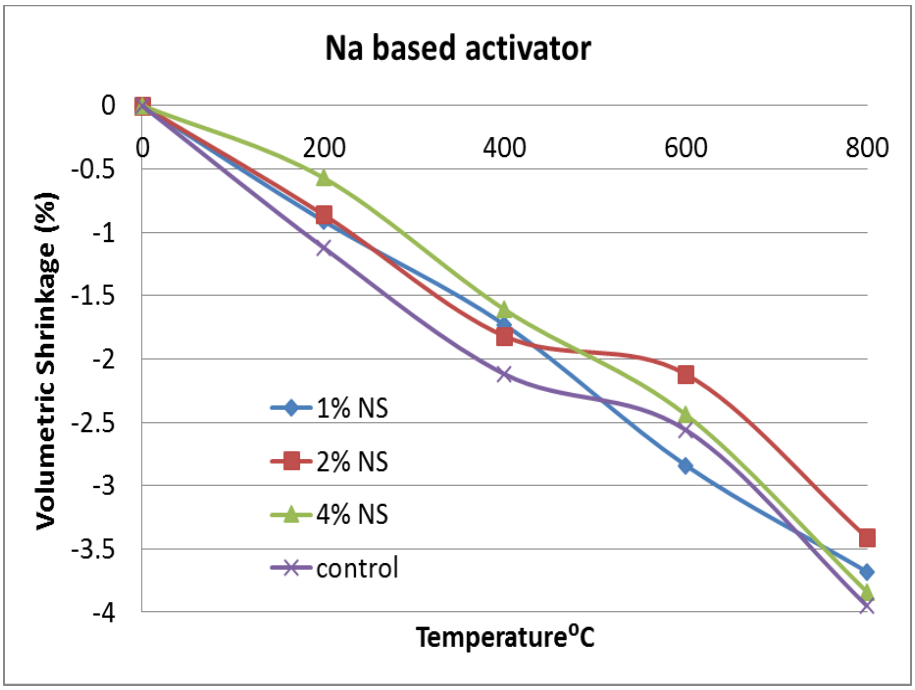


(a)

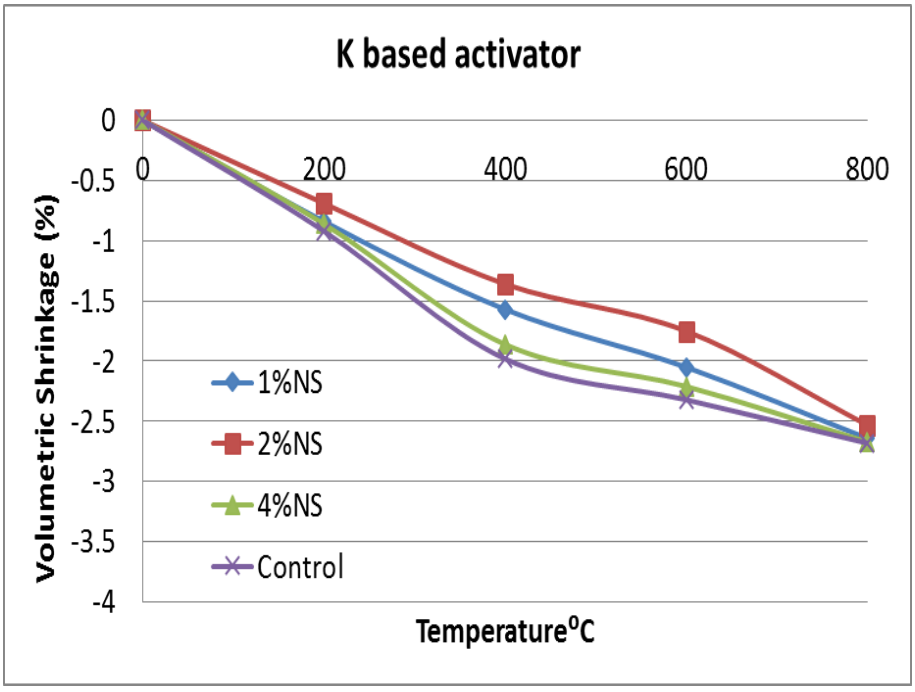


(b)

**Figure 5. 4 (a,b): Effects of various nano silica contents on the volumetric shrinkage of sodium and potassium activators synthetized geopolymer at various elevated temperatures**

The effects of nano silica and fine sand on mass loss and volumetric shrinkage of both sodium and potassium activator synthetised geopolymer are shown in Figures 5.3-5.6. It can be seen that the series with 2% nano silica shows lowest mass loss at all elevated temperatures among all series in both sodium and potassium activators synthetised geopolymers (see Figure 5.3 a,b). This series also shows better result in volumetric shrinkage than the other series in both activators cases (see Figure 5.4 a,b).

It is also interesting to note that the potassium activator synthetised geopolymer paste containing 2% nano silica exhibited the lower mass loss and volumetric shrinkage than its sodium based counterpart, which is also consistent with the measured residual compressive strength values. Similar results are also observed in Figures 5.5-5.6 in the case of sodium and potassium activator synthetised geopolymers containing fine sand, where the potassium based series showed lower mass loss and volumetric shrinkage than its sodium based counterpart and the 10% find sand content exhibited better behaviour than other fine sand contents in terms of lowest mass loss and volumetric shrinkage, which is also consistent with measured residual compressive strength values. It is also interesting to note that no significant change is observed in both mass loss and volumetric shrinkage in both geopolymers due to addition of nano silica and fine sand.

The effects of nano silica and fine sand on cracking and colour changes of both sodium and potassium activator synthetised geopolymer are shown in Figures 5.7-5.8. All the samples show little or almost no change in colour and no cracks are visible in the samples exposed to 200$^{o}$C. However, hairline cracks are appeared at 400$^{0}$C and their numbers and widths increased with increase in elevated temperatures up to 800$^{0}$C. In terms of cracking no significant difference can be seen between the sodium and potassium series irrespective of nano silica and fine sand. However, sodium based series showed higher number of cracks and more wide cracks than those observed in potassium based series. This can be attributed to the lower shrinkage of potassium synthetised geopolymer than its sodium based counterpart in the dilatometry test shown in Figure 5.9.

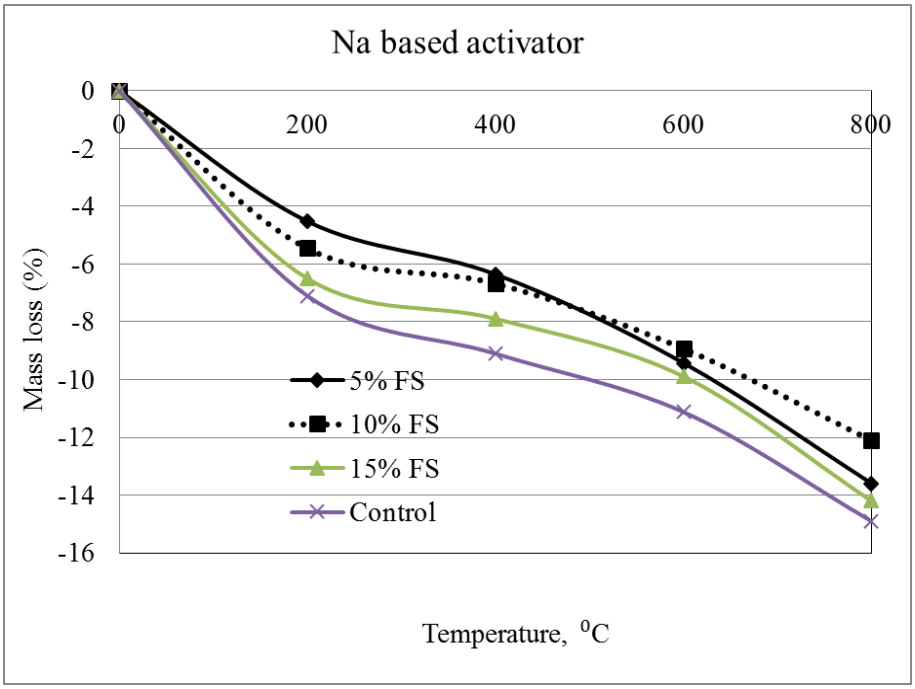


(a)

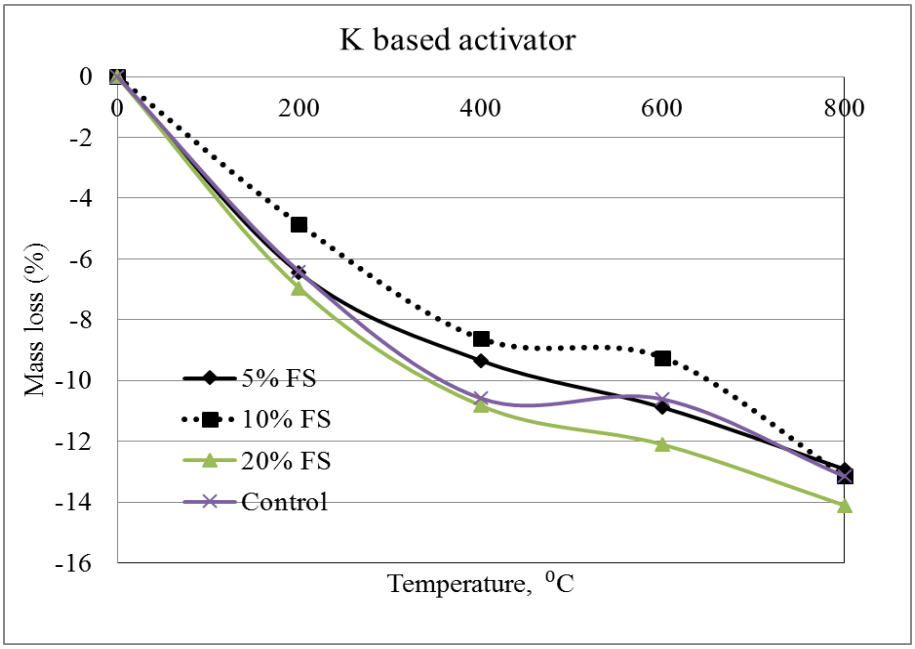


(b)

**Figure 5. 5: Effects of various fine sand contents on the mass loss of sodium and potassium activators synthetized geopolymer at various elevated temperatures**

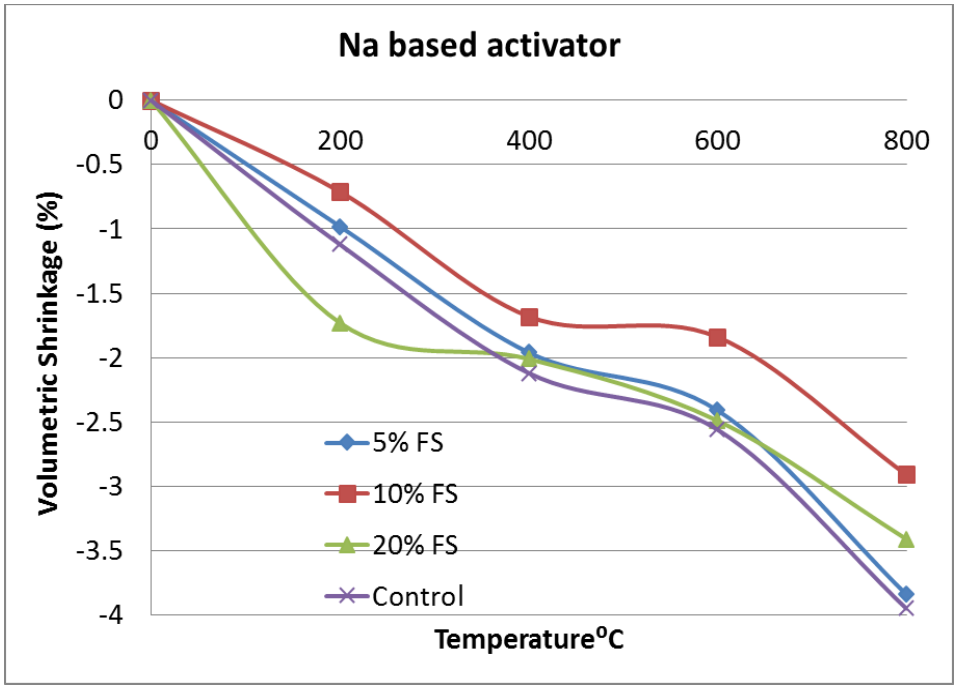


(a)

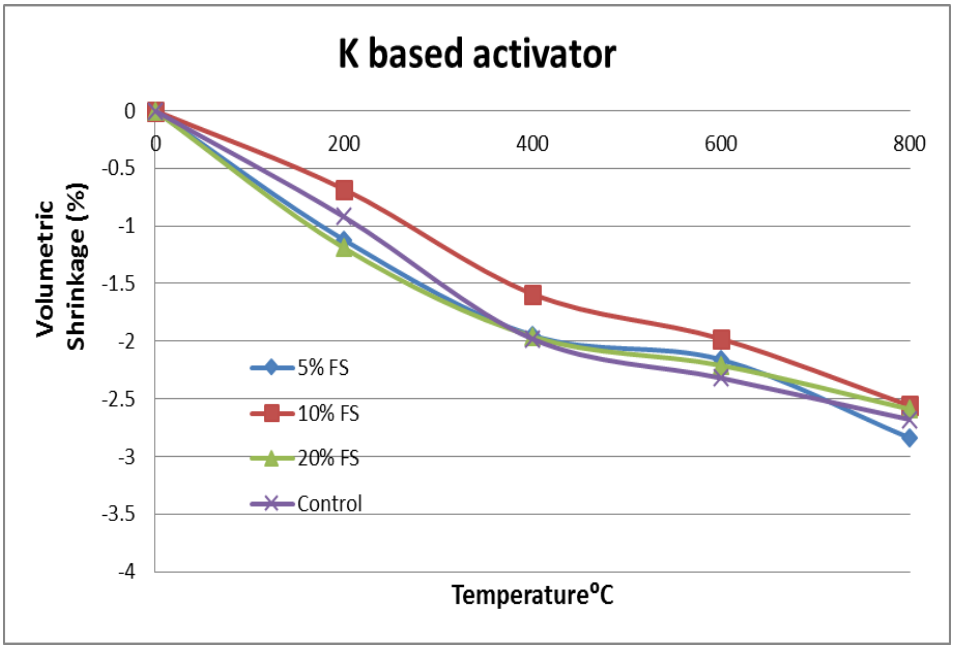


(b)

**Figure 5. 6: Effects of various fine sand contents on the volumetric shrinkage of sodium and potassium activators synthetized geopolymer at various elevated temperatures**

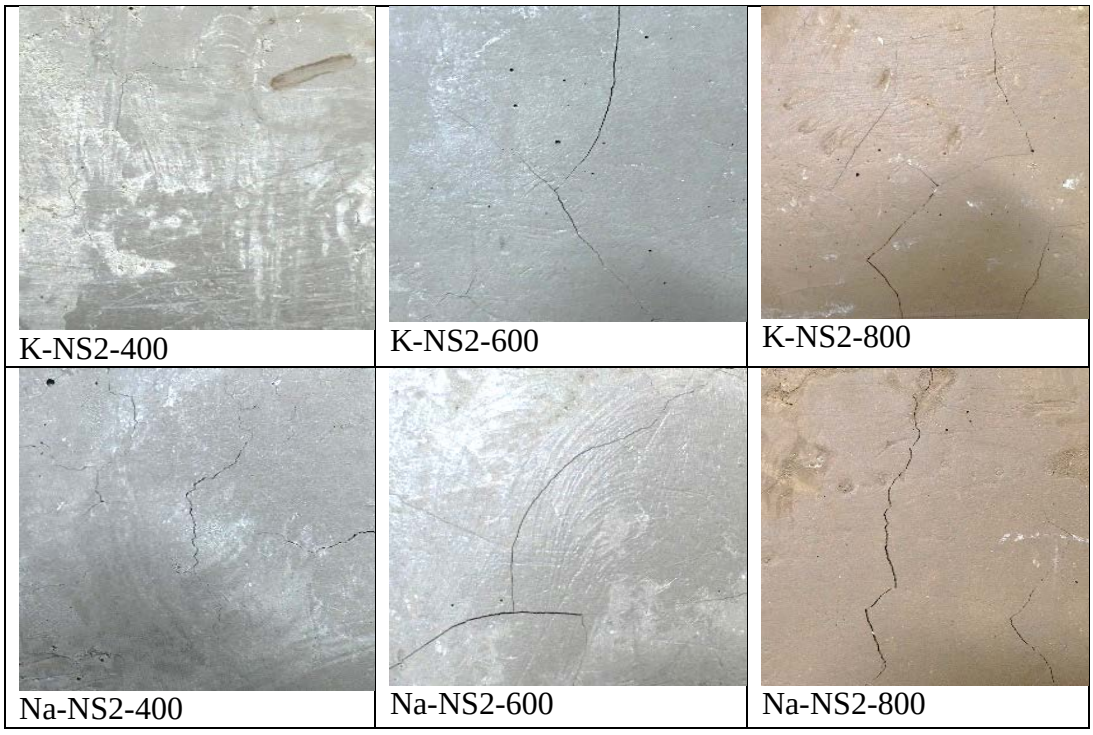


**Figure 5. 7 : Cracking pattern of sodium and potassium synthetized fly ash geopolymers containing 2% nano silica at different elevated temperatures.**


**Figure 5. 8: Cracking pattern of sodium and potassium synthetized fly ash geopolymers containing 10% fine sand at different elevated temperatures.**

### 5.3.4. Discussion considering XRD and QXRD results

The above physical behaviour and the compressive strength of sodium and potassium activators synthetised geopolymer containing nano silica and fine sand showed that the nano silica content of 2% and fine sand content of 10% performed better at various elevated temperatures than others.

In order to have better understanding in to the observed physical behaviour and compressive strength after exposure to elevated temperatures of above geopolymers, XRD and quantitative XRD analysis is performed to identify the changes of various geopolymer phases at ambient (28$^{o}$C), 400$^{o}$C and 800$^{o}$C and their results are summarised in Table 5.1 and shown in Figure 5.10. By looking in to Table 5.1 one distinct difference can be seen between geopolymer containing fine sand and nano silica. In the case of geopolymers containing fine sand significant increase in Quartz, and reduction in Amorphous and Mullite phases are observed compared to its counterpart geopolymers containing nano silica at same elevated temperatures. Generally amorphous phase contributes to the mechanical strength of geopolymer. And the observed lower compressive strength of potassium activator synthetised geopolymer containing fine sand than that containing nano silica can be attributed to this lower amorphous geopolymer gel. However, it was not the case in sodium series where slightly higher compressive strength in fine sand series than nano silica series was observed despite slightly lower amorphous geopolymer gel content in fine sand series.

It is also interesting to see in Table 5.1 that the potassium series containing nano silica shows slightly higher Mullite than sodium series and the observed higher compressive strength of potassium series at 400 and 800$^{o}$C than those of sodium series can be attributed to the higher Mullite as they are high temperature phases which contribute strength gain at elevated temperatures. It can be recalled as presented in previous section that both sodium and potassium activators synthetised geopolymers containing 2% nano silica and 10% fine sand exhibited higher compressive strength than those control geopolymers.

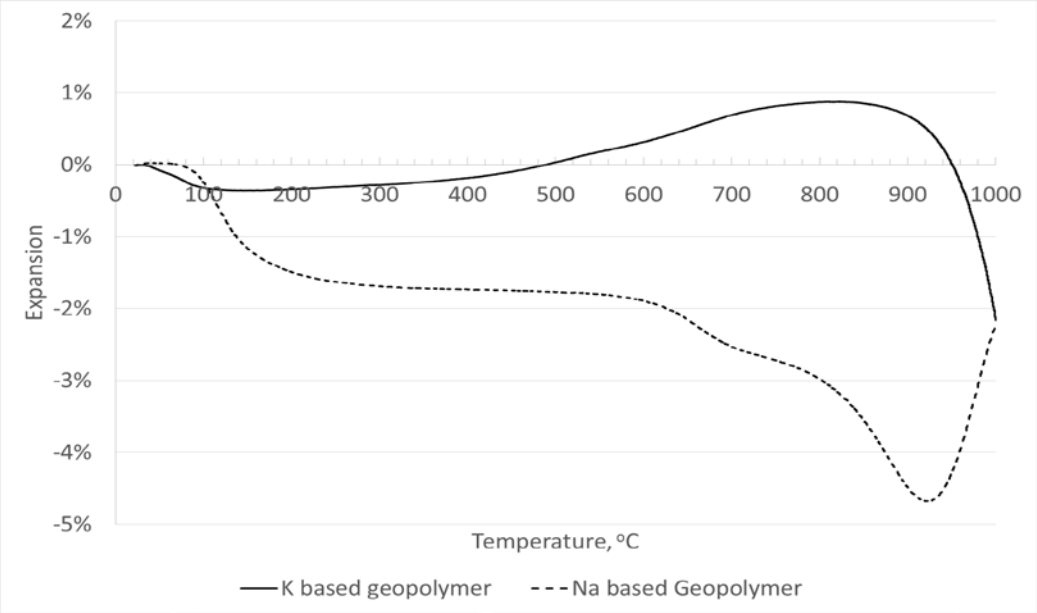


**Figure 5. 9 : Linear expansion and contraction of Na and K based geopolymer at various elevated temperatures in Dilatometer test**

The observed additional Mullite peaks in XRD patterns between 2theta angle of 35$^{o}$ and 45$^{o}$ in both geopolymers containing nano silica and fine sand shown in Figure 5.10 can be the reason for higher strength at elevated temperatures.

**Table 5. 1 : Phase abundance analysis of sodium and potassium activators synthetised geopolymer containing 2% nano silica and 10% fine sand**

| Series | Phase abundance (wt.%) | | | | |
|---|---|---|---|---|---|
| | Crystalline phases | | | | Amorphous phase |
| | Quartz (ICSD647436) | Mullite (ICSD152978) | Maghemite (ICSD79196) | Hematite (ICSD22505) | |
| Na-NS2-28 | 3.55 | 9.88 | 1.90 | 1.03 | 83.63 |
| Na-NS2-400 | 3.59 | 9.82 | 1.69 | 1.00 | 83.91 |
| Na-NS2-800 | 3.51 | 8.74 | 1.19 | 2.58 | 83.99 |
| K-NS2-28 | 3.18 | 10.27 | 1.52 | 1.26 | 83.77 |
| K-NS2-400 | 3.61 | 10.56 | 1.61 | 1.16 | 83.06 |
| K-NS2-800 | 3.34 | 8.97 | 1.92 | 2.51 | 83.26 |
| Na-FS10-400 | 11.75 | 8.42 | 1.40 | 1.18 | 77.25 |
| K-FS10-400 | 10.79 | 8.45 | 1.68 | 1.48 | 77.61 |

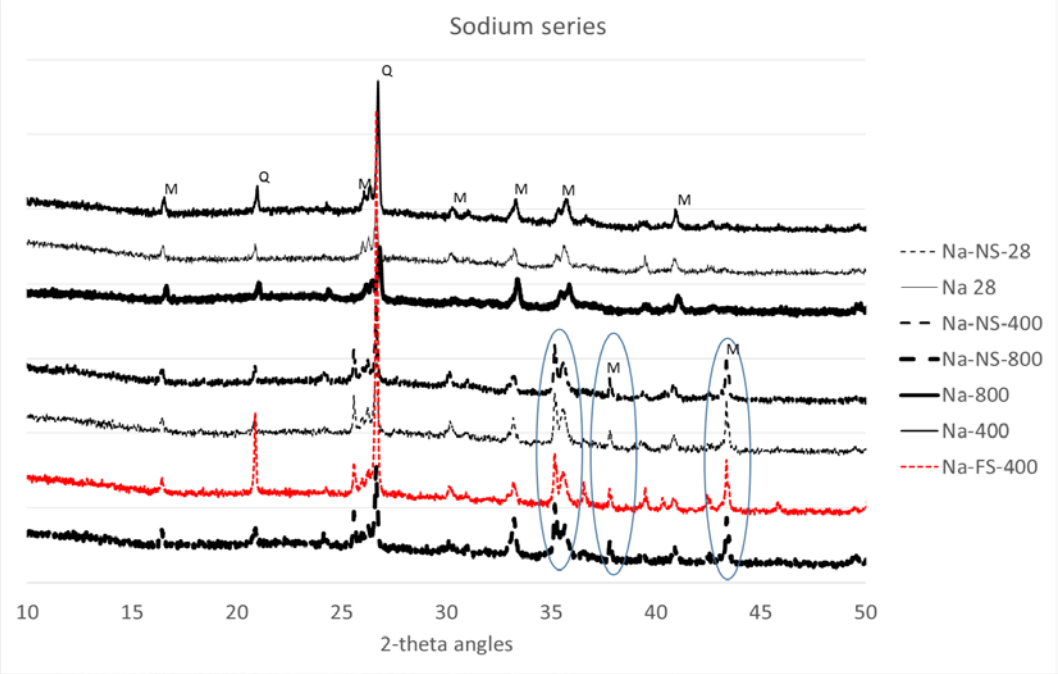


(a)

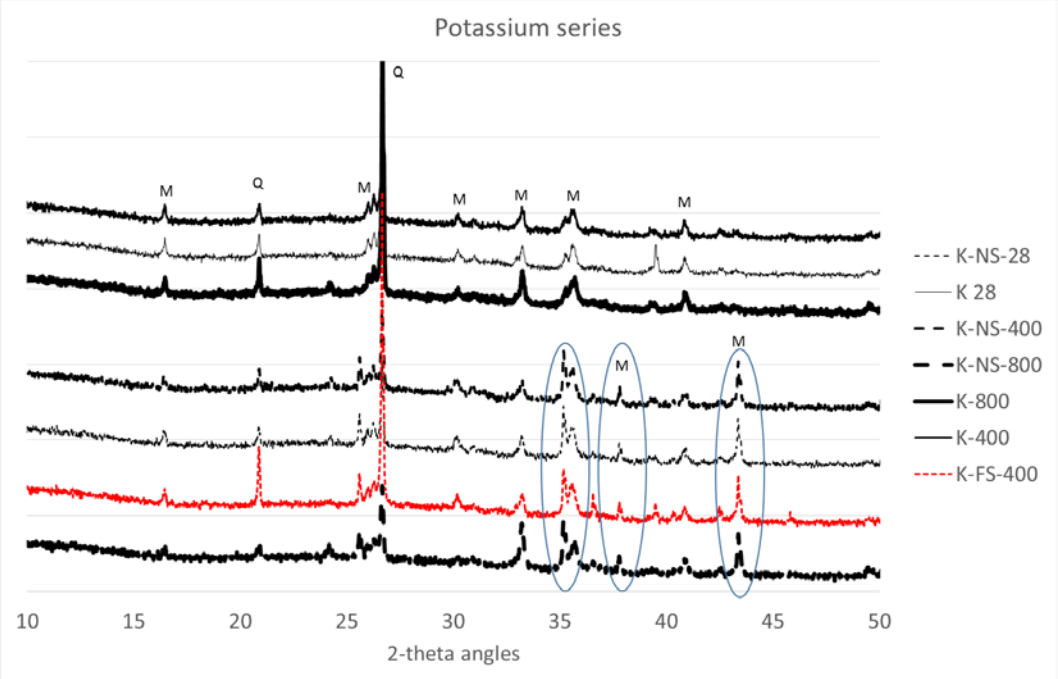


(b)

**Figure 5. 10 : XRD patterns of sodium and potassium based activators synthetized geopolymer containing 2% nano silica and 10% fine sand at ambient, 400oC and 800oC temperatures. [Note: Q=quartz and M=Mullite]**

## 5.4. CONCLUSION

This chapter illustrates the influence of nano silica and fine sand with fly ash based geopolymer at ambient and at elevated temperature. The fly ash geopolymer was activated by sodium and potassium based activator. The geopolymer samples was heated at $200^0$C, $400^0$C, $600^0$C and $800^0$C and tested for compressive strength, mass loss, XRD, dimension shrinkage and other parameters. So two different geopolymer with two different activator with five different temperature is studied and analysed in this chapter.

Among these series geopolymers containing 2% nano silica and 10% fine sand showed the lowest mass loss and lowest volumetric shrinkage at all elevated temperatures similar to those of residual compressive strengths.

Additionally nano silica improved the residual compressive strength of both sodium and potassium activators synthetized geopolymers at elevated temperatures. The potassium activator synthetized geopolymers containing nano silica exhibited higher residual compressive strength al elevated temperatures above $400^o$C than its sodium based counterparts.

No significant improvement in residual compressive strength of potassium activator synthetized geopolymer is observed at elevated temperatures due to addition of fine sand.

In the next chapter a different series of geopolymer with potassium silicate and potassium hydroxide as activator is used and basalt fibre and carbon fibre are used by 1%, 2%, and 4% for each fibre content in replacement of fly ash. The behaviour of this geopolymer matrix is analysed and described in the next chapter.

# CHAPTER VI

# BEHAVIOR OF CARBON AND BASALT FIBRE REINFORCED GEOPOLYMER AT ELEVATED TEMPERATURE

## 6.1. INTRODUCTION

This chapter presents the behaviour of potassium activators synthetized fly ash geopolymer containing carbon and basalt fibre at ambient and elevated temperature. The study is consisted of two parts. In the first part, the class F fly ash geopolymer is synthetized using potassium silicate and potassium hydroxide and the resulting matrix is reinforced with different wt.% of basalt fibre at 0.5%, 1% and 1.5% and in the second part the basalt fibre is replaced with carbon fibre without changing the fly ash, potassium silicate and potassium hydroxide ratios. As carbon and basalt fibre have a very high heat endurance capacity so this two fibres are used in this research. In both phases the fly ash based geopolymer was prepared with potassium based activators, with potassium silicate to potassium hydroxide ratios of 3 as it was found as the optimum content for fire resistant based on previous chapter. Control geopolymer paste synthetized by potassium based activators without any fibers was also cast as control. A constant activator/fly ash ratio of 0.35 was considered in all the series in both parts. For each series fibre reinforced geopolymers, six 50mm cube specimens were casted and heated at 200, 400, 600 and 800$^{o}$C temperatures. Results and discussions are discussed in the following part of this chapter.

## 6.2. PHYSICAL BEHAVIOUR OF FIBRE ADDED GEOPOLYMER

Figure 6.1 (a-b) show the effect of various wt.% of basalt and carbon fibres on the volume stability and mass loss of fly ash geopolymer at various elevated temperatures up to 800$^{o}$C. It can be seen in Figs. 6.1 and 6.2 that the geopolymer containing carbon fibres performed better in terms of measured volumetric shrinkage and mass loss at all elevated temperatures than those containing basalt fibres. Among three different contents of fibres, 1 wt.% of both carbon and basalt fibres is found to be the optimum

fibre content in terms of lowest mass loss and volumetric shrinkage at all elevated temperatures.

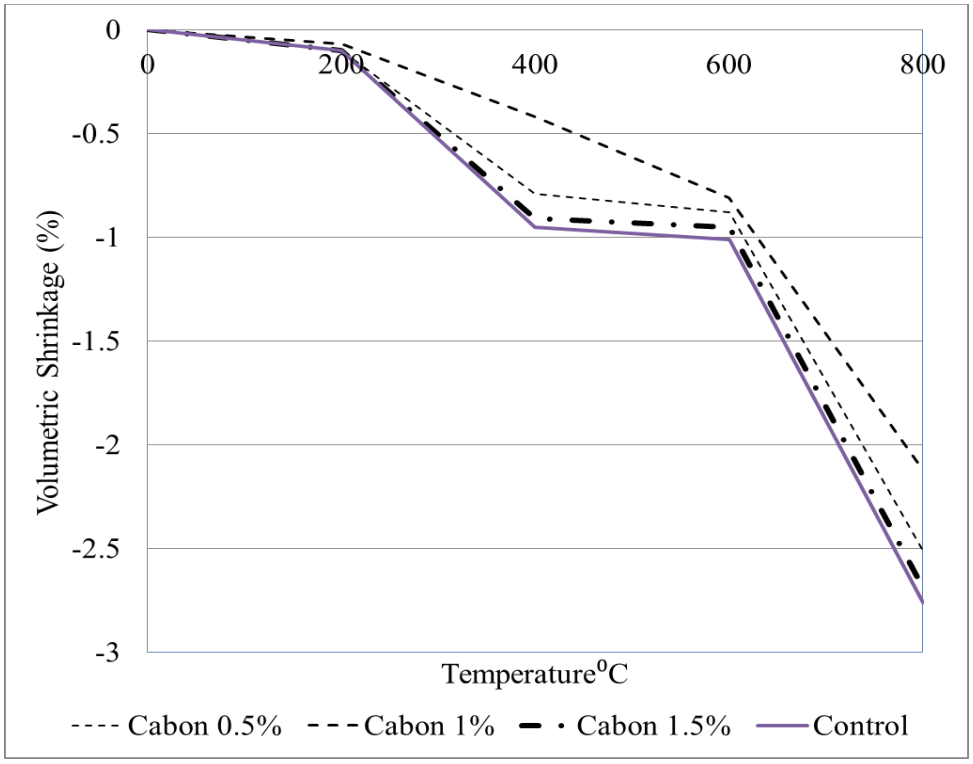


(a) Carbon fibre reinforced fly ash geopolymer composite

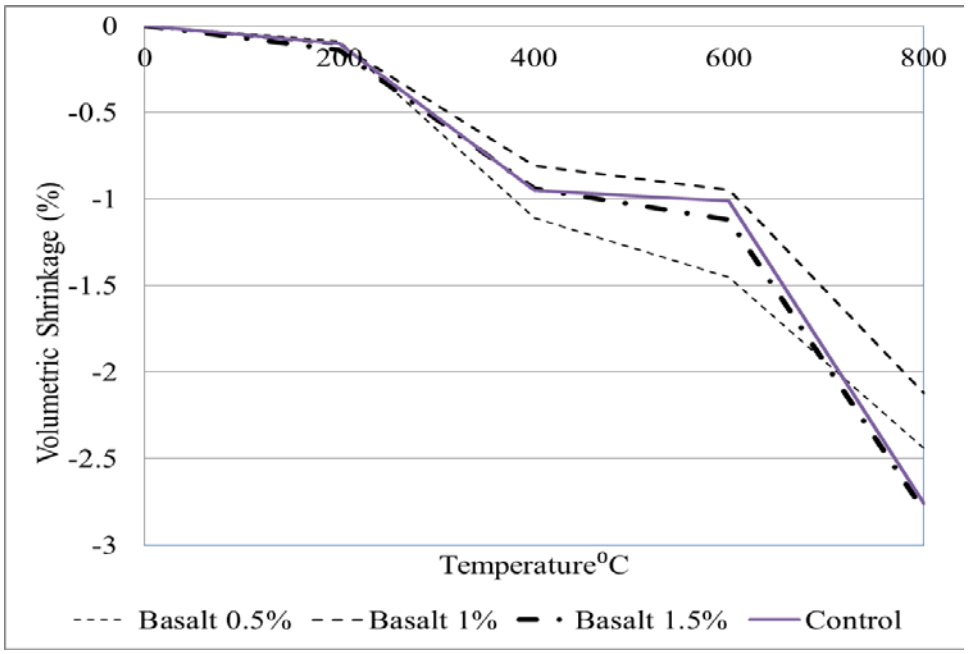


(b) Basalt fibre reinforced fly ash geopolymer composite

**Figure 6. 1: Volumetric shrinkage of carbon and basalt fibre reinforced fly ash geopolymer composites at various elevated temperatures.**

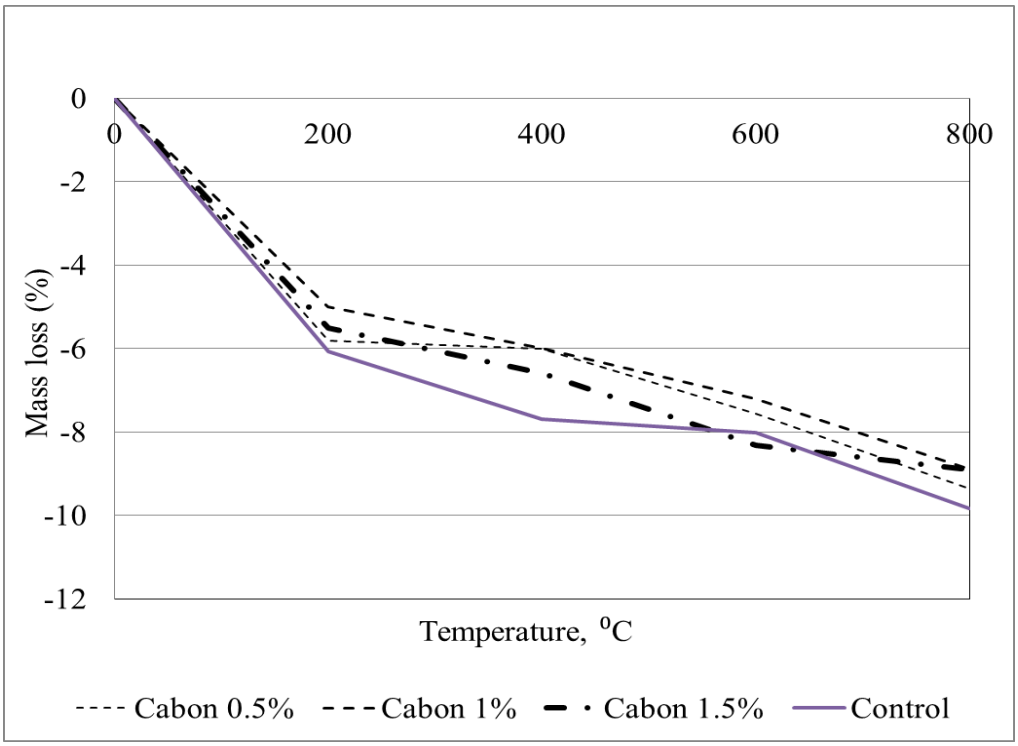


(a) Carbon fibre reinforced fly ash geopolymer composite

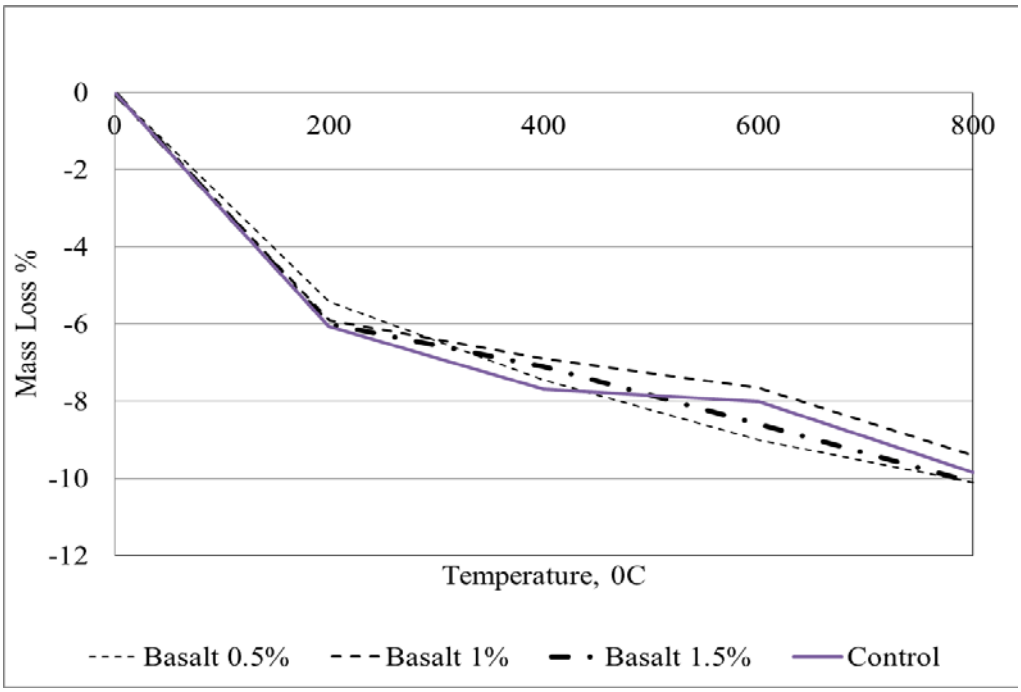


(b) Basalt fibre reinforced fly ash geopolymer composite

**Figure 6. 2 (a-b) : Mass loss of carbon and basalt fibre reinforced fly ash geopolymer composites at various elevated temperatures.**

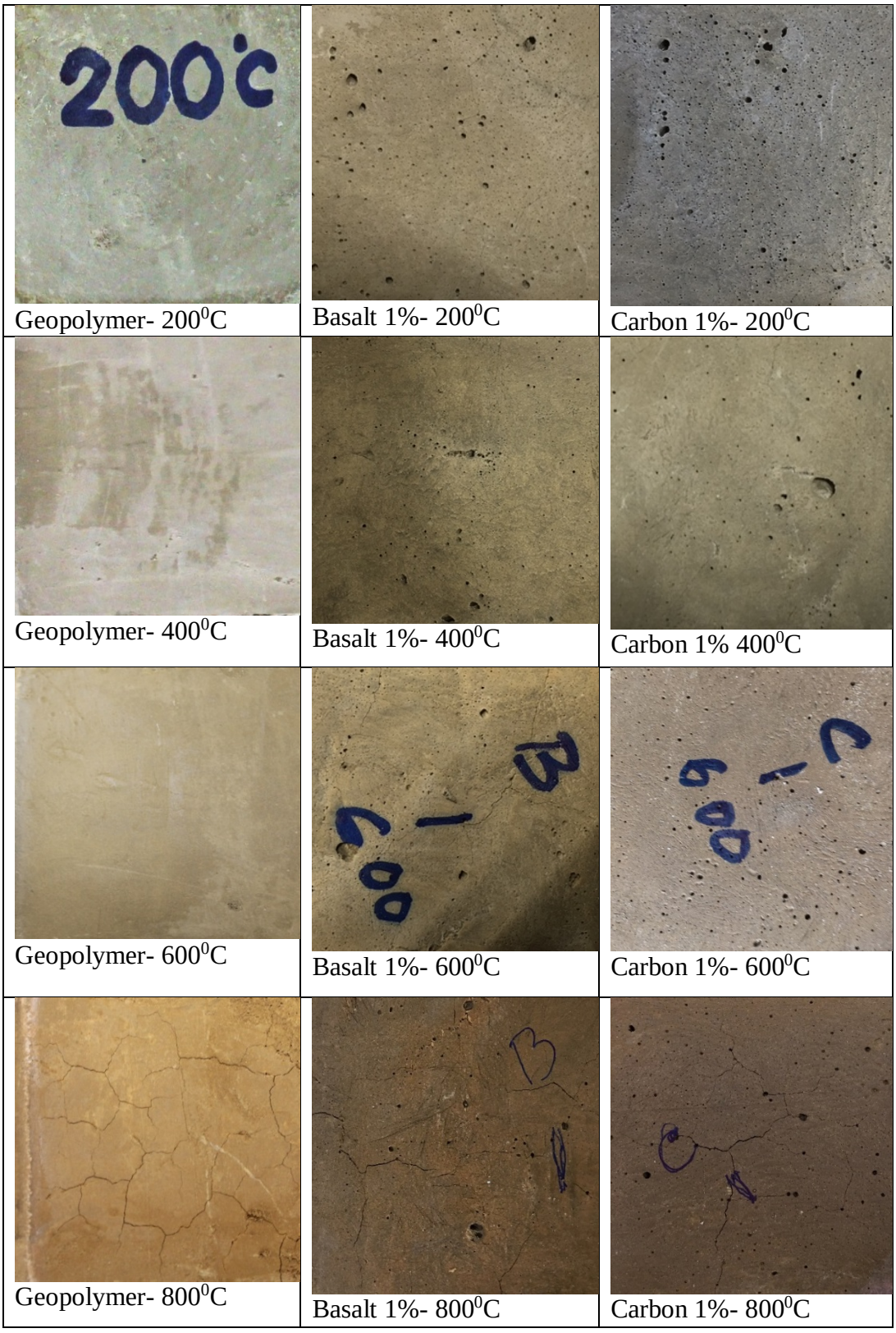


**Figure 6. 3 : Cracking behaviour of pure geopolymer and geopolymer composite containing 1 wt.% of carbon and basalt fibres at verious elevated tempetratures.**

After exposure to 200ºC, no significant change in volumetric shrinkage of geopolymer is observed in the case of both fibres. However, the addition of 1 wt.% carbon fibre significantly reduced the volumetric shrinkage of geopolymer by 79% and 19% at 400ºC and 600ºC, respectively, while in the case of basalt fibre this reduction were only 15% and 5%, respectively. After exposure to 800ºC, both fibres at 1 wt.% exhibited same reduction of volumetric shrinkage of geopolymer. Similar behaviour in terms of reduction of mass loss of geopolymer at various elevated temperatures due to addition of 1 wt.% of carbon and basalt fibres can also be seen in Fig. 6.2.

## 6.3. CRACKING BEHAVIOR OF FIBRE ADDED GEOPOLYMER

Figure 6.3 shows the cracking behaviour of the samples with 1 wt.% of both fibres content after heated at elevated temperatures (200ºC, 400ºC, 600ºC, 800ºC) and pure geopolymer samples. It can be seen from the figure that the samples containing 1 wt.% carbon fibre exhibits negligible cracking up to 600ºC compared to its pure geopolymer and basalt fibre counterpart. At 800ºC some micro cracks are formed in carbon fibre composite, however, the cracking is significantly less than pure geopolymer and slightly less intensive than that in basalt fibre composite at same temperatures. In general, the less cracking observed in carbon fibre composite at elevated temperatures than its counterpart basalt fibre geopolymer composite and pure geopolymer can be explained by the reduced volumetric shrinkage and mass loss observed in the former than the latter described before. The added reinforcing fibres aided in reducing the severity of the dehydration cracking by bridging the cracks as they developed. High temperature treatment data shows that the 1 wt.% carbon and basalt fibre reinforced geopolymer actually dehydrated slower than the pure geopolymer and there was less water loss at all temperatures, reaching about 91 wt.% of residual mass at 800°C, compared with about 90 wt.% for pure geopolymer. This can be attributed to the additional pathways for water to escape that were created by the fibre matrix interface. These pathways could help to gently dehydrate the geopolymer matrix during curing, reducing pressure gradients through the thickness of the specimen and avoiding cracking of the composite.

## 6.4. COMPRESSIVE STRENGTH OF FIBRE ADDED GEOPOLYMER

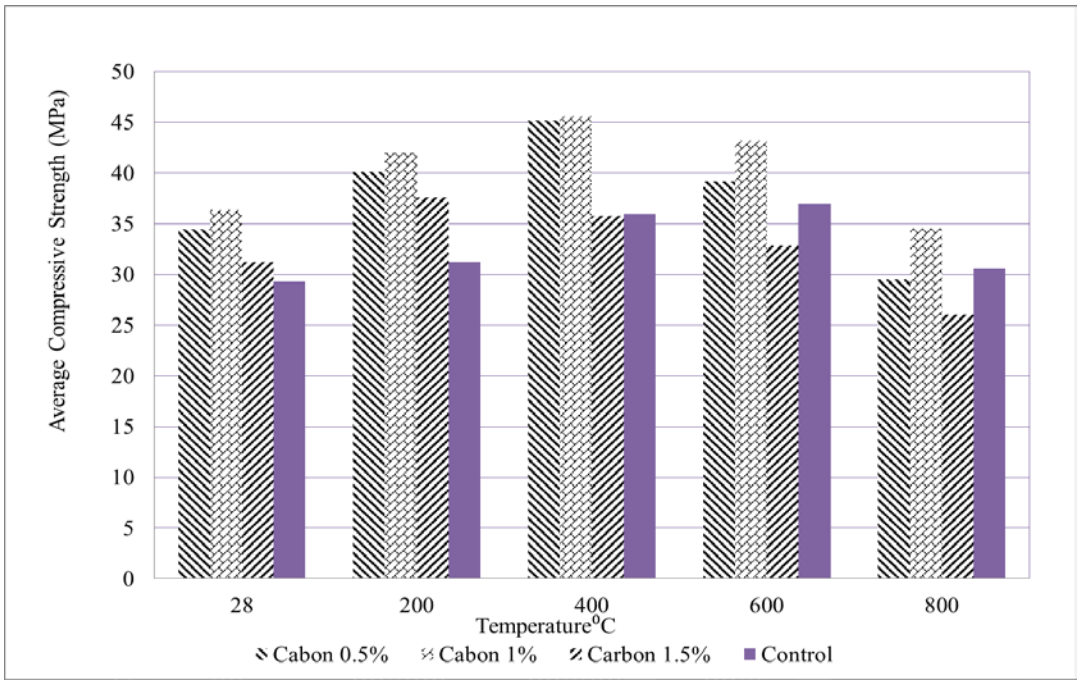


(a) Carbon fibre reinforced geopolymer composite

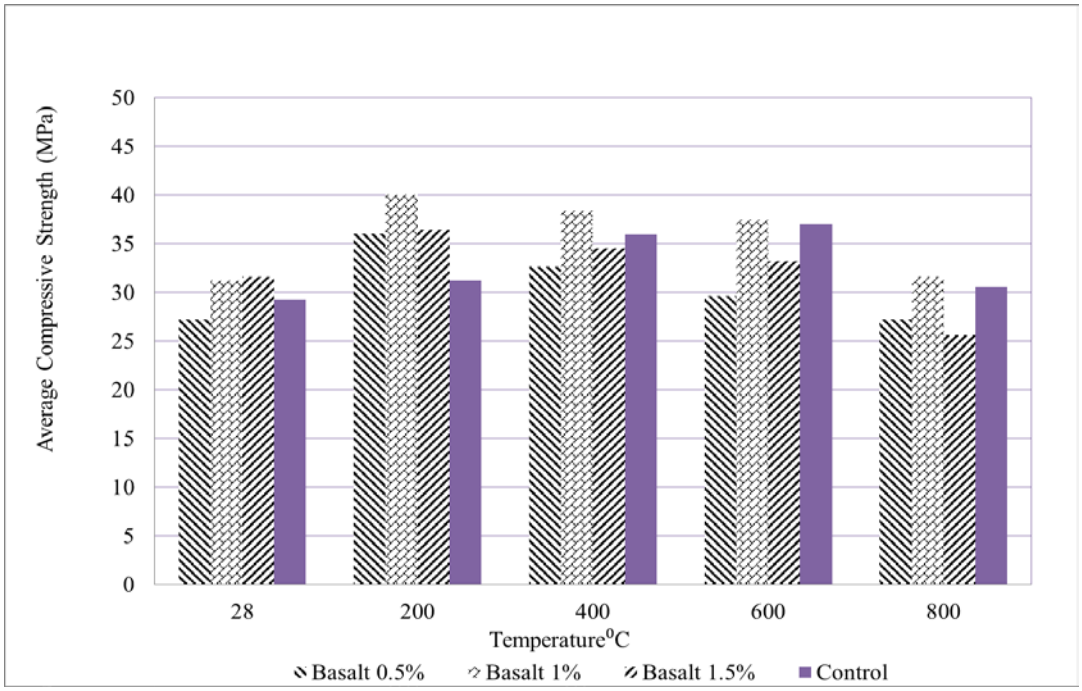


(b) Basalt fibre reinforced geopolymer composite

**Figure 6. 4 (a-b): Compressive strength of pure geopolymer and carbon and basalt fibre reinforced geopolymer at ambient and at various elevated temperatures**

The effects of various wt.% of carbon and basalt fibres on the compressive strength of fly ash geopolymer at ambient and various elevated temperatures are shown in Figs. 6.4 a-b. It can be seen that the ambient compressive strength of geopolymer is increased due to addition of both fibres at all three fibre contents except 0.5 wt.% of basalt fibre which showed about 7% reduction in ambient temperature compressive strength.

The carbon fibre at all three fibre contents showed higher improvement in compressive strength of geopolymer than those of basalt fibre contents at all elevated temperatures. This can be attributed to the formation of excessive voids due to non-uniform dispersion of long basalt fibre than carbon fibres and higher number of cracks in basalt fibre geopolymer composite than its carbon fibre counterpart at elevated temperatures especially at 600 and 800$^{o}$C. After exposure to various elevated temperatures, it can be seen that the compressive strength of 1 wt.% carbon fibre reinforced geopolymer improved significantly by about 35%, 27%, 16% and 12% at 200, 400, 600 and 800$^{o}$C, respectively compared to control geopolymer. On the other hand in the case of 1 wt.% basalt fibre geopolymer composite, these improvements are 28%, 7%, 1% and 3%, respectively. The other fibre contents at both fibres composites showed lesser improvement in compressive strength of geopolymer than 1 wt.%. It can be seen that the compressive strength of 1 wt.% carbon fibre geopolymer at elevated temperatures of 200, 400, 600 and 800$^{o}$C is about 5%, 18%, 15% and 10%, respectively higher than its basalt fibre geopolymer counterpart at the corresponding elevated temperatures, however, it is also interesting to see that the compressive strength gain with increase in elevated temperatures is comparable in both fibre reinforced geopolymer composites. Hence, based on compressive strength, volumetric shrinkage and mass loss measurements, the 1 wt.% can be considered as optimum fibre content of both carbon and basalt fibres for fire resistance of fly ash geopolymer.

## 6.5. POROSITY MEASUREMENT OF GEOPOLYMER WITH FIBRE

Mercury intrusion porosimetry (MIP) analysis is widely used to evaluate total porosity and size distributions of pores in cement, polymer and geopolymer matrix. The MIP results of the geopolymer samples containing 1 wt.% of carbon and basalt

fibres after exposure to 400 and 800ºC temperatures and at ambient temperature are shown in Figure 6.5 and Figure 6.6.

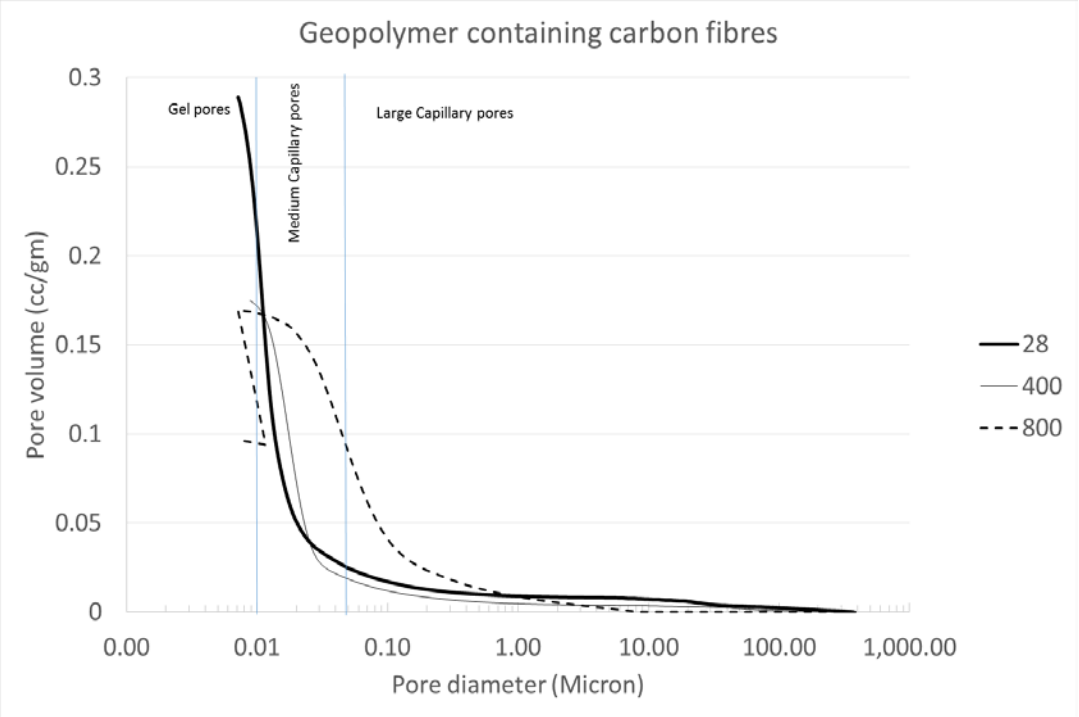


(a) Carbon fibre reinforced geopolymer composite

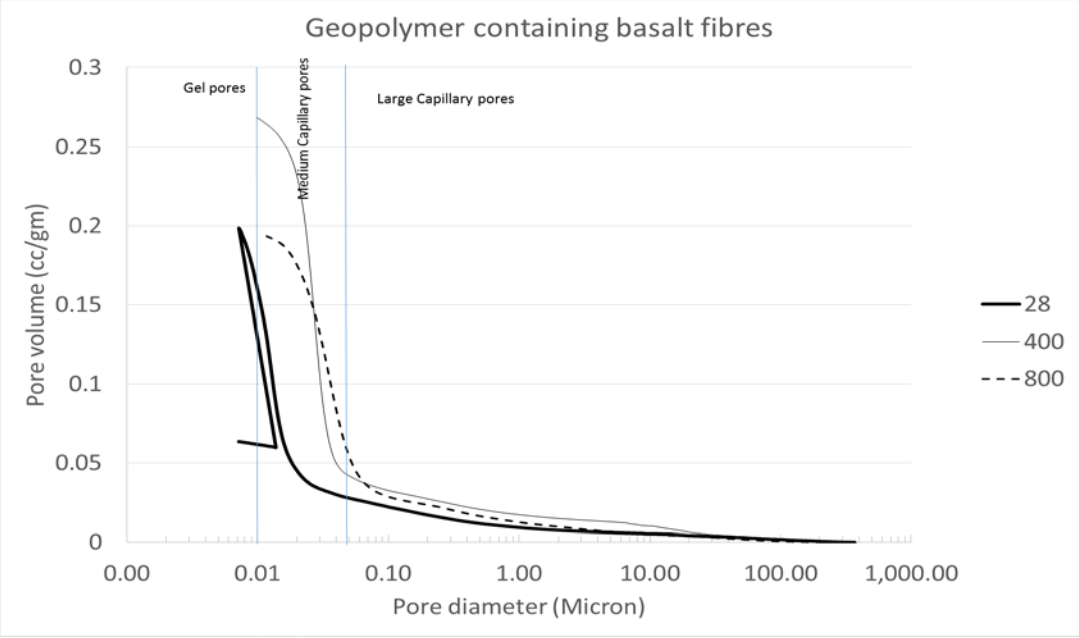


(b) Basalt fibre reinforced geopolymer composite

**Figure 6. 5 (a-b) : Cumulative pore volume of 1 wt.% carbon and basalt fibre reinforced geopolymer at ambient and at various elevated temperatures**

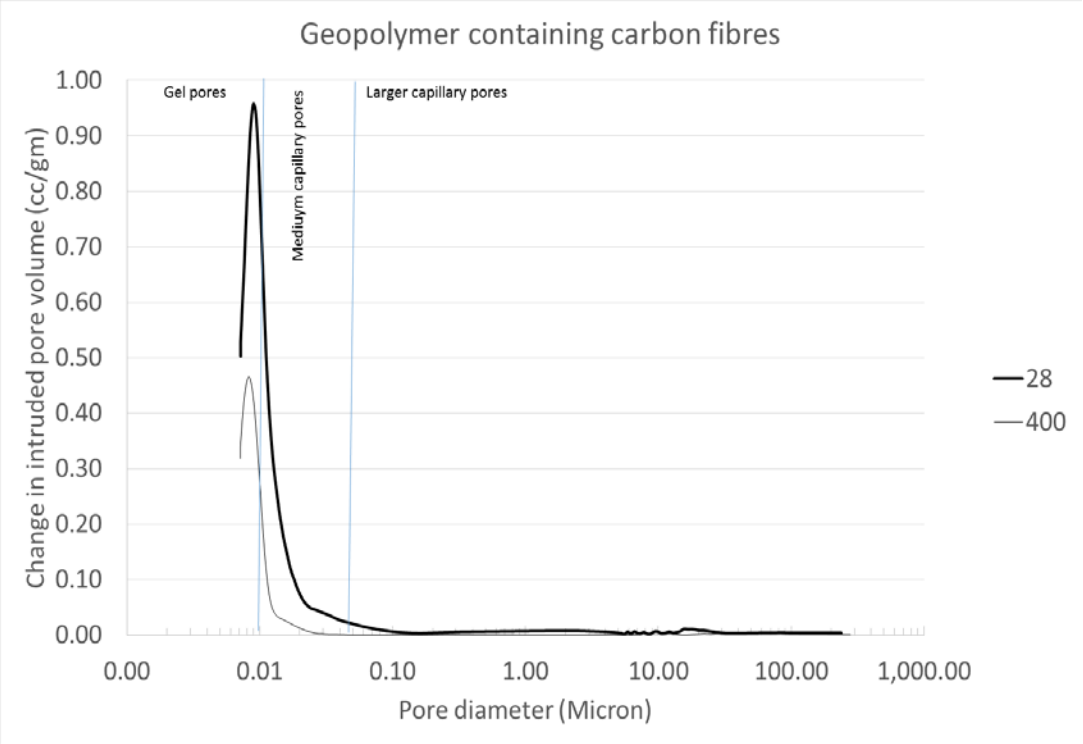


(a) Carbon fibre reinforced geopolymer composite

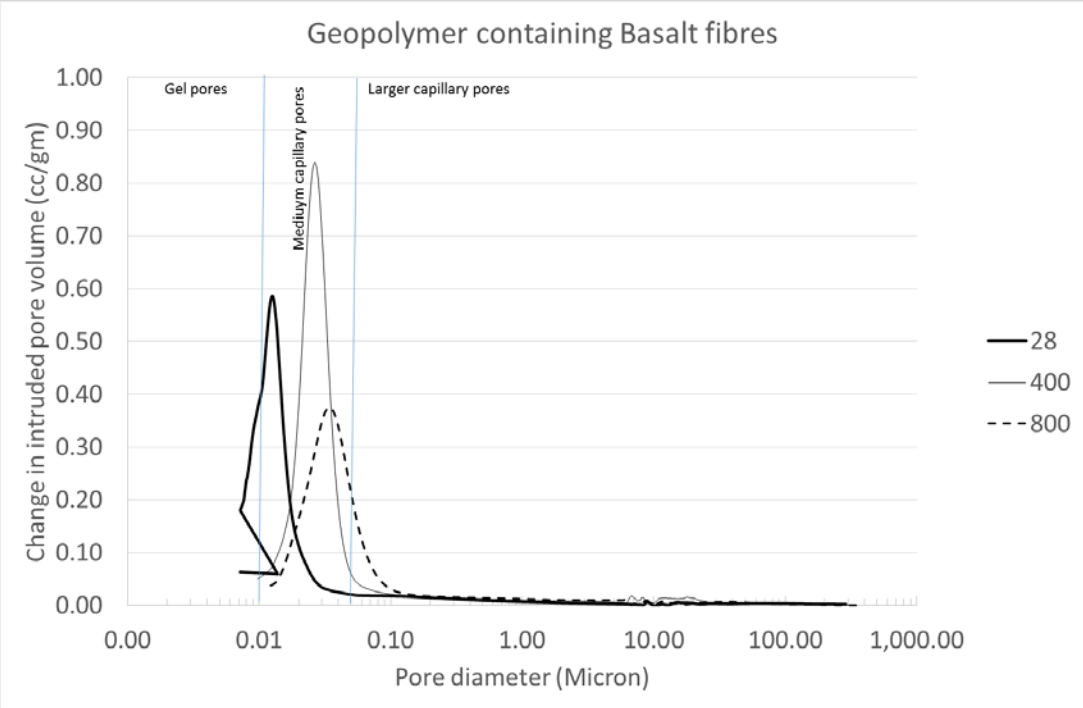


(b) Basalt fibre reinforced geopolymer composite

**Figure 6. 6 (a-b) : Pore volume distribution of 1 wt.% carbon and basalt fibre reinforced geopolymer at ambient and at various elevated temperatures**

It shows the relationship between cumulative pore volume and pore diameter in the range of 0.01–100 micron. Zhang and Islam (2012) classified the pores from 10 to 0.05 micron as large capillary pores, from 0.05 to 0.01 micron as medium capillary pores and <0.01 micron as gel pores.

From Fig. 6.5 it can be seen that the pore size distributions of both carbon and basalt fibre reinforced geopolymer at ambient temperature have the same general shape as those exposed to 400 and 800$^{o}$C temperatures. However, the basalt fibre reinforced geopolymer is found more porous than the corresponding carbon fibre geopolymer at both 400 and 800$^{o}$C temperatures with higher pore volume of large diameter pores. In particular the total cumulative pore volume of both medium and large capillary pores of basalt fibre geopolymer increased significantly after exposure to elevated temperatures (Fig. 6.5 b), which can explain the lower compressive strength observed in this composite at elevated temperatures than that of carbon fibre composite. Fig. 6.6 b also supports this observation where the maximum concentration of pores of basalt fibre composites are shifted towards medium to large capillary pores after exposure to elevated temperatures. No significant increase pore volume of pore size above 1 micron can be seen in the case of carbon fibre geopolymer composites nor any shift in the maximum concentration of pores after exposures to 400 and 800$^{o}$C temperatures. This might explain the better results observed in carbon fibre geopolymer than its basalt fibre counterpart.

## 6.6. MICROSTRUCTURE ANALYSIS OF THE GEOPOLYMER COMPOSITE

The change in microstructure of geopolymer composites after exposure to elevated temperature is also studied using scanning electron microscope (SEM) and the SEM images are shown in Fig. 6.7 (a-f).


a) Carbon fiber (ambient temperature)

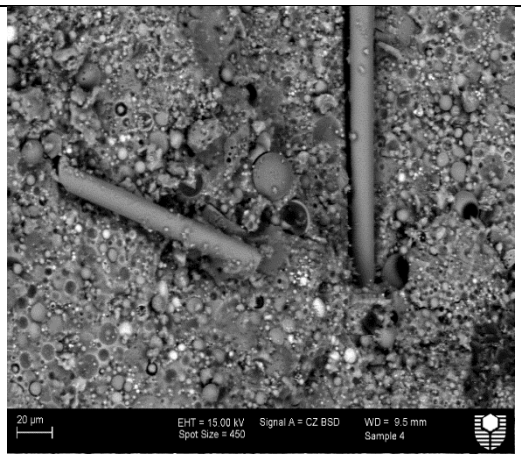


b) Basalt fiber (ambient temperature)

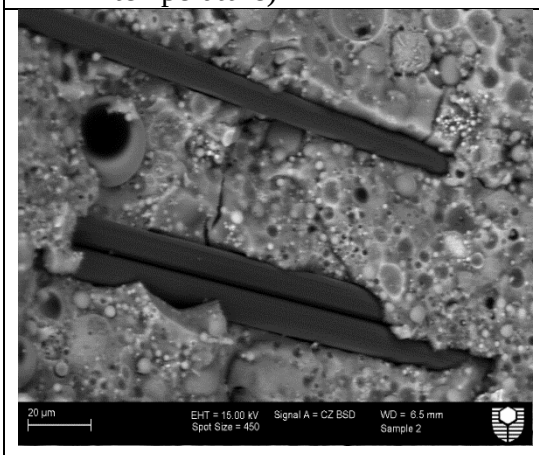


c) Carbon fiber ($400^0$ C temperature)


d) Basalt fiber ($400^0$C temperature)

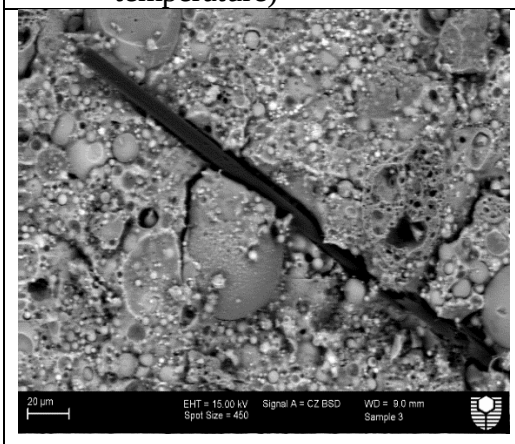


e) Carbon fiber ($800^0$C temperature)

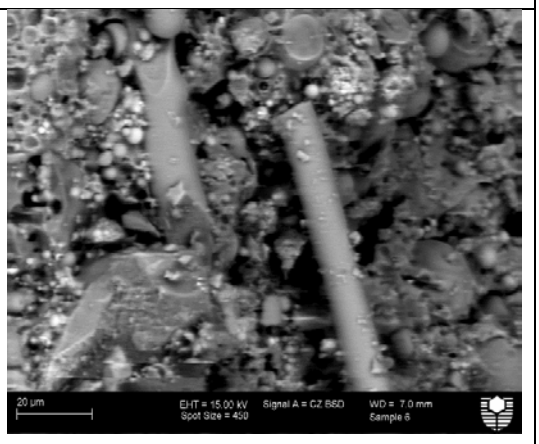


f) Basalt fiber ($800^0$C temperature)

**Figure 6. 7 (a-f) : SEM images of fly ash based geopolymer with Carbon and Basalt fibre at different elevated temperatures**

By comparing the surfaces of both carbon and basalt fibres in geopolymer after exposure to $400^0$C and $800^0$C temperatures with those at ambient condition, it can be seen no significant damage and change in diameter of both fibres at elevated temperatures, hence, indicating high temperature resistance characteristics of these two fibres.

By comparing microstructures of both composites, the carbon fibre geopolymer composite exhibited more compact microstructures even after exposure to elevated temperatures than its counterpart basalt fibre composite, which is consistent with the observed higher compressive strength, lower volumetric shrinkage and mass loss of the former than the latter as discussed earlier.

## 6.7. CONCLUSION

Based on the steps of the research it can be stated that the geopolymer series with 1% basalt fibre and also with 4% carbon fibre exhibit lower volumetric shrinkage, less mass loss and improved compressive strength after elevated temperature exposure. Among these two fibre content (Basalt and Carbon fibre) carbon fibre performs better after elevated temperature exposure.

Damage and change in diameter of both fibres at elevated temperatures are insignificant at elevated temperature as observed in SEM analysis. The results also support the fact that carbon fibre is better than basalt fibre at elevated temperature and showed better bonding with geopolymer at elevated temperature.

The better compressive strength, lower mass loss and also lower volumetric shrinkage of carbon fibre fly ash based geopolymer at various different elevated temperature than basalt fibre geopolymer summerizes the fact that carbon fibre is better as a filler than basalt fibre.

The next chapter will continue by summarizing the results and effects of the geopolymer coating on timber and the coating performance at elevated temperature as well as on direct fire.

The higher compressive strength and lower mass loss and volumetric shrinkage of carbon fibre reinforced fly ash geopolymer at various elevated temperatures up to $800^0$C indicate its superior role as filler in geopolymer at fire than that of basalt fibre.

# CHAPTER VII

# BEHAVIOUR OF GEOPOLYMER COATED TIMBER IN FIRE

## 7.1. INTRODUCTION

The previous chapters present fly ash based geopolymer matrix and its properties at elevated temperature. Properties of geopolymer with different additives like Nano silica, fine sand, basalt fibre and carbon fibres were described in the previous chapters. This chapter presents the fire resistant behaviour of geopolymer coated timber. The geopolymer coating was applied in a very thin layer and analysed at an elevated temperature. The bond between timber plates and geopolymer was also analysed and described in this chapter. The coated timber plates were also subjected to a direct fire test and interestingly the geopolymer coating behaves excellent on fire. The fire test result and the analysis is described in this chapter.

## 7.2. BOND TEST OF GEOPOLYMER COATING ON TIMBER

Results show that the bond strength of both geopolymer coatings (Na- and K-based) with timber is very similar. The Na-based geopolymer exhibited slightly higher bond strength of 0.9 MPa than that of K-based geopolymer which achieved a bond strength value of 0.85 MPa. These values are the average of two bond tests results. While no literature is available on adhesion bond strength values of geopolymer or cement paste with timber, these values seem reasonable as reported adhesion strength of paint with particleboard was about 0.97 MPa (Dilik et al., 2015). In another study, adhesion strength of about 1 MPa of alkaline aluminosilicate based coating with timber is reported by Krivenko et al. (2013). Adhesion bond strength of about 1-2.2 MPa of kaolin based geopolymer coating is also reported by Ramasamy et al. (2016). Fig. 7.1 shows the typical failure mode of the timber/geopolymer interface surface. It can be seen that the failure happened between the geopolymer coating and the timber. It can also be seen in Fig. 7.1 that some Na-based geopolymer coating still bonded with timber indicating consistency with the measured bond strength above. In addition to this mechanical test, visual inspection also shows strong adhesion of geopolymer with

timber as great effort was require to break the geopolymer coating from the timber surface using any steel plate.

**Figure 7. 1 : Typical bond failure mode of geopolymer/timber interface**

## 7.3. FIRE RESISTANCE BEHAVIOUR OF THIN GEOPOLYMER COATED TIMBER

The behaviour of geopolymer coated timber directly exposed to fire is shown in Fig. 7.2. It should be noted that the fire source was kept 30 mm away from the geopolymer coating and maintained for about 12 minutes during which about 1100$^{o}$C temperature was generated as measured by the thermocouple on the coating side. In the figure five different measured temperatures are shown. The thick black line indicates the fire temperature on the coating side, this was the surface temperature of the geopolymer coating. This temperature was first measured for about 2 minutes using a thermocouple and once it was stable at 1100$^{o}$C, its monitoring was stopped as the rate of fire through the gas torch was constant. Due to this reason a thick black line up to 12 minutes is shown representing of constant fire temperature of 1100oC. Fire temperature of 1100oC is chosen based on standard hydrocarbon fire curve shown in Fig. 7.3, where the 1100oC temperature quickly reached in less than 20 minutes. Although cellulosic fire is more appropriate in the case of timber buildings, however, the performance of geopolymer coated timber subjected to 1100oC is a conservative estimate.

The thin solid lines are the measured temperature inside the drilled hole in the timber plate which is few millimetres behind the geopolymer coating and can be seen that the

temperature increased from room temperature at the start of the test to about 300oC at the end of the test. It can also be seen that the measured temperature difference between Na- and K-based geopolymer coatings is not significant after 12 minutes fire exposure. On the other hand, the temperature of the timber side was in the range of 70-80oC at the end of the fire test in both cases. This clearly shows that the geopolymer coating significantly reduced the temperature rise inside the timber plate while the geopolymer side experienced very high 1100oC temperature. By comparing the damage of both geopolymer coatings in Fig. 7.4 it can be clearly seen that the extent of fire damage of K-based geopolymer is much lower than that of Na-based geopolymer. In the case of Na-based geopolymer coating several cracks are formed contrary to no significant cracking of K- based geopolymer coating. The measured lower contraction of K-based geopolymer than that of Na-based geopolymer observed in dilatometer test, shown in Fig. 7.5, and slightly lower thermal conductivity of 0.30 W/m$^o$C for K-based geopolymer than 0.33 W/m$^o$C for Na-based geopolymer can explain less cracking upon heating in k-based geopolymer coating. It is also interesting to note that no sign of fire spread on the geopolymer coated surface of the timber was observed during the fire tests, indicating excellent resistance against fire spread. To further examine the extent of damage of timber behind the geopolymer coating the coated timber plates were cut through the location where fire was applied and the extent of damage in the cross-section of the plate can be seen in Fig. 7.6. By comparing the Na- and K-based system it can be seen that while the spread and extend of damage on the K-based geopolymer coating is less, the damage across the thickness is more (about 14mm maximum char depth) than that of timber coated with Na-based geopolymer coating (about 11mm maximum char depth). Nevertheless, in both cases the fire damage did not reached the end of the timer which was about 20mm thick and no sign of fire in the timber was also observed during the test as shown in Fig. 7.7. Published data on fire resistance performance of cementitious materials coated timber is limited, the only study where 40mm thick Douglas fir tongue-and-groove timber plank was coated with cementitious coating of 50mm thickness and was exposed to standard ASTM E119 fire conditions for 30 minutes (Richardson and Cornelissen, 1987). After fire exposure a char depth of 12mm was observed in that study. It should be noted that in ASTM E119 fire test the fire temperature of about 800oC is reached

in 20 minutes and a maximum of about 1050$^0$C is reached after 3 hours. By comparing that result with this result it can be seen that the 2mm thick geopolymer coating showed excellent fire resistance in terms of 11-14mm char depth, which is expected to be much smaller in the case of much thicker geopolymer coatings and geopolymer coating containing any fillers e.g. high temperature resistant carbon and basalt fibres, the results whose are presented in next section.

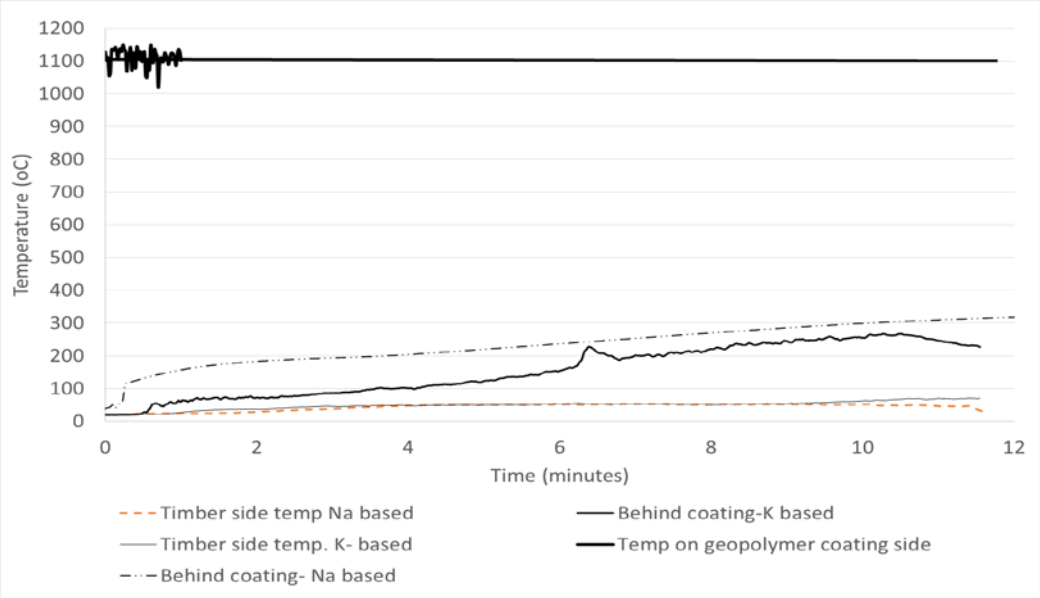


**Figure 7. 2: Measured temperatures of thin and thick geopolymer coated timber during fire test**

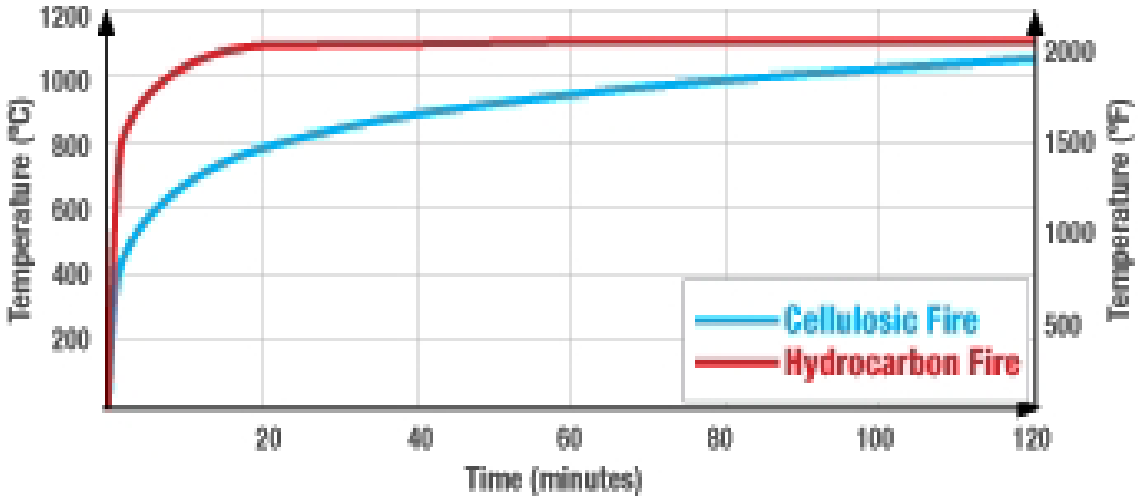


**Figure 7. 3 : Standard fire curves**

**Figure 7. 4: Coating side damage of both geopolymers due to direct application of fire for 12 minutes (Top image is Na-based geopolymer coating and bottom image is K-based geopolymer coating)**

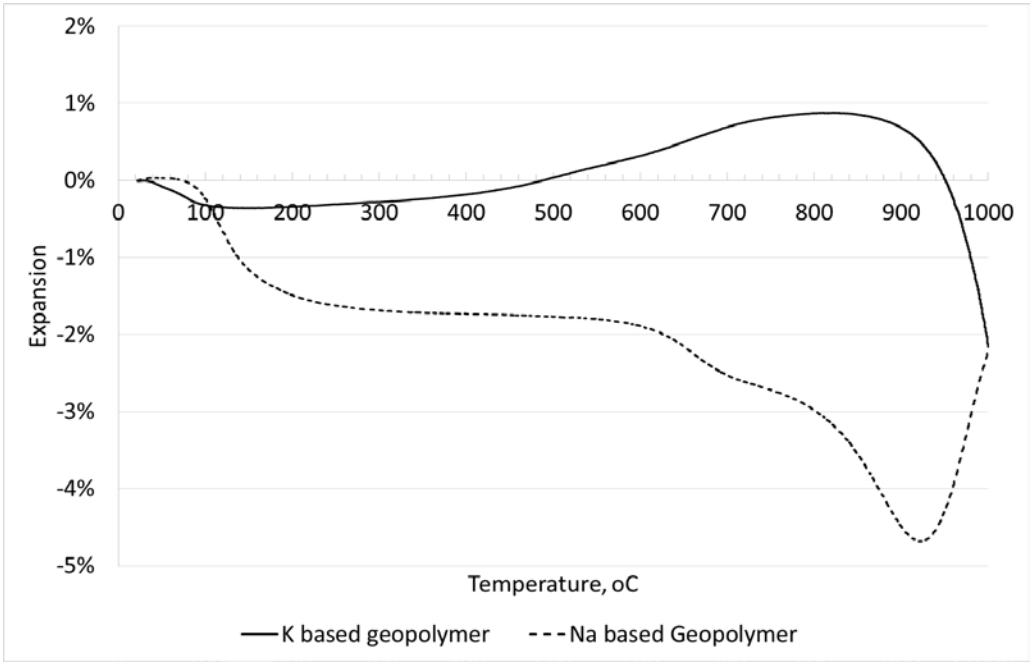


**Figure 7. 5: Linear expansion and contraction of geopolymer in dilatometer test.**

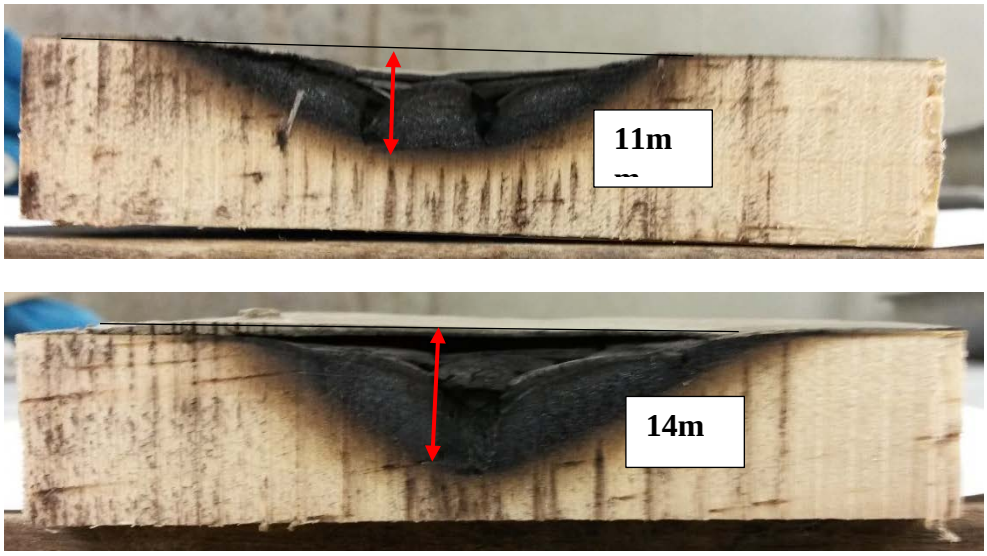


**Figure 7. 6: Char thickness after fire tests (Top: Na-based geopolymer coated timber; Bottom: K-based geopolymer coated timber).**

## 7.4. EFFECT OF THICK GEOPOLYMER COATING AND FILLER ON FIRE RESISTANCE

The effect of thick coating of about 4 mm thickness in fire resistance of both geopolymers coated timbers is also evaluated in this study. Thick geopolymer coated timbers are also exposed to the same fire testing regime and a fire temperature of about 1100oC is also maintained for about 20 minutes. In Fig. 7.7 the comparison of char depth of both 2mm and 4mm thick geopolymers coated timber is shown and it can be seen that by doubling the geopolymer coating the char depth of the timber is reduced by about 35-45%. In the case of Na-based geopolymer coating the char depth is reduced from 11mm to 6mm and in K-based geopolymer coating the reduction of from 14mm to 9mm due to doubling the coating thickness, both reduced by 5mm. The results also show that by increasing the coating thickness the char depth is not only reduced significantly but also the time required to form thick char is also increased from 12 minutes to 20 minutes. This indicates that by further increasing the coating thickness the fire damage of timber in terms of char depth can be reduced significantly which is the future study of this test.

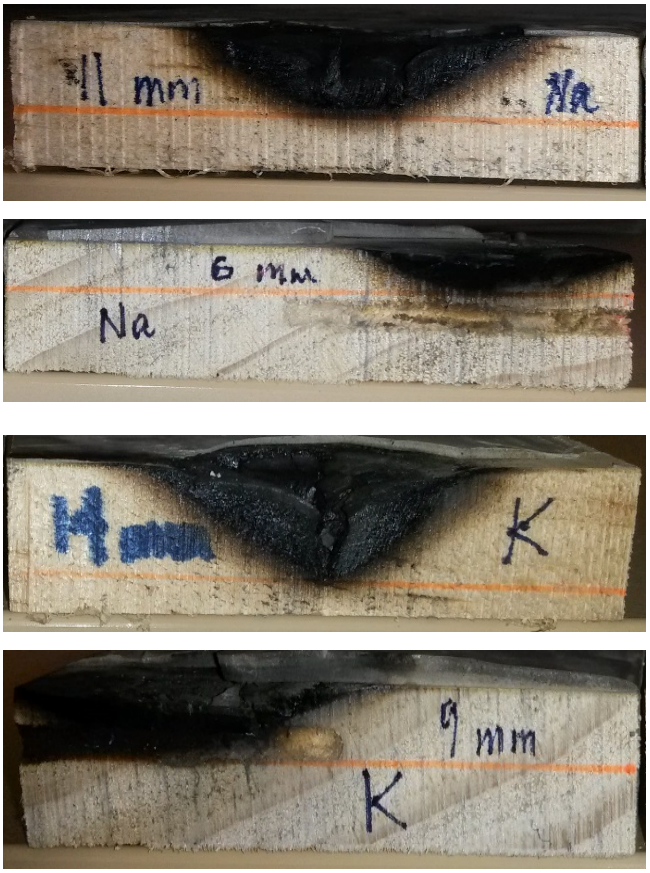


**Figure 7. 7: Comparison of char depth of Na-based geopolymer (Top) and K-based geopolymer coated timber.**

The addition of fillers or fibres adversely affect the workability of any cementitious materials. In this study the K-based geopolymer paste exhibited better workability than its Na-based counterpart. While both Na-based and K-based geopolymer coating exhibited quite comparable fire resistance, the K-based geopolymer is selected to reinforce with various volume fractions of carbon fibre (CF) and basalt fibre (BF) as significant reduction in workability of Na-based geopolymer is expected. The effects of inclusion of CF and BF of various volume fractions in fire resistance behaviour of thick (~4mm thick) geopolymer coated timber is shown in Figs. 7.8-7.12. Fig. 7.8 shows the measured temperatures behind the geopolymer coating containing increasing volume fractions of CF and BF from 0.5% to 1.5% while the geopolymer coating surface is subjected to a fire for about 10 minutes during which a temperature

of about 1100oC is maintained. It can be seen that the measured temperatures behind the geopolymer coating containing CF and BF are significantly lower than that of applied fire temperature and geopolymer coating containing 0.5% and 1.5% CF (and BF) exhibited the lower temperature than those of 1.0% CF (and BF). Among CF and BF reinforced geopolymer, no significant difference in measured temperature behind geopolymer coating can be seen. However, significant difference can be seen in the char depths shown in Figs. 7.10-7.12. The effect of CF and BF of various volume fractions on the char depth of geopolymer coated timber is shown in Fig. 7.10. It can be seen that the measured char depths of BF reinforced geopolymer coated timber are much higher than its CF counterpart. The char depths of geopolymer coated timber decreases with increase of both CF and BF. In the case of geopolymer coating containing 1.0% CF the char depth of about 3 mm is observed which is about 67% lower than non-fibrous geopolymer coating of same thickness and similar reduction is also observed in the case of 1.5% CF. Figs. 7.10-7.11 show the comparison of char depths of both CF and BF reinforced geopolymer coated timber and the effectiveness of CF in reducing the char depth of geopolymer coated timber compared to BF can be clearly seen. Fig. 7.12 also evidence the significantly lower level of damage of CF reinforced geopolymer coating layer after exposure to direct fire compared to its non-fibrous geopolymer coating in Fig. 7.4. Due to higher temperature resistance of CF, it bridges the micro cracks which develop due to contraction of geopolymer coating layer on timber and reduced the damage of timber behind the coating which is observed in this study. It is also interesting to see that the char depths of both CF and BF reinforced geopolymer coated timber are much lower than that of unreinforced geopolymer coating especially in the case of CF reinforced geopolymer but the measured temperatures behind the geopolymer coating exhibit opposite trend. It is well know that the thermal conductivity (TC) of CF is much higher than the BF and the geopolymer, therefore, the TC of geopolymer containing CF will be much higher than pure geopolymer and due to this reason the measured temperature behind the geopolymer coating containing CF is much higher than that of pure geopolymer. The higher TC of the CF reinforced geopolymer diffuses the heat outside easily, which makes the material flame resistant due to higher heat diffusion and restrain the ignition temperature of timber. This phenomenon is believed to be the reason for smaller char

depth of the CF reinforced geopolymer coated timber specially at higher CF content e.g. at 1.5% CF. On the other hand inferior performance of BF reinforced same geopolymer coated timber in terms of bigger char depth can be attributed to the lower TC of BF reinforced geopolymer due to lower TC of BF than that of CF.

As can be seen that the char depth can significantly be reduced by increasing the geopolymer coating thickness and addition of fibres. Char depth also depends of timber species e.g. burning rate is different for different timbers and the pine timber used in this study is considered as the highly combustible due to low-density and soft wood than other types e.g. Jarrah which is high density and hard wood. Therefore, significantly lower char depth and longer time required to develop the char can be achieved using the same geopolymer coating applied to high density hard wood timber. More research is need by considering other popular commercial timber species as well as manufactured timbers e.g. cross-laminated timber panel.

The development of char depth of timber also depends on the concentration of fire. In this study due to limitation of fire testing facility and to examine the hypothesis of fire resistant geopolymer coating fire test was performed in small scale, where fire was applied using gas torch on the coated timber which results in concentration of fire on a very small area. However, in real fire situation, the fire often spread over a larger area. Therefore, quite a different behaviour in terms of char depth can be expected in the same coated timber. Nevertheless, the effectiveness of CF reinforced geopolymer coating as an effective heat flux barrier and passive fire protection in terms of reduced char depth of timber due to fire is established in this preliminary study and more thorough research is required.

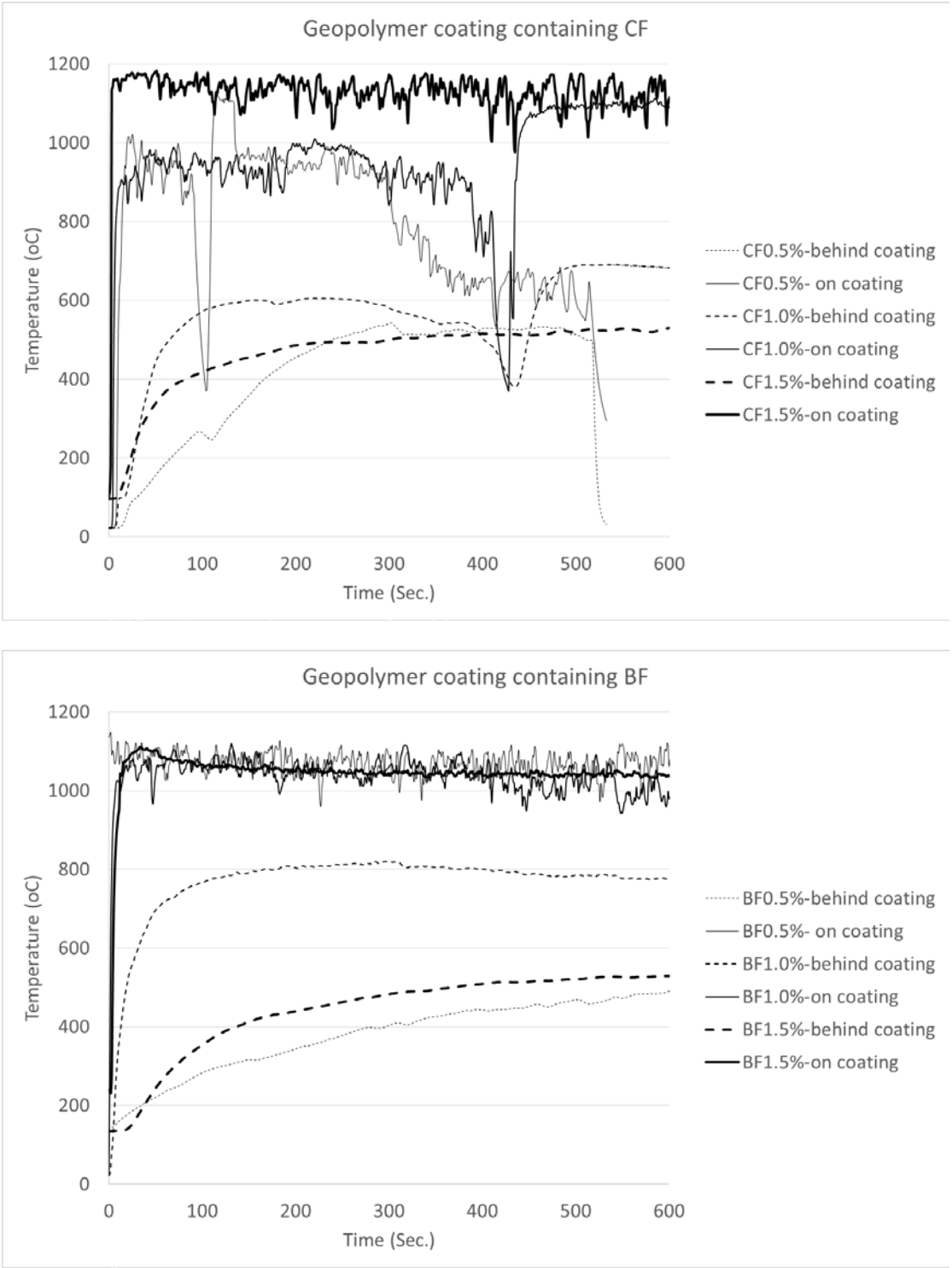


**Figure 7. 8: Measured temperatures of timber coated with thick geopolymer coating containing different volume fractions of carbon fibre (CF) (above) and basalt fibre (BF) (Below) during fire test**

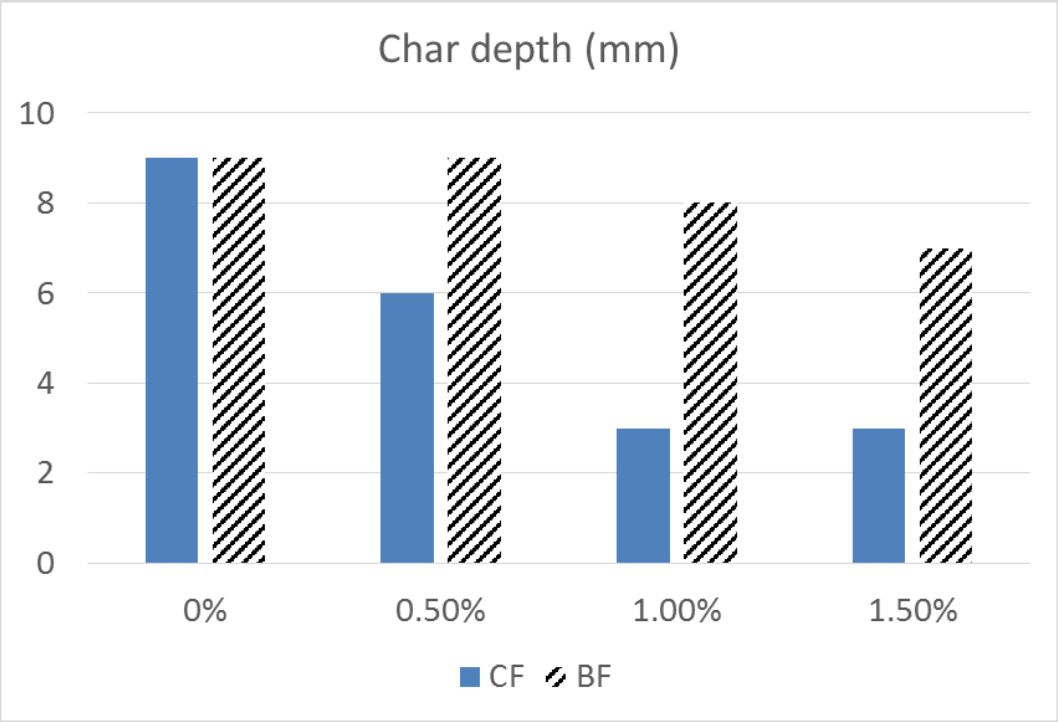


**Figure 7. 9: Effects of different volume fraction of CF and BF on char depth of thick geopolymer coated timber after 10 minutes of fire exposure**

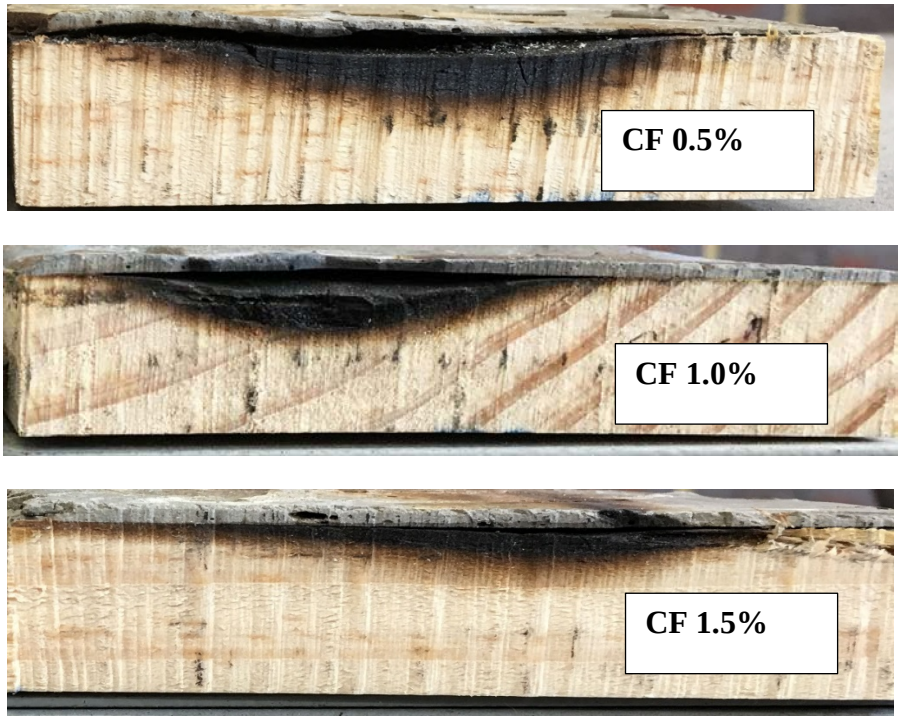


**Figure 7.10: Char depths of timber coated with thick geopolymer coating containing CF**

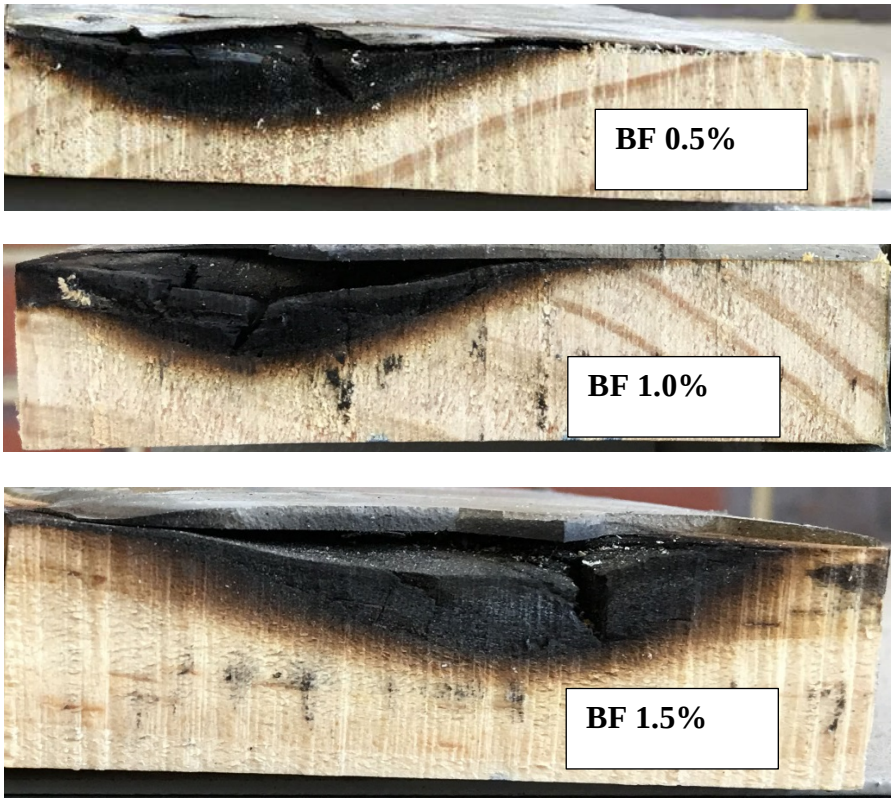


**Figure 7.11: Char depths of timber coated with thick geopolymer coating containing BF**

**Figure 7. 12: Damage of CF reinforced geopolymer coated layer after fire test**

## 7.5. MODELLING OF GEOPOLYMER COATED TIMBER IN FIRE

This section describes the finite element modelling of geopolymer coated timber subjected to fire of same temperature which was applied in the fire test in last chapter. ANSYS (2015) 16.0 a finite element based program is used to model the geopolymer coated timber subjected to fire.

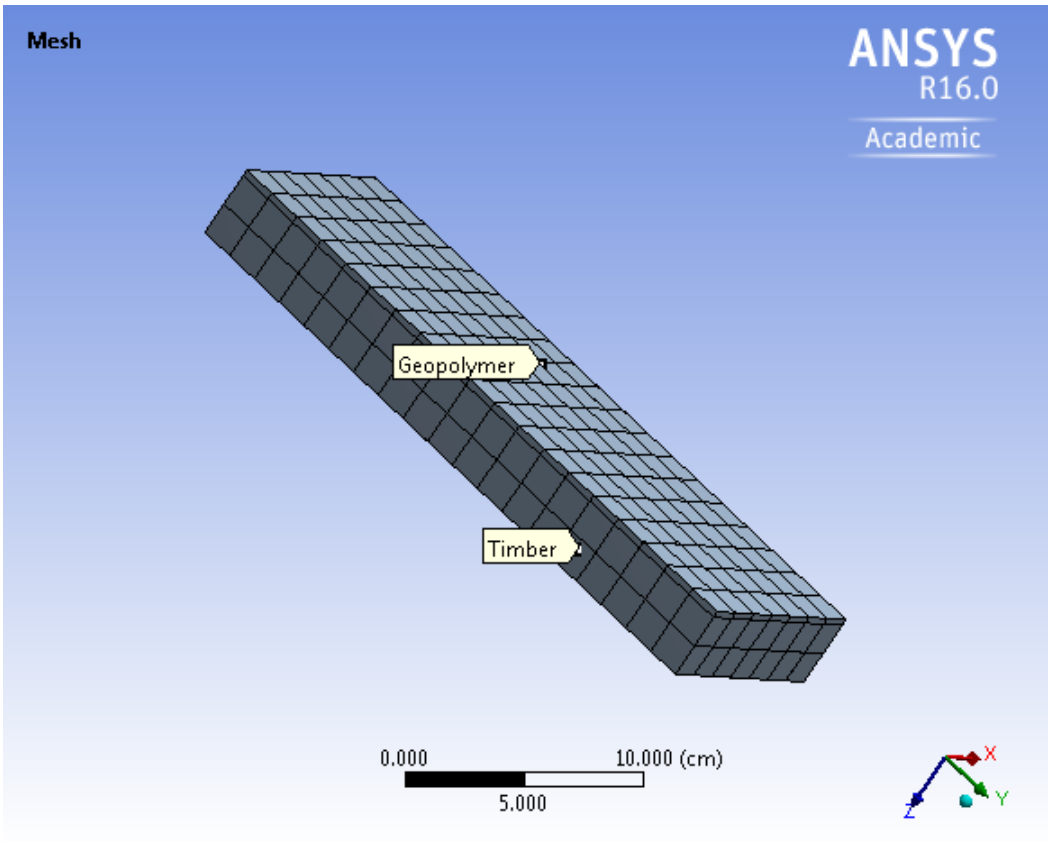


**Figure 7. 13: ANSYS model**

For modelling purpose timber is modelled using the property wood and geopolymer is modelled depending on the properties found in the previous research. A 100mm by 300 mm timber block with 20 mm thickness is modelled with a coating of geopolymer with the elements used in the ANSYS extruded by the thickness measurement. Geopolymer coating is modelled as bonded on the timber plate. Automated by ANSYS meshing was used during analysis. Transient thermal analysis is used for the analysis. The direct fire exposure to geopolymer coating is simplified by applying a constant temperature of $1100^0$C on the geopolymer coating of the model for 10 minutes as in the experiment. Specific heat of geopolymer is used as 1000 J/kg/C with a density of

2400 kg/m$^3$ (https://www.geopolymer.org/science/technical-data-sheet). Density of timber is considered as 700 kg/m$^3$, Specific heat of timber is used as 2310 J/Kg/C (http://www.timber.net.au). The ANSYS model is shown in Figure 7.13 and 7.14.

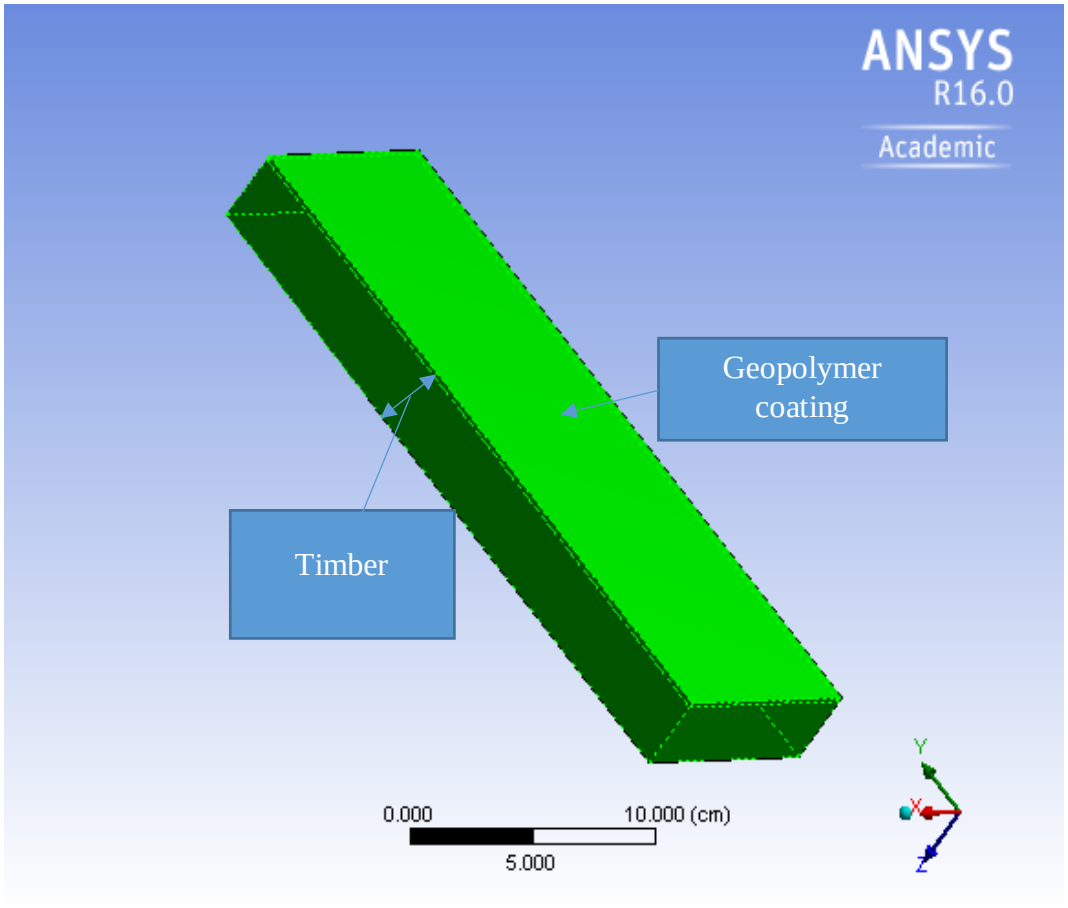


**Figure 7. 14 : Finite element model of the timber plate**

## 7.6. RESULTS AND DISCUSSION

Geopolymer is a new material with no established code yet so modelling of geopolymer might not give the same accurate result with the experiment. The thermal conductivity of K- and Na-based geopolymer was measured as 0.3 and 0.33 W/m$^0$C, respectively. Therefore, in the modelling purpose the thermal conductivity of geopolymer was used 0.3 and 0.33. Geopolymer coating thickness in the research was

2 and 4 mm. In the analysis 2 and 4 mm coating thickness was also used and compared with the test results. In the proposed model a constant $1100^0$C temperature heating is applied over the whole geopolymer coating of the timber. However, in actual test the fire was applied over a very small area on the geopolymer coating due to limitation of fire testing facility whereas in actual fire event, the fire can spread over the heating surface. Secondly the applied heating was started $1100^0$C from the beginning whereas in the lab fire test $1100^0$C was reached gradually.

### 7.6. a) Geopolymer coating with a thermal conductivity of 0.3 W/m$^0$C (Potassium based geopolymer)

The result of 2mm potassium based geopolymer coated timber in the finite element analysis is shown in Figure 7.15 and that for 4mm coating is shown in Figure 7.16. In the fire test the developed char thickness was 9mm for 4mm coating and 14mm was for 2mm coating. In the FE model it can be seen that at the same depth the temperature is $246.46^0$C for 2mm coating and $160.83^0$C for 4mm coating. The burning temperature of timber is around $232^0$C therefore any temperature below this can be considered safe and no charring can be considered at this temperature (http://www.timber.net.au). Therefore based on predicted temperature in the model it can be seen that for 2mm thick coating charring will be developed in timber. However, for 4 mm thick coating the timber will reach to burning leading to char formation.

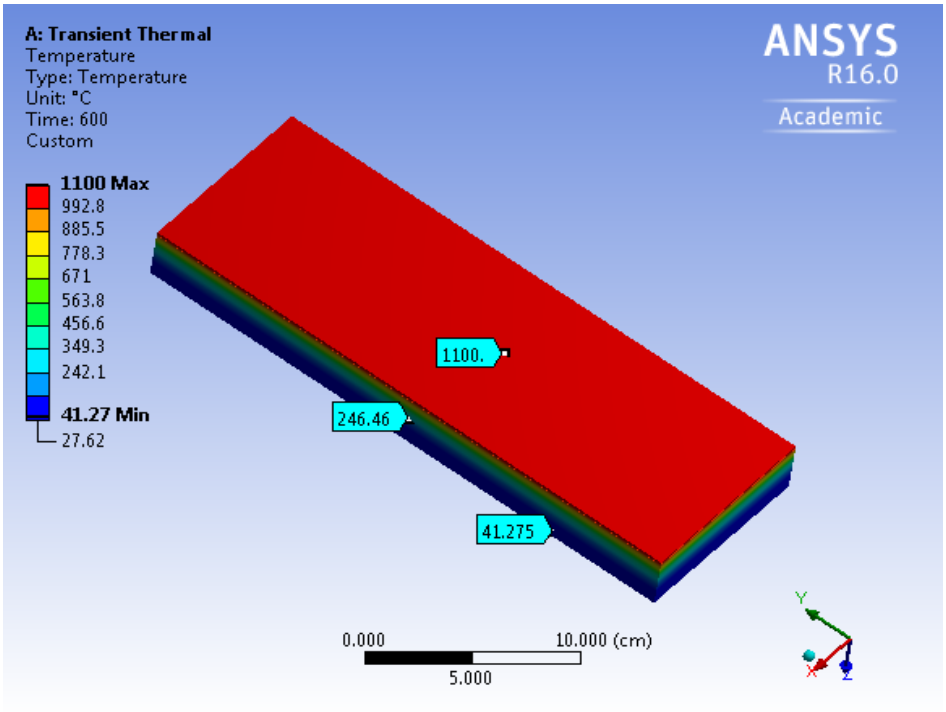


**Figure 7. 15: Finite element modelling with potassium based geopolymer 2mm coating**

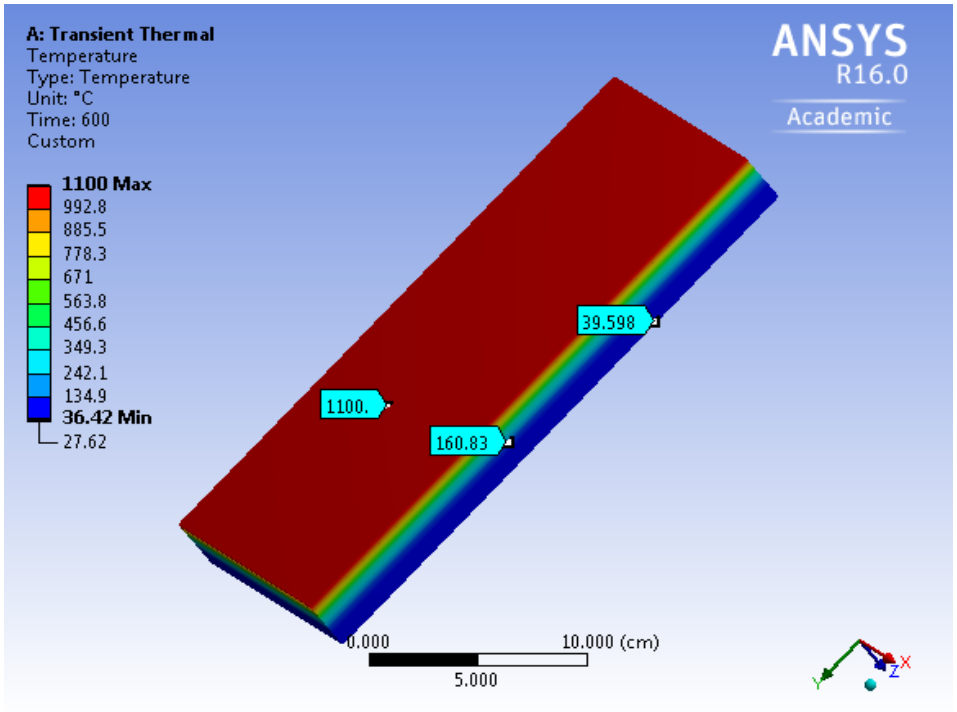


**Figure 7.16 : Finite element modelling with potassium based geopolymer 4mm coating**

### 7.6. b) Geopolymer coating with a thermal conductivity of 0.33 W/m$^0$C (Sodium based geopolymer)

Figures 7.17 and 7.18 show the predicted temperature at the char depths in the timber corresponding to coating thickness of 2 and 4mm, respectively. It can be seen that at about 7mm depth below the 2mm thick Na-based geopolymer coating the predicted temperature in timber in the model is about 263.32$^o$C (Fig. 7.17) and at about 10mm below the 4mm thick coating the predicted temperature in timber in the model is about 200.08$^o$C. As stated before the burning temperature of timber is around 232$^0$C, therefore, it can be seen that the model predicts quite reasonably the char depth in the timber. The comparison of model predicted temperatures and predicted char depths with those of fire test is summarised in Table 7.1.

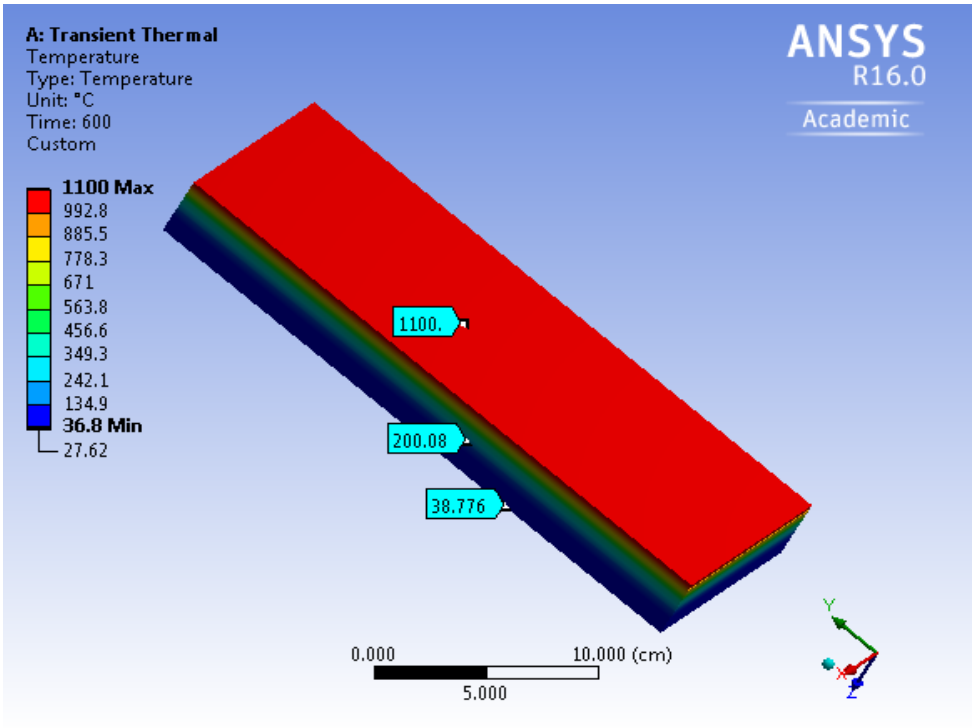


**Figure 7.17 : Finite element modelling with sodium based geopolymer 4mm coating**

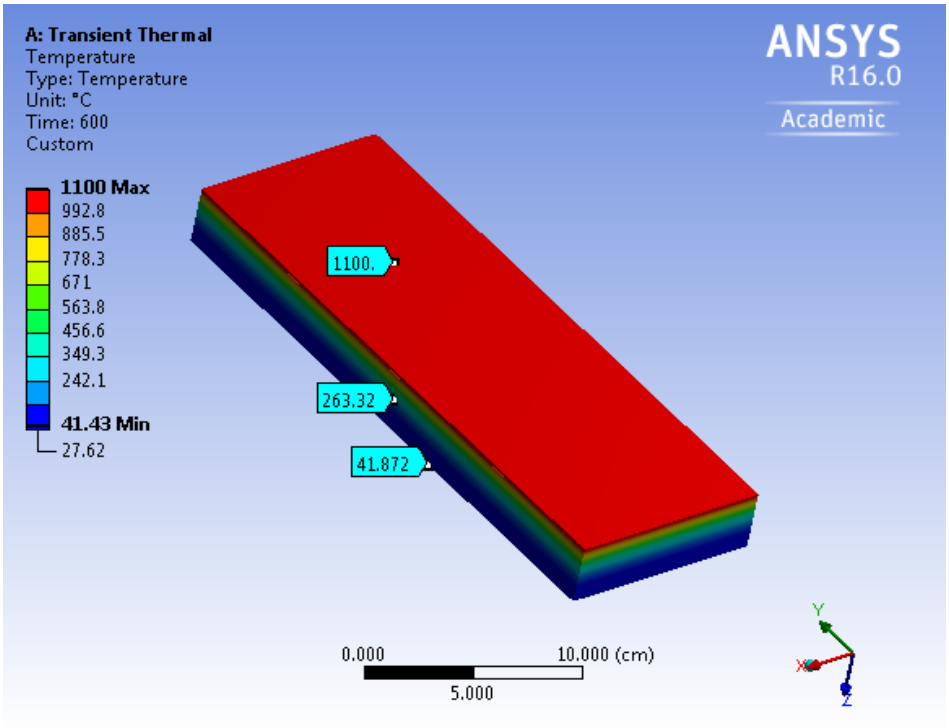


**Figure 7.18 : Finite element modelling with sodium based geopolymer 2mm coating**

**Table 7.1 : Comparison between the result from the experiment and the result from ANSYS**

| **Fire test Result** | | **FE model result** | |
|---|---|---|---|
| Geopolymer Thickness (mm) | Char thickness (mm) | Temperature at the char depth ($^0$C) | Predicted Char depth (mm) |
| 2 (Na based) | 11 | 263.32 | 10 |
| 4 (Na based) | 6 | 200.08 | 7 |
| 2 (K based) | 14 | 246.46 | 15 |
| 4 (K based) | 9 | 160.83 | 8 |

## 7.7. CONCLUSION

This chapter presents the fire resistance behaviour of two types of geopolymer coated pine timber having two different coating thickness of 2 and 4mm and containing two types of fibres. Based on small scale fire tests results the following conclusion can be drawn:

- The Na-based and K-based fly ash geopolymer coating exhibited about 0.90 MPa and 0.85 MPa, respectively of adhesion bond strength with smooth finish pine timber. The values are comparable to bond strength of alkali aluminosilicate based coating and paint coating with timber.
- Both fly ash geopolymer coatings exhibited good resistance against fire damage of timber in terms of char thickness with no sign of fire spread during the fire tests. K-based geopolymer coating exhibited fewer cracking than its Na-based geopolymer counterpart after 12 minutes of direct fire exposure at 1100$^{o}$C.
- By doubling the geopolymer coating thickness the char depth is reduced by about 35-45% and time required for char formation also increased from 12 to 20 minutes.
- The addition of carbon fibre and basalt fibre in 4mm thick k-based fly ash geopolymer coating exhibited about 50% and 79%, respectively lower char thickness than 2mm thin K-based geopolymer coating.
- The char depth of K-based geopolymer coating decreases with increase in both carbon fibre and basalt fibre volume fractions. Most significant reduction is observed in the case of 1.5% carbon fibre with about 67% reduction in char depth.
- The addition of carbon fibres significantly reduced the cracking of geopolymer coating after dire fire exposure.
- The K-based fly ash geopolymer paste also exhibited lower thermal contraction and thermal conductivity than its Na-based geopolymer counterpart.
- The proposed model predicts the charring depth of geopolymer coated timber with reasonable accuracy compared to fire test.

# CHAPTER VIII

# CONCLUSION AND RECOMMENDATION

## 8.1. OVERVIEW

This research evaluated the behaviour of geopolymer at elevated temperature. Timber structures are common around the world and these structures are very vulnerable to fire. The aim of this research was to evaluate the effectiveness of geopolymer based coating to protect the timber structures against fire and to minimize the loss. The conclusions of this research is summarized in this chapter and future recommendations are also presented in this chapter.

## 8.2. SUMMARY OF GEOPOLYMER WITH SODIUM AND POTASSIUM BASED ACTIVATOR

Based on limited experimental variables in terms of Na and K-based activators, the ratios of silicate to hydroxide of above activators, elevated temperatures on the residual compressive strengths, volumetric shrinkage and mass loss of geopolymer pastes the following conclusions can be drawn:

a. The geopolymer pastes containing Na-based activator exhibited higher compressive strength at ambient temperature and higher compressive strength at elevated temperatures up to 400$^{o}$C than its K-based counterpart.
b. At 600$^{o}$C the compressive strength of geopolymer containing K-based activator is slightly higher than its Na-based counterpart.
c. The geopolymer paste containing K-based activator exhibited higher residual compressive strengths at all elevated temperatures compared to ambient temperature than its Na-based counterpart.
d. The geopolymer paste containing K-based activator with $K_2SiO_3$/KOH ratio of 3 exhibited the highest residual compressive strengths at all elevated temperatures compared to ambient temperature than its Na-based counterpart.
e. The volumetric shrinkage and mass loss of geopolymer paste containing K-based activator is lower than its Na-based counterpart.

f. The geopolymer pastes containing K-based activator exhibited fewer surface cracks than that of Na-based activator.
g. XRD peaks of quartz and mullite are observed in both geopolymers after exposure to 400 and 800$^{o}$C temperatures like those observed in ambient condition. The presence of quartz and mullite peaks are believed to be the reason for maintaining residual compressive strength by both geopolymers after exposure to elevated temperatures.
*h.* The Na-based fly ash geopolymer exhibited higher weight loss in TGA and higher DTA peak at about 100$^{o}$C than its K-based counterpart after exposure to 400$^{o}$C. The higher weight loss and DTA peak is associated with the loss of absorbed and combined water in geopolymer gels, which indicate that higher geopolymer gels are remained in Na based geopolymer after 400$^{o}$C exposure than K-based system, which agrees well with the observed compressive strength results. An opposite trend is observed after exposure to 800$^{o}$C.

## 8.3. EFFECT OF NANO SILICA AND FINE SAND ON GEOPOLYMER

Based on available results of this phase of the research the following conclusion can be summarised:

a. Addition of nano silica improved the residual compressive strength of both sodium and potassium activators synthetized geopolymers at elevated temperatures. The potassium activator synthetized geopolymers containing nano silica exhibited higher residual compressive strength al elevated temperatures above 400$^{o}$C than its sodium based counterparts.
b. The 2% nano silica as partial replacement of fly ash by weight exhibited the optimum content among all nano silica contents at all elevated temperatures in both geopolymers.
c. The sodium activator synthetized geopolymer containing fine sand exhibited higher residual compressive strength at all elevated temperatures compared to those containing nano silica. The potassium activator synthetized geopolymer containing fine sand exhibited lower residual compressive strength at 400, 600 and 800$^{o}$C compared to those containing nano silica.

d. No significant improvement in residual compressive strength of potassium activator synthetized geopolymer is observed at elevated temperatures due to addition of fine sand.
e. The 10% fine sand as partial replacement of fly ash by weight exhibited the optimum content at all elevated temperatures in both geopolymers.
f. Irrespective of nano silica and fine sand contents, the potassium activator synthetized geopolymers exhibited lower mass loss and lower volumetric shrinkage than its sodium based counterpart at all elevated temperatures.
g. The geopolymers containing 2% nano silica and 10% fine sand exhibited the lowest mass loss and lowest volumetric shrinkage among other contents at all elevated temperatures similar to those of residual compressive strengths.
h. The potassium activator synthetized geopolymers also exhibited fewer cracks and smaller crack widths at elevated temperatures compared to those of sodium based counterparts.
i. The X-ray diffraction patterns of geopolymers showed new Mullite peaks between 2theta angle of 35$^{o}$ and 45$^{o}$ due to addition of nano silica and fine sand in both geopolymers. The quantitative X-ray diffraction analysis also showed higher Mullite phase in potassium activator synthetized geopolymers than that of sodium based series, which is the reason for observed higher residual compressive strength, lower mass loss and volumetric shrinkage and fewer cracking at elevated temperatures.

## 8.4. EFFECT OF BASALT AND CARBON FIBRE ADDITION ON GEOPOLYMER

Based on limited studies on physical, mechanical and microstructural characteristics of carbon and basalt fibre reinforced geopolymer composites at various elevated temperatures exposure the following conclusions can be drawn:

a. Geopolymer containing 1wt.% basalt and 1wt.% carbon fibre exhibited better compressive strength, lower volumetric shrinkage and mass loss than other fibre contents at all elevated temperatures. Among two fibres composites, the carbon fibre geopolymer exhibited better performance than its basalt fibre

counterpart at all elevated temperatures and ambient temperature. 1 wt.% of carbon and basalt fibres are the optimum fibre content in fly ash geopolymer at elevated temperatures. 1 wt.% carbon fibre reinforced geopolymer exhibited negligible cracking than its basalt fibre counterpart and pure geopolymer up to 600$^{o}$C. At 800$^{o}$C the cracking in 1 wt.% carbon fibre reinforced geopolymer is less than its basalt fibre counterpart and pure geopolymer.

b. The microstructure of carbon fibre reinforced geopolymer composite is also better in terms of lower pores/voids and more compact microstructure than its basalt based counterpart at elevated temperatures. Pore volume of larger diameter pores is increased at elevated temperatures in basalt fibre geopolymer than that of carbon fibre geopolymer. The maximum concentration of pores of basalt fibre composites are shifted towards medium to large capillary pores after exposure to elevated temperatures.
c. No significant damage and change in diameter of both fibres at elevated temperatures are observed in SEM analysis. The results also support the fact that carbon fibre is better than basalt fibre at elevated temperature and showed better bonding with geopolymer at elevated temperature, which is indicated by more compact microstructure of carbon fibre geopolymer.
d. The higher compressive strength and lower mass loss and volumetric shrinkage of carbon fibre reinforced fly ash geopolymer at various elevated temperatures up to 800oC indicate its superior role as filler in geopolymer at fire than that of basalt fibre.

## 8.5. GEOPOLYMER COATED TIMBER AT ELEVATED TEMPERATURE

a. Adhesive bond strength of about 0.90 MPa and 0.85 MPa of geopolymer coating containing Na- and K-based activators, respectively with timber were obtained in this study.
b. The timber cubes coated with both Na and K-based geopolymers survived up to about 600$^{o}$C temperatures inside the kiln. However, at 800$^{o}$C temperature significant damage of timber cubes were observed.

c. Failure of bond of geopolymer coating with timber at all elevated temperatures are observed and the damage of timbers are believed to be initiated due to the bond failure.
d. Both geopolymer coatings exhibited reasonable resistance against fire damage of timber with no sign of fire spread and burning of timber during the fire tests.
e. The proposed model reasonably predicts the charring depth of geopolymer coated timber compared to fire test.

## 8.6. FUTURE RECOMMENDATIONS

From this research and analysis following are the recommendations for some further investigations:

a. The sodium hydroxide and potassium hydroxide used in this study as an activator has a concentration of 8M in this study. Some more investigation can be done with different concentrations.
b. The geopolymer was cured at elevated temperature at $70^0$C. Ambient temperature curing will be beneficial for practical purpose. So research need to be done for ambient temperature curing geopolymer.
c. In the case of addition of nano silica, fine sand, basal fibre and carbon fibre more ratio with more varying parameters need to be done.
d. Coating thickness on the timber can be varied to check its effectiveness at elevated temperature and on fire.
e. Fly ash based geopolymer is used in this study. The same study can be done with metakaolin or slag to check its effectiveness at elevated temperature.
f. Study the fire resistance behaviour of ambient cured geopolymer coated timber.
g. Bending strength and tensile strength can also be done for each sample series.

# REFERENCES


Adak, D., Sarkar, M. and Mandal, S. (2014). Effect of nano silica on strength and durability of fly ash based geopolymer mortar. Construction and building materials, Vol.70:453-459.

Alomayri, T. Vickers, L. Shaikh, F.U.A. and Low, I.M. (2014). Mechanical properties of cotton fabric reinforced geopolymer composites at 200-1000C. *Journal of Advanced Ceramics*, DOI:10.1007/s40145-014-0109-x.

Arioz Van Jaarsveld, J. G. S., van Deventer, J. S. J., & Lorenzen, L. (1997) The potential use of geopolymeric materials to immobilise toxic metals: Part I. Theory and applications. *Minerals Engineering*, *10*(7), 659-669. doi:10.1016/s0892-6875(97)00046-0

Arioz, O. (2007). Effects of elevated temperatures on properties of concrete. Fire safety journal, Volume 42, Issue 8, November 2007, Pages 516–522

AS 1012.9 (2014). Methods of testing concrete - Compressive strength tests - Concrete, mortar and grout specimens. Standards Australia.

Askeland, D.R., Fulay, P.P. and Wright, W.J. (2010) The science and engineering for materials. 6th ed. Cengage learning, USA.

Assaedi, H. Shaikh, F.U.A. Low, I.M. (2015). Effect of nano-clay on mechanical and thermal properties of geopolymer. Journal of Asian Ceramic Societies.

ASTM C 109, (2012). Standard test method for compressive strength of hydraulic cement mortars (using 50 mm cube specimens), American Soceity for Testing and Materials, Pennsylvania, USA.

ASTM COMMITTEE E37 (2011). E228-11 Standard Test Method for Linear Thermal Expansion of Solid Materials With a Push-Rod Dilatometer. *ASTM Standard*, 10.

ASTM COMMITTEE E37 (2012). E831-12 Standard Test Method for Linear Thermal Expansion of Solid Materials by Thermomechanical Analysis. *ASTM Standard*, 4.

ASTM D4541 (2009) Standard test method for pull-off strength of coatings using portable adhesion testers. American society for testing and materials, West Conshohocken, PA, USA.

ASTM D4541 (2009). Standard test method for pull-off strength of coatings using portable adhesion testers. American society for testing and materials, West Conshohocken, PA, USA.

ASTM E119 (2016) Standard test methods for fire testing of building construction and materials. American society for testing and materials, West Conshohocken, PA, USA.

Bakharev, T. (2006). Thermal behaviour of geopolymers prepared using class F fly ash and elevated temperatures curing. Cem. Concr. Res. 36, 1134–1147.

Bakharev. T (2005). Geopolymeric materials prepared using class F fly ash and elevated temperature curing". Cement and Concrete Research 35, 1224–1232. Department of Civil Engineering, Monash University, Clayton, Victoria 3800, Australia.

Barbosa, V.F.F. MacKenzie, J. D. (2003). Synthesis and thermal behaviour of potassium sialate geopolymers. Mater. Lett. 57 (9) 1477-1482.

Barbosa, V.F.F., MacKenzie, K.J.D. & Thaumaturgo, C. (2000). Synthesis and characterisation of materials based on inorganic polymers of alumina and silica: sodium polysilate polymers. *International Journal of Inorganic Materials*, Vol. 2, pp. 309 – 317

Barnes, R. and Fidell, J. (2006) Performance in fire of small scale CFRP strengthened concrete beams. *Journal of composite for construction*. 10(6):503-508.

Bastami,M. Baghbadrani, M. and Aslani, F. (2014). Performance of nano silica modified high strength concrete at elevated temperatures. Construction and building materials, Vol.68:402-408.

Bell, J. Gordon, M. Kriven, W.M. Comrie, D. (2005). Graphite fiber reinforced geopolymer molds for near net shape casting of molten diferrous silicide,

conference paper, in: Workshop on Geopolymers and Geopolymer Concrete, Perth, Western Australia, p. 12.

Blissett, R.S. Rowson, N.A. A review of the multi-component utilization of coal fly ash Fuel. 97 (2012), pp. 1–23

Cheng, T.W. Chiu, J.P. (2003). Fire-resistant geopolymer produced by granulated blast furnace slag. Miner. Eng. 16, 205–210.

Chen-Tan, N. van Riessen, A. LY, C. & Southam, D. (2009). Determining the Reactivity of a Fly Ash for Production of Geopolymer. *Journal of the American Ceramic Society*, *92*(4), 881-887. doi:10.1111/j.1551-2916.2009.02948.x

Chew, M.Y.L. (1993). The assessment of fire damaged concrete. Build. Environ, 28 (1) 97–102.

Chindaprasirt, P. Jaturapitakkul, C., Chalee, W. Rattanasak, U. (2009). Comparative studies on the characteristics of fly ash and bottom ash Geopolymers. Waste Management 539–543.

Daniel, K. L.Y. Sanjayan, J. G. (2008). Effect of elevated temperatures on geopolymer paste, mortar and concrete. Department of Civil Engineering, Monash University, Clayton, Victoria 3800, Australia.

Daniel, L. Y. Kong, Jay G. Sanjayan , Kwesi Sagoe-Crentsil, (2007). Cement and Concrete Research. 37, 1583-1589.

Davidovits J, Davidovics M. (1988). Geopolymer room temperature ceramic matrix for composites. Ceramic Eng Sci Proc;9:842–53.

Davidovits Joseph (1994). Geopolymers Man made Rock Geosynthesis and the resulting development of very high strength cement, Geopolymer Institute 02100 Saint-Quentin, France. Journal of materials education vol. 16 (2&3), pp 91-139.

Davidovits, J. (1989). Geopolymers and geopolymer new materials. *J. Therm. Anal.*, vol. 35, no 2, pp. 429-444, 1989.

Davidovits, J. (1991). Geopolymers – inorganic polymeric new materials, J. Therm. Anal., 37 (8) , pp. 1633–1656

Davidovits, J. (1993). Geopolymer cement to minimize carbon-dioxide greenhouse-warming Cement-Based Materials: Present, Future and Environmental Aspects. Ceramic Transactions, 37, pp. 165–182

Davidovits, J. (1994). Global warming impact on the cement and aggregates industries. *World Resource Review*, 6(2), 263–278.

Davidovits, J. (2008). Geololymer, Chemistry and Applications Institute Geopolymer, Saint-Quentin, France.

Davidovits, J. Kurz, S. Balaguru, P. Lyon, R. (1999) *Second International Conference Geopolymere'99*.

Deb, P.S., Sarker, P.K. and Barbhuiya, S. (2015). Effects of nano silica on the development of geopolymer cured at room temperature. Construction and building materials, Vol.101:675-683.

Diaz, E. I., Allouche, E. N., & Eklund, S. (2010). Factors affecting the suitability of fly ash as source material for geopolymers. *Fuel*, *89*(5), 992-996. doi:10.1016/j.fuel.2009.09.012

Dilik, T., Erdinlet, S., Hazir, E., Koc, H. and Hiziroglu, S. (2015). Adhesion strength of wood based composites coated with cellulosic and polyurethane paints. Advances in materials and science and engineering. DOI:http://dx.doi.org/10.1155/2015/745675.

Dimitrios, P., Ioanna, P. Giannopoulou, Theodora Perraki. (2007). Effect of synthesis parameters on the mechanical properties of fly ash-based Geopolymers. Colloids and Surfaces A: Physicochem. Eng. Aspects 301, 246–254.

Duxon, P. Fernandez-Jiminez, A. Provis, JL. Luckey, GC. Palomo, A. Van Deventure JSJ. (2007). Geopolymer technology: the current state of the art. J Mater Sci ;42:2917–33.

Duxson, P. Mallicoat, S.W. Lukey, G.C. Kriven, W.M. van Deventer, J.S.J. (2007). The effect of alkali and Si/Al ratio on the development of mechanical properties of metakaolin-based geopolymers. Colloids Surf., A – Physiochem. Eng. Aspects, 292, pp. 8–20 http://dx.doi.org/10.1016/j.colsurfa.2006.05.044

Duxson, P. Provis, J. L. Lukey, G. C. Mallicoat, S. W. Kriven, W. M. and J. S. J. v. (2005). Deventer : Colloids Surf. A Vol 269, p. 47 - 58.

Duxson, P., Fernández-Jiménez, A., Provis, J. L., Lukey, G. C., Palomo, A., & van Deventer, J. S. J. (2007). Geopolymer technology: The current state of the art. *Journal of Material Science*, 42, 2917–2933.

Dylmar, D. Clelio, T. (2005). Fracture toughness of geopolymeric concretes reinforced with basalt fibers. Cement and Concrete composites, 27 (1) 49-54.

Estrada-Arreola, F. Perez-Bueno, J.J. Flores-Ruiz, F.J. Leon-Sarabia, E. and Espinoza-Beltran, F.J. (2014). The effect of temperature on micromechanical properties of fly ash based geopolymers activated with nano silica by sol-gel technique. Microscopy: advances in scientific research and education, Pp.986-991.

Fernández-Jiménez, A., & Palomo, A. (2003). Characterisation of fly ashes. Potential reactivity as alkaline cements. Fuel, 82(18), 2259-2265. doi:10.1016/s0016-2361(03)00194-7

Fernandez-Jimenez, A., Palomo, A. and Criado, M. (2006). Alkali activated fly ash binders. A comparative study between sodium and potassium activators. Materials de Construction, 56(281):51-65.

Ghosh, S. Ravindra, N. T. (2009). Effect on Mix Composition on Compressive strength & Microstructure of Fly Ash Based Geopolymer Composites. ARPN Journal of Engineering & Applied Sciences. Vol 4, No. 4.

Global Mining Conference, September (2010). (https://www.slideshare.net/objectivecapital/siegfried-konig-recycling-flyash-waste-day-1-session-1-strategic-metals-and-the-cleantech-revolution)

Gouny, F. Fouchal, F. Maillard, P. Rossignol, S. (2012). A geopolymer mortar for wood and earth structures, Constr. Build. Mater., 36, pp. 188–195

Gouny, F. Fouchal, F. Pop, O. Maillard, P. Rossignol, S. (2013). Mechanical behavior of an assembly of wood-geopolymer-earth bricks, Constr. Build. Mater., 38, pp. 110–118

Gourley, J. Johnson, G. (2005). Developments in geopolymer precast concrete: In proceedings of fourth world congress geopolymer, Saint-Quentin, France; P 133-7.

Guerrieri, M., Sanjayan, J. G. (2010) Behaviour of combined fly ash/slag based geopolymers when exposed to high temperatures, Fire Mater. 34 (2010) 163–175.

Haider, J.G. Sanjayan, P.G. Ranjith (2014) Complete triaxial stress–strain curves for geopolymer Constr. Build. Mater., 69, pp. 196–202

Hardito, D. Wallh, S.E. Sumajouw, D.M.J. Rangan, B.V. (2004). On the development of fly ash based geopolymer concrete. ACI Materials Journal, 101(6) 467-472.

Hardjito Djwantoro, Wallah Steenie E., Sumajouw Dody M. J., Rangan B.Vijaya. (2004). On the Development of Fly Ash-Based Geopolymer Concrete, ACI Materials Journals, Vol- 101-6; pp 467-472.

Hardjito, D. Cheak Chua Chung, Lee Ing Carrie Ho, (2008). Strength and Setting Times of Low Calcium Fly Ash-based Geopolymer Mortar. Vol 2, No 4 July.

Hardjito, D. Wallah, S. E. Sumajouw, D. M.J. Rangan, B.V. (2003). Geopolymer concrete: Turn waste into Environmentally Friendly Concrete, International Conference on Recent Trends in Concrete Technology and Structures, INCONTEST, 10-11 September, Coimbatore, India.

Hardjito, D. Wallah, S.E.. Sumajouw, D.M.J. Rangan, V. (2005). Fly ash based geopolymer concrete. Aust. J. Struct. Eng. 6, 1–10.

Hardjito, D. Wallah, SE. Sumajouw, DMJ. Rangan, BV. (2004). On the development of fly ash – based geopolymer concrete. ACI Mater J ;101(6):467–72.

Hassaan, M.M., Khater, H.M., El-Mahllawy, M.S. and El-Nagar, A.M. (2015). Production of geopolymer composites enhanced by nano kaolin material. Journal of advanced ceramics, Vol.4(4):245-252.

Heah, CY. Kamarudin, H. Al Bakri, AMM. Binhussain, M. Luqman, M. Nizar, IK et al. (2011). Effect of curing profile on Kaolin-based geopolymers. Phys Procedia, 22:305–11.

Hosan, A., Haque, S. and Shaikh, F.U.A. (2016). Compressive behaviour of sodium and potassium activators synthetised fly ash geopolymer at elevated temperatures: a comparative study. Journal of Building Engineering.

Jaarsveld, J. S. J. van Deventer, and L. Lorenzen. (1999). The potential use of geopolymer materials to immobilize toxic metals: part I. Theory and applications. *Miner. Eng.*, vol. 10, pp.659-669, 1999.

Jang-Ho, J.K. Yun, M.L. Jong, P. W. Hae, G.P. (2010) Fire resistant behavior of newly developed bottom-ash-based cementitious coating applied concrete tunnel lining under RABT fire loading. Construction and Building Materials 24 (2010) 1984–1994.

Johnson, G. High performance geopolymer concrete railway sleepers, in: Presented at Annual Geopolymer meeting of CSRP, 21–22 April Perth, Australia, 2008.

Kamseu, E. Rizzuti, A. Leonelli, C. Perera , D. (2010). Enhanced thermal stability in $K_20$-metakaolin based geopolymer concretes by $Al_2O_3$ and $SiO_2$ fillers addition, J. Mater. Sci. 45(7) 1715-1724.

Kamseu, E. Rizzuti, A. Leonelli, C. Perera, D. (2009). Dehydration, dihydroxylation, densification and deformation during sintering of geopolymers based on the $K_2O$-$Al_2O_3$-$SiO_2$ system, Brittle Matrix Compose.

Kani, EN. Allahverdi, A. (2009). Effects of curing time and temperature on strength development of inorganic polymeric binder based on natural pozzolan. J Mater Sci, 44:3088–97.

Khale, D. and Chaudhary, R. (2007). Mechanism of geopolymerization and factors influencing its development: a review. *J. Mater. Sci.*, vol. 42, pp. 729-746, 2007.

Kiatsuda, S. Jaturapitakkul, C. Kajitvichyanukul, P. Chindaprasirt, P. (2011). NaOH activator ground fly ash Geopolymer cured at ambient temperature. Fuel 90, 2118-2124.

Kim, J.J., Lim, Y.M., Won, J.P. and Park, H.G. (2010) Fire resistant behaviour of newly developed bottom ash based cementitious coating applied concrete tunnel lining under RABT fire loading. *Construction and building materials*. 24:1984-1994.

Kong, D. L.Y. Sanjayan J. G. (2010). Damage behavior of geopolymer composites exposed to elevated temperatures, Department of Civil Engineering, Monash University, Clayton, Victoria 3800, Australia.

Kong, D.L.Y. Sanjayan, J.G. (2008). Damage behaviour of geopolymer composites exposed to elevated temperatures. Cement and Concrete Composites 30(10), 986-991.

Kriven,W.M. Inorganic polysialates or geopolymers. Am. Ceram. Soc. Bull., 89 (4) (2010), pp. 31–34

Krivenko, P., Guzil, S. and Kravchenko, A. (2013). Protection of timber from combustion and burning using alkaline aluminosilicate based coatings. Advanced materials research. Vol. 688, pp3-9.

Krivenko, P.V. Kovalchuk, P.V. G. YU. (2002). Heat resistant fly ash based geocements. Proceedings of the INT. Conf. Geopolymer $28^{th}$-$29^{th}$ October 2002, Melbourne, Australia.

Krivenko, P.V. Pushkareva, Ye.K. Sukhanevich, M.V. Guziy, S.G. (2008). Fireproof coatings on the basis of alkaline aluminium silicate systems. Dev. Strategic Mater.: Ceram. Eng. Sci. Proc. 29 (10) (2008) 129–142.

Lee, B.Y. Cho. C.G. Lim, H.J. Song, J.K. Yang, K.H. and Li, V.C. (2012). Strain hardening fibre reinforced alkali-activated mortar-a feasibility study. *Journal of construction and building materials*, 37: 15-20.

Li, V.C. and Leung, C.K.Y. (1992). Steady state and multiple-cracking of short random fibre composites. *ASCE Journal of Engineering Mechanics*, 118(11): 2246-2264.

Li, Z. Ding, Z. Zhang, Y. (2004). Development of sustainable cementitious materials. In proceedings of International Workshop on Sustainable Development and Concrete Technology, Beijing, China; p. 20-1

Lin, T.S. Jia, D.C. He, P.G. Wang, M.R. (2009). Thermomechanical and microstructural characterisation of geopolymers with alpha alumina particulate filler. Int. J. Thermophys, 30 (2009) 1568–1577

Lizcano, M. et al., (2012). Mechanical properties of sodium and potassium activated metakaolin based geopolymers, J. Mater. Sci. 47, 2607-2616.

Luo, X. Xu, J.Y. Li, E.M. Bai, E.L. (2014). Effect of alkali-activator types on the dynamic compressive deformation behavior of geopolymer. Concrete Mater. Lett., 124, pp. 310–312

Lyon, R.E. Sorathia, U. Balaguru, P. N. Foden, A. Davidovits, J. and Davidovics, M. (1996). *First International Conference on Fiber Composites in Infrastructure (LCCI' 96) Tucson*.

Lyon, R.E., Balaguru, P.N. Foden, A. Sorathia, U. Davidovits, J. and Davidovics, M. (1997): Fire and Matrials Vol. 21, p. 67-73.

Maholtra, VM. (2002). Introduction: sustainable development and concrete technology. ACI Concr Int ;24(7):22. international conference, France; 1999. p. 9–40.

Malhotra, V. M. (1999). Making Concrete "Greener" With Fly Ash. ACI Concrete International 21(5): 61-66.

Masi, G. Rickard, W. D. A. Bignozzi, M. C. van Riessen, A. (2015). The effect of organic and inorganic fibers on the mechanical and thermal properties of aluminate activated geopolymers. *Composites Part B* 76 218-228.

Nazari, A. Sanjayan, J.G. (2015). Hybrid effects of alumina and silica nanoparticles on water absorption of geopolymers: Application of Taguchi approach. Measurement. 60:240-6.

Nematollahi, B. Sanjayan, J. Shaikh, F. U. A. (2014). Effect of different activators on the behavior of Ductile Fiber Reinforced Geopolymer Composite

(DFRGC)..In proceedings of 38th International Conference and Expo on Advanced Ceramics and Composites" (ICACC'14), Florida, USA.

Olivia, M. Sarker, P. Nikraz, H. (2008). Water Penetrability of Low Calcium Fly Ash Geopolymer Concrete. Curtin University of Technology, AUSTRALIA. ICCBT 2008 - A - (46) – pp517-530.

Omar, A.A. Al Bakri Abdullah, Hussin, M.M. K. Khairul Nizar, I. (2013). Lightweight Fly Ash-Based Geopolymer Concrete. Advanced Materials Research, Vol. 626, pp. 781-785.

Omar, G. J. Zheng, X. M. Cui, W. P. Zhang, and Zhang, F. T. (2009). Preparation of geopolymer precursors by sol–gel method and their characterization. *J. Mater. Sci.* 2009; vol. 44, no 15, pp. 3991-3996.

Östman, B., Voss, A., Hughes, A., Jostein Hovde, P. and Grexa, O. (2001). Durability of fire retardant treated wood products at humid and exterior conditions review of literature. Fire Mater., 25: 95–104. doi:10.1002/fam.758

Pacheco-Torgal, F. Castro-Gomes, J. Jalali, S. (2008). Alkali-activated binders: A review Part I. Historical background, terminology, reaction mechanisms and hydration products. J. Constr. Build Mater Vol. 22, pp. 1305-1314.

Palomo A. Grutzek M.W. Blanco M.T, (1999). Alkali activated fly ash A cement for the future" Cement and Concrete Research 29, 1323–1329.

Palomo, A. Macias, A. Blanco, MT. Puertas, F. (1992). Physical, chemical and mechanical characterization of geopolymers. In: Proceedings of the 9th International Congress on the Chem of Cem; p. 505–\

Pan, P. Z. Sanjayan, J. G. Rangan, B. V. (2009). An investigation of the mechanisms for strength gain or loss of geopolymer mortar after exposure to elevated temperature, Springer Science, Business Media, LLC.

Part, W.K. Ramli, M. Cheah, C. (2015). An overview on the influence of various factors on the properties of geopolymer concrete derived from industrial by-products Constr. Build Mater., 77, pp. 370–395.

Pavel, R. (2010). Effect of curing Temperature on the structure of metakaolin-base geopolymer. Construction and building materials, Vol 24-7, July 2010, Page 1176-1183.

Pavel, V.K. Sergey, G.G. (2013). Aluminosilicate coatings with enhanced heat- and corrosion resistance. Applied Clay Science. Volume 73, March 2013, Pages 65-70.

Pelisser, E.L. Guerrino, M. Menger, M.D. Michel, J.A. Labrincha (2013). Micromechanical characterization of metakaolin-based geopolymers Constr. Build. Mater., 49, pp. 547–553

Phoo-nhernkham, T., Chindaprasirt, P., Sata, V., Hanjitsuwan, S. and Hatanaka, S. (2014). The effect of adding nano silica and nano alumina on properties of high calcium fly ash geopolymer cured at ambient temperature. Materials and Design, Vol.55:58-65.

Provis , J. L. (2014). Green concrete of red herring?- Future of alkali activated materials, Adv. Appl. Cream. 113 (8), 472-477.

Provis, J. L. Duxson, P. Harrex, R M. Yong, C. Z. and Van Deventer, J. S. J. (2008). Valorisation of fly ashes by geopolymerization. *Glob. Nest. J.*, vol.11, no. 2; pp. 147-154.

Provis, J.L. & van Deventer, J.S.J. (2007a). Geopolymerisation kinetics. 1. In situ energy-dispersive X-ray diffractometry. Chemical Engineering Science, Vol. 62, pp. 2309 – 2317.

Provis, J.L. & van Deventer, J.S.J. (2007b). Geopolymerisation kinetics. 2. Reaction kinetic modelling. Chemical Engineering Science, Vol. 62, pp. 2318 –2329.

Ramasamy, S., Hussin, K., Abdullah, M.M.A-B, Ghazali, C.M.Z., Sandhu, A.V. and Binhussain, M. and Shahedan, N.F. (2016). Adhesiveness of kaolin based coating materials on lumber wood. *Key engineering materials*. 673:47-54.

Ranjbar, N., Mehrali, M., Alengaram, U.J., Metselaar, H.S.C. and Jumaat, M.Z. (2014). Compressive strength and microstructural analysis of fly ash/palm oil fuel ash based geopolymer mortar under elevated temperatures. *Construction and Building Materials*, Vol.65:114-121.

Rashad, A.M. Zeedan, S.R. (2011). The effect of activator concentration on the residual strength of alkali-activated fly ash pastes subjected to thermal load. Constr. Build. Mater, 25, 3098–3107.

Rattanasak, U. Chindaprasirt, P. (2009). Influence of NaOH solution on the synthesis of fly ash Geopolymer. Minerals Engineering, 22, 1073–1078.

Rees, C. Lukey, G.C. Van Deventer, J.S.J. (2004). The role of solid silicates on the formation of geopolymers derived from coal ash. In International Symposium of Research Student on Material Science and Engineering, Chennai: India, pp. 1-13.

Richardson, L.R. and Cornelissen, A.A. (1987). Fire resistant coatings for roof/ceiling deck timbers. *Fire and materials*. 11:191-194.

Rickard, W. D. A., Vickers, L. And van Riessen, A. (2012). Performance of fibre reinforced, low density metakaolin geopolymers under simulated fire conditions. *Applied Clay Science* 73 (2013) 71-77

Rickard, W.D.A. Temuujin, J. van-Riessen, A. (2012). Thermal analysis of geopolymer pastes synthesized from five fly ashes of variable compositions. J. Non-Cryst. Solids, 358 ,1830–1839.

Rickard, W.D.A., Riessen, A. and Walls, P. (2010). Thermal character of geopolymer synthetized from class F fly ash containing high concentretions of iron and quartz. *Applied ceramic technology*. 7(1):81-88.

RILEM TC 129-MHT (2000). Test methods for mechanical properties of concrete at high temperatures. *Materials and structures*, Vol. 33:219-223

Rovnanik, P. (2010). Effect of curing temperature on the development of hard structure of metakaolin-based geopolymer. *Construction and Building Materials*, 24, pp. 1176-1183.

Şahmaran, M., Özbay, E., Yücel, H.E., Lachemi, M. and Li, V.C. (2011). Effect of Fly Ash and PVA Fiber on Microstructural Damage and Residual Properties of Engineered Cementitious Composites Exposed to High Temperatures. Journal of materials in civil engineering, Vol. 23(12), pp.1735-1745.

Sahmaran,M. Lachemi, M. and Li, V.C. (2010). Assessing Mechanical Properties and Microstructure of Fire-Damaged Engineered Cementitious Composites. ACI Materials journal, Vol. 107(3), pp.297-304.

Sarker, P. K. (2011). Bond strength of reinforcing steel embedded in fly ash-based geopolymer concrete. Materials and Structures 44 (5): 1021-1030.

Shaikh, F.U.A. (2013). Deflection hardening behaviour of short fibre reinforced fly ash based geo-polymer composites. *Materials and Design,* Vol. 50: 674-680.

Shaikh, F.U.A. and Hosan, A. (2016). Mechanical properties of steel fibre reinforced geopolymer concretes at elevated temperatures. Construction and building materials, Vol. 114:15-28.

Shaikh, F.U.A. and Supit, W.M.S. (2014). Mechanical and durability properties of high volume fly ash (HVFA) concrete containing calcium carbonate ($CaCO_3$) nanoparticles. *Construction and building materials.* Vol. 70:309-321.

Shaikh, F.U.A. and Vimonsatit, V. (2015). Compressive strength of fly ash based geopolymer concrete at elevated temperatures. *Fire and Materials,* Vol. 39:174-188.

Shaikh, F.U.A., Supit, S. and Sarker, P. (2014). A study on the effect of nano silica on compressive strength of high volume fly ash mortar and concrete. *Materials and design,* Vol.60: 433-442

Silva, F.J. Mathias, A.F. Thaumaturgo, C. (1999). Evaluation of the fracture toughness in poly(sialate-siloxo) composite matrix, conference paper, Geopolymer 99 (1999) 97–106.

Skvara Frantisek, Kopecky Lubomir, Myskova Lenka, Smilauer Vit, Alberovska Lucie, Vinsova Lenka, (2007). Effect of curing temperature on the development of hard structure of metakaolin-base Geopolymer, Institute of chemistry, faculty of civil engineering, Brno University of technology. Czech Republic.

Skvara, F. (2007). Alkali activated materials or geopolymers. Ceram.-Silik. 51, 173–177.

Sofi, M. van Deventer, J.S.J. Mendis, P.A Lukey, G.C. (2007). Engineering properties of inorganic polymer concretes (IPCs). Cement and Concrete Research 37, 251–257.

Songpiriyakij S. (2010). Effect of Temperature on Compressive Strength of Fly Ash-based Geopolymer Mortar. Department of Civil and Environmental Engineering Technology, King Mongkut‟s Institute of Technology North Bangkok, Thailand.

Songpiriyakij. Smith, (2006). Engineering properties of MAE MOH fly ash Geopolymer concrete, International Conference on Pozzolan, Concrete and Geopolymer Khon Kaen, Thailand, May 24-25, 2006.

Steins, P., Poulesquen, A., Frizon, F., Diat, O., Jestin, J., Causse, J., Lambertin, D. & Rossignol, S. (2014). Effect of aging and alkali activator on the porous structure of a geopolymer. *Journal of Applied Crystallography*, 47, 1, 316-324.http://dx.doi.org/10.1107/s160057671303197x

Subaer, A. van Riessen, (2007). Thermo-mechanical and microstructural characterisation of sodium-poly(sialate-siloxo) (Na-PSS) geopolymers. J. Mater. Sci. 42; 3117–3123.

Sun, D. S. Wang, A. G. and Hu, P. H. (2005). Geopolymer research and application prospect. *Mater. Rev.*, vol. 7, pp.61-65.

Supit, W.M.S. and Shaikh, F.U.A. (2014). Durability properties of high volume fly ash concrete containing nano silica. *Materials and structures*, 48:2431-2445.

Swanepoel, J.C. Strydom, C.A. (2002). Utilisation of fly ash in a geopolymeric material. Appl Geochem;17(8):1143–8.

Temuujin, J. Minjigmaa, A. Rickard, W. Lee, M. Williams, I. van Riessen, A. (2010). Fly ash based geopolymer thin coatings on metal substrates and its thermal evaluation. J. Hazard. Mater. 180, 748–752

Thakur R. N. and Ghosh S. (2009). Performance of Fly Ash base Geopolymer composite at elevated temperature. International Journal of Applied Engineering Research Volume 4,No,4, April 2009.

Thokchom, S. Ghosh, P. Ghosh, S. (2009). Effect of water absorption, porosity and sorptivity on durability of Geopolymer mortar. Vol. 4, NO. 7, September. ARPN Journal of Engineering and Applied Sciences.

Tippayasam, C. Balyore, P. Thavorniti, P. Kamseu, E. C. Leonelli, C. Chindaprasirt, P. Chaysuwan, D. (2016). Potassium alkali concentration and heat treatment affected metakaolin-based geopolymer. Constr. Build. Mater., 104, pp. 293–297

Univ. of Michigan, ACE MRL. (2008). Some ECC applications. ⟨http://ace-mrl.engin.umich.edu/NewFiles/eccapp.html⟩

Valeria, F.F. Barbosa, K. Mackenzie, J. D. (2003). Thermal behavior of inorganic Geopolymer and composites derive from sodium polysialate Materials research Bulletin 38 319-331 New Zealand institute for industrial Research and Development, P.O. Box 31-310, Lower Hutt.

Van Jaarsveld J.G.S., van Deventer, J.S.J and Lukey G.C (2003). The characterisation of source materials in fly ash-based geopolymers, Materials Letters 57, 1272–1280. Department of Chemical Engineering, the University of Melbourne, Victoria 3010, Australia.

Vit Petranek, Lenka, N. Dana, Z. Sergey, G. (2014) Thermal Insulating Materials for Energy Storage Application. Advanced Materials Research Vol. 911, pp 30-35. Trans Tech Publications, Switzerland.

Wallah, S.E. Rangan, B.V. (2006). Low-calcium fly ash based geopolymer concrete: long term properties. Research Report GC 2, Curtin University of Technology, Australia.

Wang, M.R. Jia, D.C. He, P.G. Zhou, Y. (2010). Influence of calcination temperature of kaolin on the structure and properties of final geopolymer Mater. Lett., 64 (22), pp. 2551–2554

Washburn, E.W. (1921). Note on a method of determining the distribution of pore sizes in a porous material, Proc. Natl. Acad. Sci. USA 7 (4). 115–116.

Welter, M. Schmücker, M. MacKenzie, K.J.D. (2015). Evolution of the Fibre-Matrix Interactions in Basalt-Fibre-Reinforced Geopolymer-Matrix Composites after Heating. J. Ceram. Sci. Tech., 06 [01] 17-24.

Xu H. & van Deventer J.S.J. (2000). The geopolymerisation of alumina-silicate minerals. International Journal of Mineral Processing. Vol. 59, pp. 247 – 266

Zanotti, C., Borges, P.H.R., Bhutta, A., Du, Y. and Banthia, N. (2016). Bond strength of PVA fibre reinforced geopolymer repair to Portland cement concrete substrate. 9th international symposium on fibre reinforced concrete – BEFIB2016, Vancouver, Canada. 90-100.

Zhang, H. Kodur, V. Cao, L. and Qi, S. (2014). Fibre reinforced geopolymers for fire resistance applications. Procedia engineering, 71: 153-158.

Zhang, M.H. Islam, J. (2012). Use of nano-silica to reduce setting time and increase early strength of concretes with high volume fly ash or slag. Constr Build Mater ; 29: 573–80.

Zhang, Y. S. Sun, W. and Li, Z. J. (2010). Composition design and microstructural characterization of calcined kaolin-based geopolymer cement. *Appl. Clay. Sci.* vol. 47, pp.271-275.

Zoulgami, M. Lucas-Girot, A. Michaud, V. Briard, P. Gaudé, J. and Oudadesse, H. (2002). Synthesis and physico-chemical characterization of a polysialate-hydroxyapatite composite for potential biomedical application. *Eur. Phys. J. AP*, 19, 173-179.

# APPENDIX

## A.1 COMPRESSIVE STRENGTH SETUP AND CRACKING

This shows the compressive strength setup and some cracking figures.


Figure A. 1: Compressive strength test of samples

Figure A. 2 Cracking of samples after compressive strength test

Figure A. 3 Samples heated at $800^0$C after compressive st test

Figure A. 4 Samples after compressive st test (ambient temperature)

## A.2. SEM IMAGE OF FIBRE SAMPLES

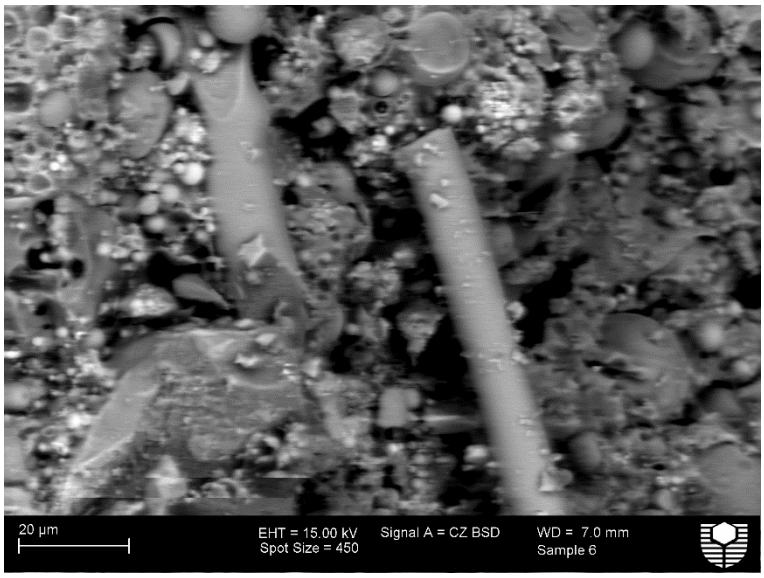


Figure A. 5 SEM image (sample with basalt fibre, 800 deg C)

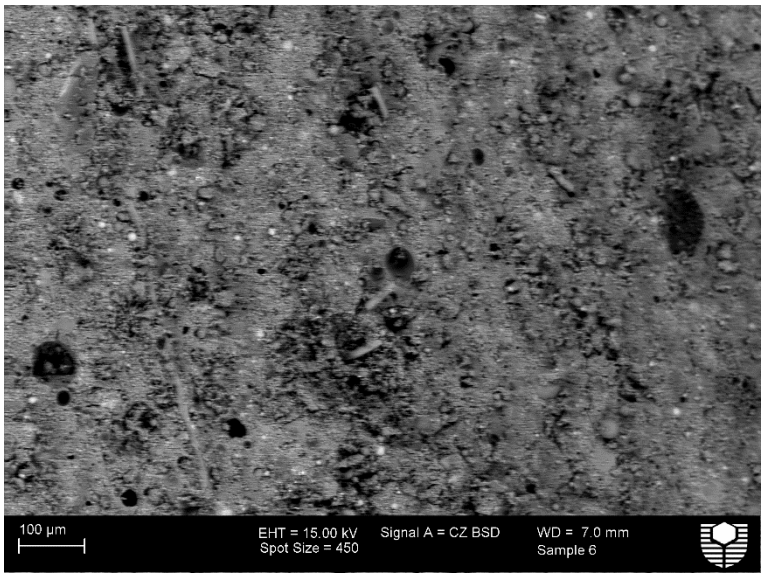


Figure A. 6 SEM image (sample with basalt fibre, 800 deg C)

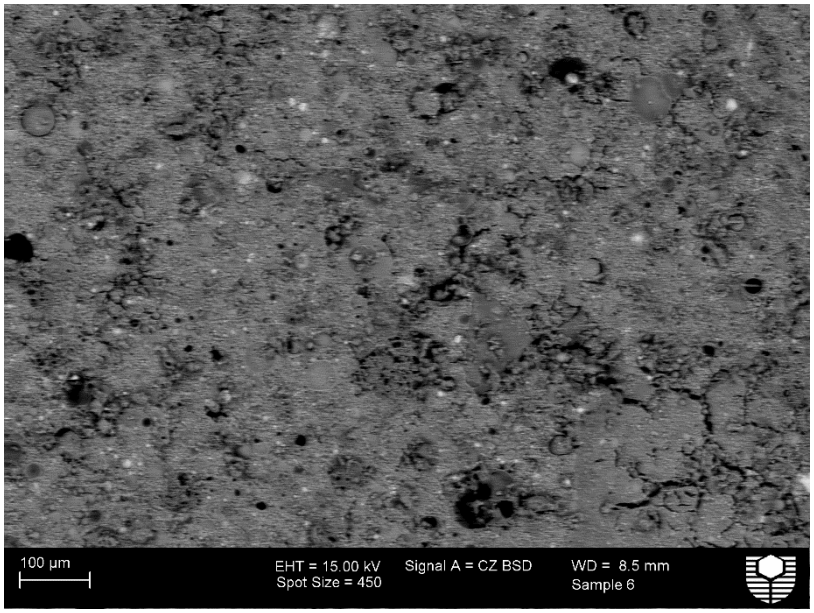


Figure A. 7 SEM image (sample with basalt fibre, 800 deg C)

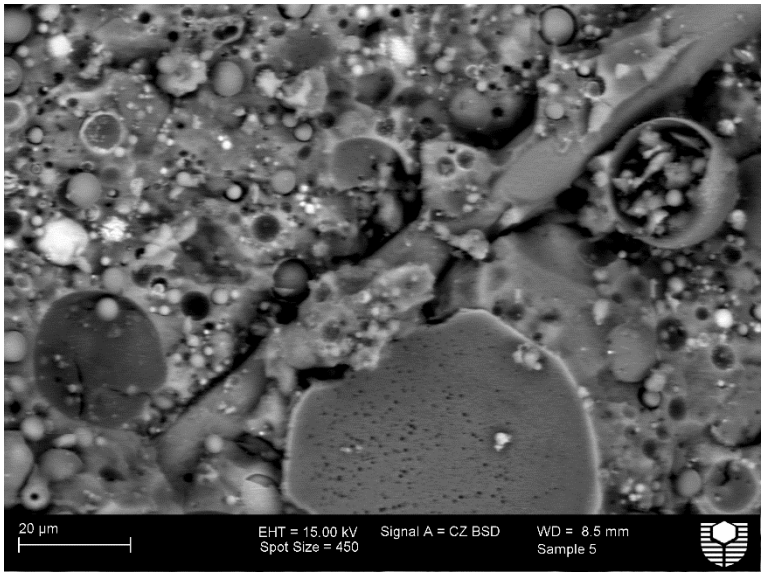


Figure A. 8 SEM image (sample with basalt fibre, 400 deg C)


Figure A. 9 SEM image (sample with basalt fibre, 400 deg C)


Figure A. 10 SEM image (sample with basalt fibre, 400 deg C)


Figure A. 11 SEM image (sample with basalt fibre, 28 deg C)

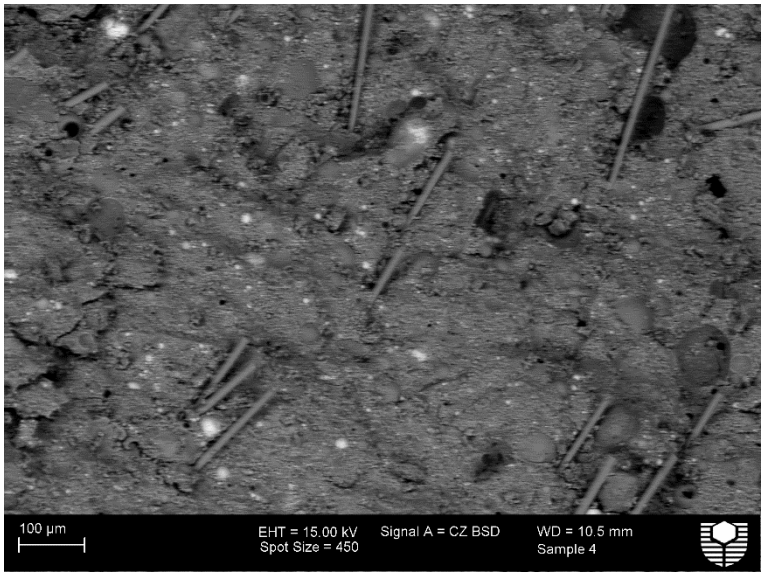


Figure A. 12 SEM image (sample with basalt fibre, 28 deg C)


Figure A. 13 SEM image (sample with basalt fibre, 28 deg C)

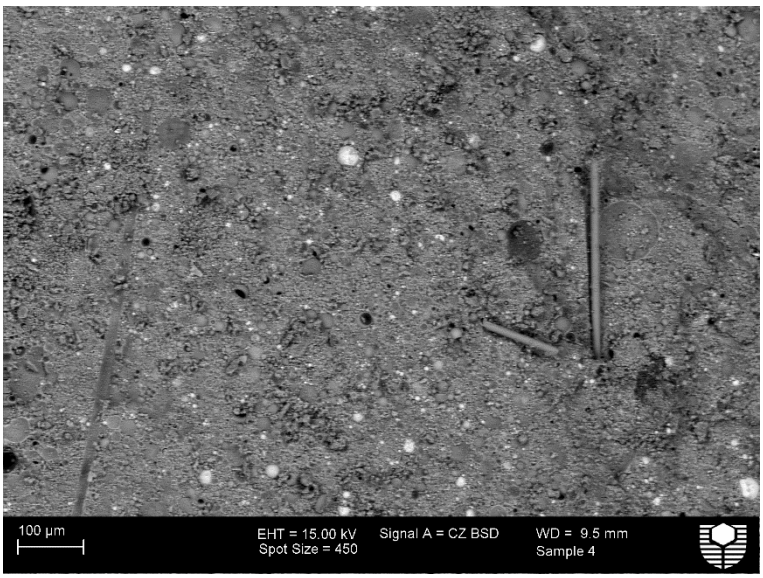


Figure A. 14 SEM image (sample with basalt fibre, 28 deg C)

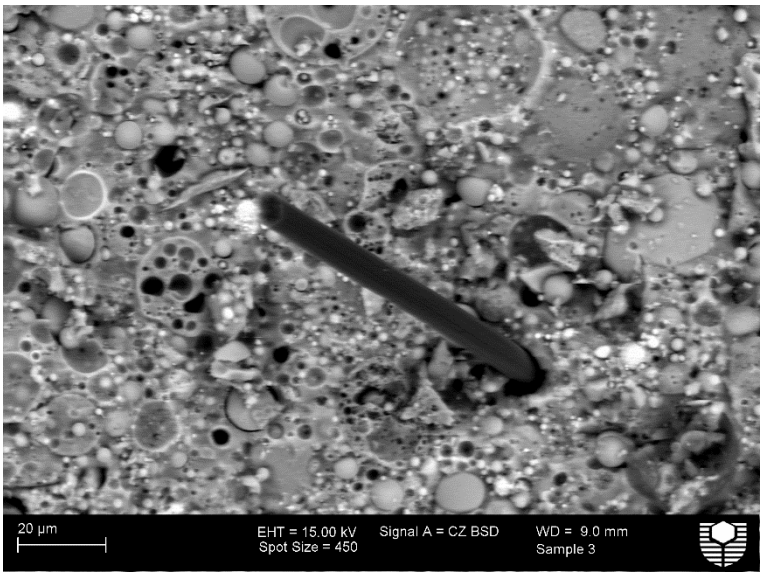


Figure A. 15 SEM image (sample with carbon fibre, 800 deg C)

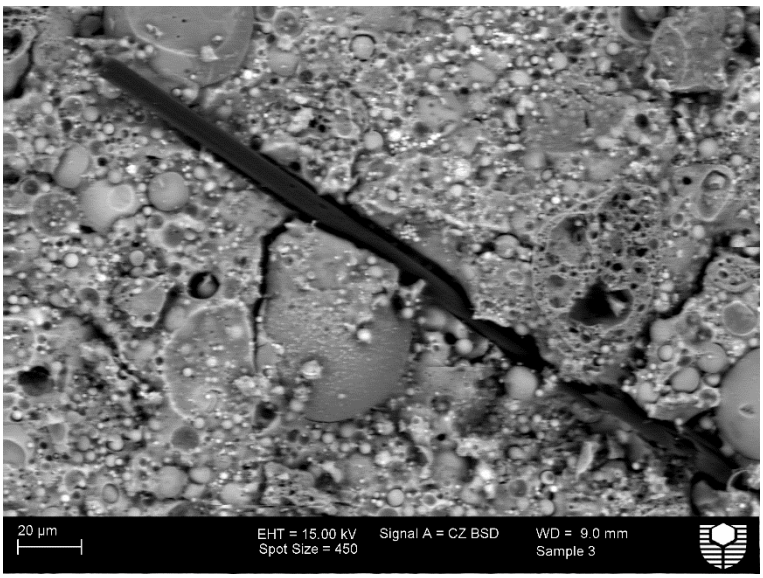


Figure A. 16 SEM image (sample with carbon fibre, 800 deg C)

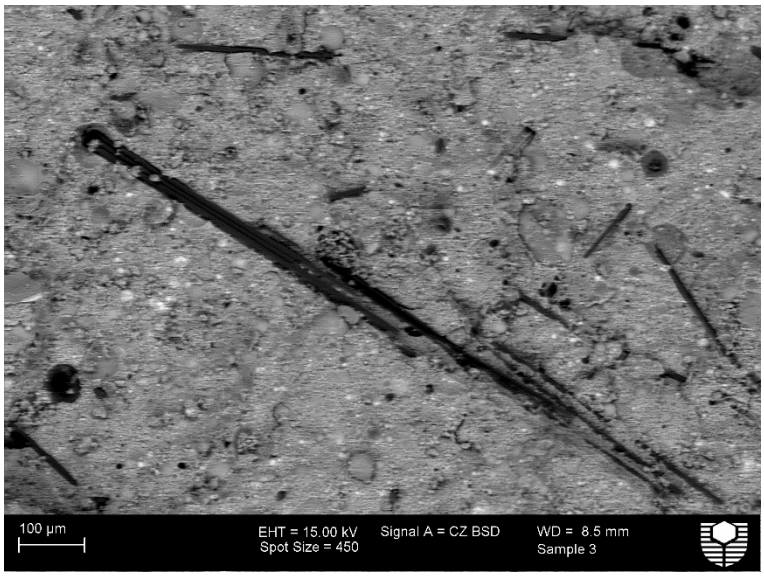


Figure A. 17 SEM image (sample with carbon fibre, 28 deg C)

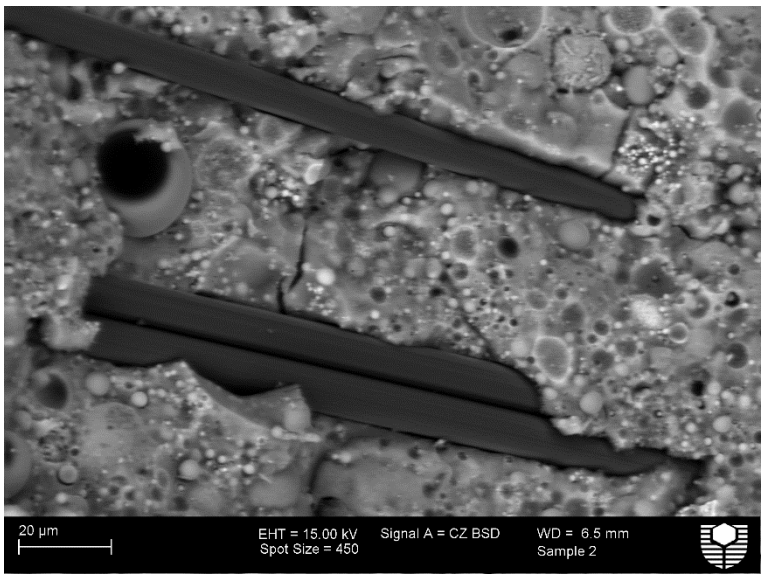


Figure A. 18 SEM image (sample with carbon fibre, 400 deg C)

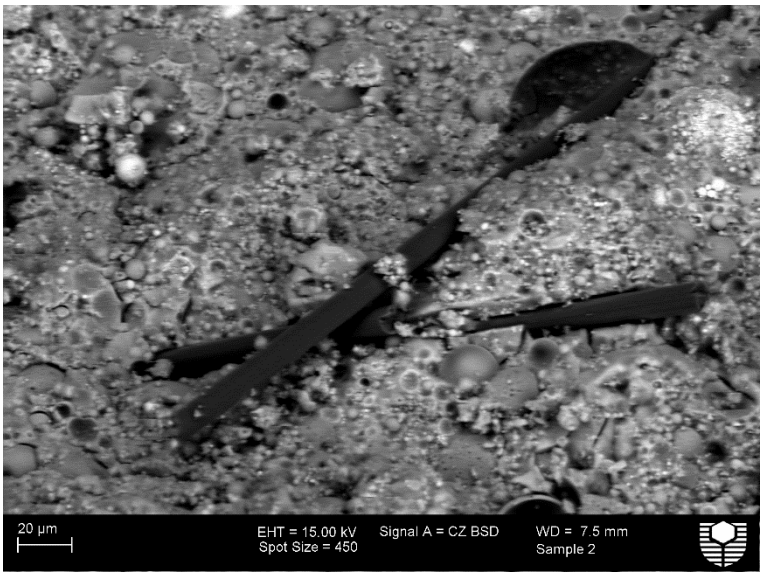


Figure A. 19 SEM image (sample with carbon fibre, 400 deg C)

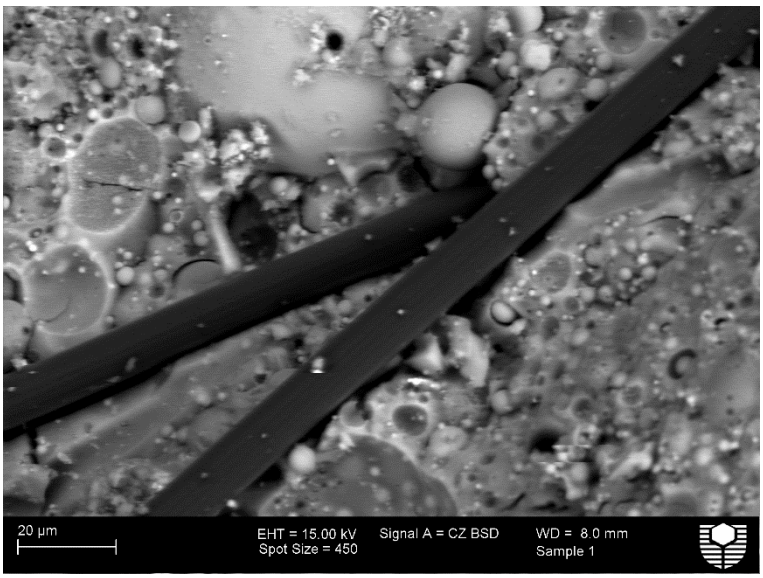


Figure A. 20 SEM image (sample with carbon fibre, 28 deg C)

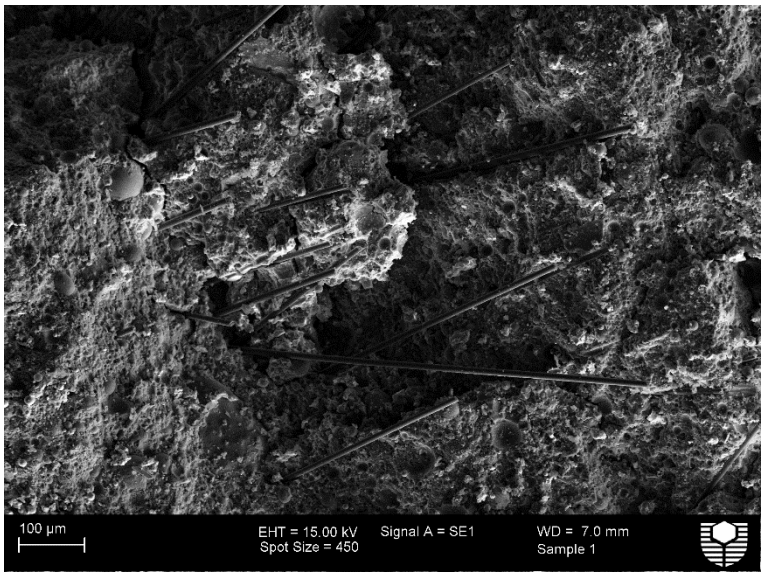


Figure A. 21 SEM image (sample with carbon fibre, 28 deg C)

## A.3. THERMAL CONDUCTIVITY

This part states the result from the thermal conductivity test

**Table A. 1 Thermal conductivity test data**

| | Na based system | | K based system | |
|---|---|---|---|---|
| TC test | 23-11-15 | 24-11-15 | | |
| Sample | GPNa test | | | |
| Thickness | 0.01789 | 0.01789 | 0.01813 | 0.0187 |
| Area | 0.004094155 | 0.0040942 | 0.003914707 | 0.003919 |
| T (H) | 36.3 | 36.6 | 35.04 | 36.36 |
| T (C ) | 17.7 | 17.75 | 17.7 | 17.72 |
| | | | | |
| V (sensor) | 0.0222 | 0.0221 | 0.02 | 0.01754 |
| Q (W/m2) | 350.1025075 | 348.52547 | 315.4076644 | 276.6125 |
| Q' (J/s) | 1.433373918 | 1.4269173 | 1.234728652 | 1.084084 |
| | | | | |
| therefore | | | | |
| k | 0.337 | 0.331 | 0.330 | 0.278 |
| | | | | |
| **Average K** | **0.334** | | **0.304** | |
| | | | -9 | % |

**B.1 Compressive strength results of Na-based geopolymer paste mixtures after exposure to elevated temperatures of 200, 400, 600, and 800ºC.**

B.1.1 Compressive strengths of Na-based geopolymer pastes at ambient temperature

| Series | Specimen No. | Size(mm) | Ultimate Load, KN | Compressive strength (MPa) | Average strength (MPa) |
|---|---|---|---|---|---|
| Na-2 | 1 | 50.4x51.4x50.5 | 98.5 | 38.62 | 53.59 |
| | 2 | 50.9x51.4x50.5 | 152 | 58.09 | |
| | 3 | 50.6x51.0x50.6 | 120 | 46.50 | |
| | 4 | 50.8x51.0x50.6 | 154 | 59.44 | |
| | 5 | 50.6x51.4x51.4 | 132 | 50.75 | |
| | 6 | 50.6x51.0x50.7 | 113 | 43.79 | |

B.1.2 Compressive strengths of Na-based geopolymer pastes at 200ºC temperature

| Series | Specimen No. | Size(mm) | Ultimate Load, KN | Compressive strength (MPa) | Average strength (MPa) |
|---|---|---|---|---|---|
| Na-2 | 1 | 50.2x51.5x50.5 | 96.20 | 37.21 | 58.35 |
| | 2 | 50.4x51.5x50.2 | 134.32 | 51.75 | |
| | 3 | 50.7x50.8x50.3 | 82.5 | 32.03 | |
| | 4 | 51.0x50.5x50.5 | 172.7 | 67.05 | |
| | 5 | 50.3x50.0x50.8 | 98.3 | 39.08 | |
| | 6 | 50.3x51.2x50.7 | 146.7 | 56.96 | |

B.1.3 Compressive strengths of Na-based geopolymer pastes at 400ºC temperature

| Series | Specimen No. | Size(mm) | Ultimate Load, KN | Compressive strength (MPa) | Average strength (MPa) |
|---|---|---|---|---|---|
| Na-2 | 1 | 50.4x50.8x50.5 | 76.3 | 30.03 | 55.71 |
| | 2 | 50.7x50.0x50.5 | 169.5 | 66.86 | |
| | 3 | 50.0x50.3x50.9 | 157.0 | 62.42 | |
| | 4 | 50.4x50.0x50.6 | 114 | 45.18 | |
| | 5 | 50.2x50.0x51.4 | 121.5 | 48.40 | |
| | 6 | 50.0x49.7x50.7 | 78.7 | 31.35 | |

B.1.4 Compressive strengths of Na-based geopolymer pastes at 600ºC temperature

| Series | Specimen No. | Size(mm) | Ultimate Load, KN | Compressive strength (MPa) | Average strength (MPa) |
|---|---|---|---|---|---|
| Na-2 | 1 | 49.4x50x49.9 | 149 | 60.32 | 52.20 |
| | 2 | 50.1x49.5x49.3 | 121 | 48.79 | |
| | 3 | 49.2x48.3x49.2 | 120 | 50.5 | |
| | 4 | 49.7x50.1x49.7 | 128 | 51.40 | |
| | 5 | 49.2x49.5x49.0 | 139 | 50.07 | |
| | 6 | 49.1x49.7x49.1 | 127.5 | 52.24 | |

B.1.5 Compressive strengths of Na-based geopolymer pastes at 800ºC temperature

| Series | Specimen No. | Size(mm) | Ultimate Load, KN | Compressive strength (MPa) | Average strength (MPa) |
|---|---|---|---|---|---|
| Na-2 | 1 | 49.5x48.8x50 | 54 | 22.35 | 24.78 |
| | 2 | 49.0x49.5x49.4 | 59 | 24.32 | |
| | 3 | 49.5x49.0x48.1 | 65 | 26.80 | |
| | 4 | 49.0x49.0x48.5 | 65 | 27.07 | |
| | 5 | 50x48.7x48.5 | 57 | 23.40 | |
| | 6 | 48.8x48.5x49.6 | 28.5 | - | |

B.1.6 Compressive strengths of Na-based geopolymer pastes at ambient temperature

| Series | Specimen No. | Size(mm) | Ultimate Load, KN | Compressive strength (MPa) | Average strength (MPa) |
|---|---|---|---|---|---|
| Na-2.5 | 1 | 51.0x50.3x51.1 | 98.0 | 38.20 | 55.95 |
| | 2 | 50.8x50.4x50.4 | 95.0 | 37.10 | |
| | 3 | 50.6x52.0x50.9 | 133.0 | 50.50 | |
| | 4 | 50.7x52.0x50.6 | 168.0 | 63.72 | |
| | 5 | 50.8x50.9x50.9 | 141.0 | 54.53 | |
| | 6 | 51.1x51.7x50.4 | 145.5 | 55.07 | |

B.1.7 Compressive strengths of Na-based geopolymer pastes at 200ºC temperature

| Series | Specimen No. | Size(mm) | Ultimate Load, KN | Compressive strength (MPa) | Average strength (MPa) |
|---|---|---|---|---|---|
| Na-2.5 | 1 | 51.2x49.9x50.2 | 180 | 70.49 | 62.33 |
| | 2 | 50.3x51.5x50.6 | 206 | 79.52 | |
| | 3 | 51.0x50.2x50.6 | 130 | 50.78 | |
| | 4 | 50.0x52.0x50.8 | 255 | - | |
| | 5 | 51.1x50.0x50.1 | 201 | 78.66 | |
| | 6 | 50.3x51.5x50.5 | 84 | 32.42 | |

B.1.8 Compressive strengths of Na-based geopolymer pastes at 400ºC temperature

| Series | Specimen No. | Size(mm) | Ultimate Load, KN | Compressive strength (MPa) | Average strength (MPa) |
|---|---|---|---|---|---|
| Na-2.5 | 1 | 50.9x49.4x49.8 | 162.5 | 64.62 | 49.78 |
| | 2 | 49.6x49.7x49.1 | 71.10 | - | |
| | 3 | 49.4x50.1x59.7 | 70.0 | - | |
| | 4 | 50.7x49.7x49.5 | 111.5 | 44.25 | |
| | 5 | 49.3x49.5x50.3 | 121.0 | 49.58 | |
| | 6 | 50.6x50.5x50.5 | 138.0 | 54.0 | |

B.1.9 Compressive strengths of Na-based geopolymer pastes at 600ºC temperature

| Series | Specimen No. | Size(mm) | Ultimate Load, KN | Compressive strength (MPa) | Average strength (MPa) |
|---|---|---|---|---|---|
| Na-2.5 | 1 | 50x49.3x49.4 | 137 | 55.58 | 49.04 |
| | 2 | 49.6x49.4x49.3 | 135 | 55.09 | |
| | 3 | 49.2x50.2x49.5 | 99 | 40.08 | |
| | 4 | 49.5x49.6x49.4 | 127 | 51.72 | |
| | 5 | 50.0x49.0x49.2 | 105.5 | 43.06 | |
| | 6 | 49.1x49.3x49.5 | 118 | 48.75 | |

B.1.10 Compressive strengths of Na-based geopolymer pastes at 800ºC temperature

| Series | Specimen No. | Size(mm) | Ultimate Load, KN | Compressive strength (MPa) | Average strength (MPa) |
|---|---|---|---|---|---|
| Na-2.5 | 1 | 48.9x48.7x49.5 | 67.6 | 28.38 | 25.40 |
| | 2 | 48.6x49.7x50.3 | 61.6 | 25.5 | |
| | 3 | 49.0x48.8x48.7 | 67.5 | 28.22 | |
| | 4 | 49.0x49.4x48.1 | 59.8 | 25.0 | |
| | 5 | 49.0x48.8x48.5 | 50.3 | 21.03 | |
| | 6 | 49.3x49.3x48.2 | 59.2 | 24.35 | |

B.1.11 Compressive strengths of Na-based geopolymer pastes at ambient temperature

| Series | Specimen No. | Size(mm) | Ultimate Load, KN | Compressive strength (MPa) | Average strength (MPa) |
|---|---|---|---|---|---|
| Na-3 | 1 | 51.2x50.4x50.5 | 64 | - | 39.47 |
| | 2 | 50x50.6x50.7 | 106 | 41.89 | |
| | 3 | 50.5x50.3x50.6 | 94.5 | 37.20 | |
| | 4 | 51.0x50.6x51.3 | 96.0 | 37.20 | |
| | 5 | 50.7x50.7x506 | 103.5 | 40.26 | |
| | 6 | 51.2x51.5x50.3 | 107.7 | 40.77 | |

B.1.12 Compressive strengths of Na-based geopolymer pastes at 200ºC temperature

| Series | Specimen No. | Size(mm) | Ultimate Load, KN | Compressive strength (MPa) | Average strength (MPa) |
|---|---|---|---|---|---|
| Na-3 | 1 | 49.5x50.2x51.1 | 46.5 | - | 53.35 |
| | 2 | 49.8x51x51.5 | 123.5 | 48.62 | |
| | 3 | 50x50.1x50.2 | 108.0 | 43.11 | |
| | 4 | 50.0x50.2x50.1 | 172.0 | 68.52 | |
| | 5 | 49.8x50.6x50.5 | 134.0 | 53.17 | |
| | 6 | 49.8x50x50.0 | 81.5 | - | |

B.1.13 Compressive strengths of Na-based geopolymer pastes at 400ºC temperature

| Series | Specimen No. | Size(mm) | Ultimate Load, KN | Compressive strength (MPa) | Average strength (MPa) |
|---|---|---|---|---|---|
| Na-3 | 1 | 49.8x49.6x49.6 | 170 | - | 51.68 |
| | 2 | 49.8x49.6x49.5 | 125 | 50.6 | |
| | 3 | 49.9x49.0x50.0 | 129 | 52.75 | |
| | 4 | 49.8x50.2x49.8 | 134 | 53.60 | |
| | 5 | 49.6x49.7x49.8 | 109 | 44.22 | |
| | 6 | 49.6x49.3x50.4 | 140 | 55.25 | |

B.1.14 Compressive strengths of Na-based geopolymer pastes at 600ºC temperature

| Series | Specimen No. | Size(mm) | Ultimate Load, KN | Compressive strength (MPa) | Average strength (MPa) |
|---|---|---|---|---|---|
| Na-3 | 1 | 49.9x49.8x50 | 102 | 41.04 | 49.86 |
| | 2 | 49.3x49.0x49.5 | 136 | 56.29 | |
| | 3 | 49.5x49.5x49.5 | 138 | 56.32 | |
| | 4 | 49.0x49.2x49.8 | 120 | 49.78 | |
| | 5 | 49.5x49.5x49.4 | 104 | 42.44 | |
| | 6 | 49.4x49.0x49.2 | 129 | 53.29 | |

B.1.15 Compressive strengths of Na-based geopolymer pastes at 800ºC temperature

| Series | Specimen No. | Size(mm) | Ultimate Load, KN | Compressive strength (MPa) | Average strength (MPa) |
|---|---|---|---|---|---|
| Na-3 | 1 | 49.0x48.5x49.0 | 45.5 | 19.14 | 25.15 |
| | 2 | 49.1x49.1x49.0 | 65.0 | 26.96 | |
| | 3 | 49.0x48.7x49.2 | 71.0 | 29.75 | |
| | 4 | 49.4x49.0x48.6 | 70.5 | 29.12 | |
| | 5 | 49.0x48.5x49.2 | 42.0 | 17.67 | |
| | 6 | 49.4x49.0x49.6 | 68.4 | 28.25 | |

**B.2 Compressive strength results of K-based geopolymer paste mixtures after exposure to elevated temperatures of 200, 400, 600, and 800ºC.**

B.2.1 Compressive strengths of K-based geopolymer pastes at ambient temperature

| Series | Specimen No. | Size(mm) | Ultimate Load, KN | Compressive strength (MPa) | Average strength (MPa) |
|---|---|---|---|---|---|
| K-2 | 1 | 50.2x50.1x50.4 | 84.0 | 33.4 | 36.97 |
| | 2 | 49.3x50.7x50.5 | 84.0 | 33.60 | |
| | 3 | 49.4x50.6x50.8 | 87.5 | 35.0 | |
| | 4 | 50.8x50.1x50.1 | 125.5 | 49.31 | |
| | 5 | 50.2x50.1x50.5 | 90.5 | 35.98 | |
| | 6 | 50.4x50.5x50.5 | 88.0 | 34.57 | |

B.2.2 Compressive strengths of K-based geopolymer pastes at 200ºC temperature

| Series | Specimen No. | Size(mm) | Ultimate Load, KN | Compressive strength (MPa) | Average strength (MPa) |
|---|---|---|---|---|---|
| K-2 | 1 | 50.0x49.5x50.2 | 90.0 | 36.36 | 38.42 |
| | 2 | 49.8x50.1x50.2 | 120.0 | 48.09 | |
| | 3 | 50.2x50.4x50.6 | 98.0 | 38.73 | |
| | 4 | 50.2x49.4x50.5 | 88.0 | 35.48 | |
| | 5 | 50.2x50.3x50.0 | 79.0 | 31.28 | |
| | 6 | 50.7x50.8x50.2 | 104.5 | 40.57 | |

B.2.3 Compressive strengths of K-based geopolymer pastes at 400ºC temperature

| Series | Specimen No. | Size(mm) | Ultimate Load, KN | Compressive strength (MPa) | Average strength (MPa) |
|---|---|---|---|---|---|
| K-2 | 1 | 49.1x49.5x49.5 | 132.5 | 54.51 | 53.13 |
| | 2 | 49.7x49.0x49.8 | 102.5 | 42.08 | |
| | 3 | 50.1x50.0x50.0 | 139.0 | 55.49 | |
| | 4 | 49.5x49.7x50.1 | 132.0 | 53.65 | |
| | 5 | 49.4x49.6x49.8 | 65.5 | - | |
| | 6 | 50.1x50.1x50.2 | 150.5 | 59.95 | |

B.2.4 Compressive strengths of K-based geopolymer pastes at 600ºC temperature

| Series | Specimen No. | Size(mm) | Ultimate Load, KN | Compressive strength (MPa) | Average strength (MPa) |
|---|---|---|---|---|---|
| K-2 | 1 | 50.1x49.5x50.0 | 142.0 | 57.25 | 58.25 |
| | 2 | 49.5x50.2x49.7 | 157.5 | 63.38 | |
| | 3 | 49.7x49.5x49.7 | 138.5 | 56.29 | |
| | 4 | 49.8x49.6x50.2 | 167.5 | 67.81 | |
| | 5 | 49.5x49.5x49.6 | 108.5 | 44.28 | |
| | 6 | 49.8x49.8x49.6 | 150.0 | 60.48 | |

B.2.5 Compressive strengths of K-based geopolymer pastes at 800ºC temperature

| Series | Specimen No. | Size(mm) | Ultimate Load, KN | Compressive strength (MPa) | Average strength (MPa) |
|---|---|---|---|---|---|
| K-2 | 1 | 48.2x48.0x48.4 | 74.5 | 32.20 | 33.28 |
| | 2 | 48.6x48.7x49.1 | 64.0 | 27.04 | |
| | 3 | 49.0x48.8x49.6 | 93.5 | 39.10 | |
| | 4 | 48.5x48.8x48.4 | 78.0 | 32.96 | |
| | 5 | 49.1x49.0x48.8 | 80.5 | 33.46 | |
| | 6 | 48.9x49.8x49.5 | 85.0 | 34.70 | |

B.2.6 Compressive strengths of K-based geopolymer pastes at ambient temperature

| Series | Specimen No. | Size(mm) | Ultimate Load, KN | Compressive strength (MPa) | Average strength (MPa) |
|---|---|---|---|---|---|
| K-2.5 | 1 | 50.8x49.5x50.2 | 62.0 | 24.65 | 28.08 |
| | 2 | 50.1x50.0x50.1 | 68.0 | 27.14 | |
| | 3 | 50.4x50.3x50.4 | 69.0 | 27.21 | |
| | 4 | 50.1x50.1x50.2 | 88.0 | 35.06 | |
| | 5 | 50.2x49.8x50.2 | 75.0 | 30.0 | |
| | 6 | 50.2x49.8x50.0 | 61.0 | 24.40 | |

B.2.7 Compressive strengths of K-based geopolymer pastes at 200ºC temperature

| Series | Specimen No. | Size(mm) | Ultimate Load, KN | Compressive strength (MPa) | Average strength (MPa) |
|---|---|---|---|---|---|
| K-2.5 | 1 | 50.2x50.3x50.5 | 103.0 | 40.80 | 31.26 |
| | 2 | 50.4x50.5x50.2 | 65.0 | 25.54 | |
| | 3 | 50.0x50.2x51.1 | 69.0 | 27.49 | |
| | 4 | 50.6x50.2x50.4 | 65.0 | 25.60 | |
| | 5 | 50.4x50.3x49.9 | 62.0 | 24.45 | |
| | 6 | 50.1x50.2x51.0 | 110.0 | 43.73 | |

B.2.8 Compressive strengths of K-based geopolymer pastes at 400ºC temperature

| Series | Specimen No. | Size(mm) | Ultimate Load, KN | Compressive strength (MPa) | Average strength (MPa) |
|---|---|---|---|---|---|
| K-2.5 | 1 | 49.8x49.9x50.0 | 151.0 | 60.76 | 42.89 |
| | 2 | 49.7x49.2x49.4 | 73.0 | 29.85 | |
| | 3 | 49.4x49.9x50.1 | 93.0 | 37.73 | |
| | 4 | 50.0x49.8x50.0 | 68.0 | 27.30 | |
| | 5 | 49.9x49.0x49.9 | 115.0 | 47.03 | |
| | 6 | 49.8x49.2x50.4 | 134.0 | 54.69 | |

B.2.9 Compressive strengths of K-based geopolymer pastes at 600ºC temperature

| Series | Specimen No. | Size(mm) | Ultimate Load, KN | Compressive strength (MPa) | Average strength (MPa) |
|---|---|---|---|---|---|
| K-2.5 | 1 | 50.8x49.8x49.8 | 110.0 | 43.48 | 40.60 |
| | 2 | 50.0x50.2x49.7 | 108.0 | 43.02 | |
| | 3 | 49.7x49.7x49.6 | 86.0 | 34.81 | |
| | 4 | 49.8x49.8x49.4 | 102.0 | 41.10 | |
| | 5 | 49.8x50.1x49.8 | 47.0 | - | |
| | 6 | 50.0x49.7x49.7 | 66.0 | - | |

B.2.10 Compressive strengths of K-based geopolymer pastes at 800ºC temperature

| Series | Specimen No. | Size(mm) | Ultimate Load, KN | Compressive strength (MPa) | Average strength (MPa) |
|---|---|---|---|---|---|
| K-2.5 | 1 | 49.2x49.0x49.5 | 51.0 | 21.15 | 26.60 |
| | 2 | 49.6x48.9x48.4 | 76.0 | 31.33 | |
| | 3 | 48.5x49.1x48.7 | 67.0 | 27.72 | |
| | 4 | 48.9x49.0x48.8 | 62.0 | 25.88 | |
| | 5 | 48.9x49.0x49.2 | 59.0 | 25.62 | |
| | 6 | 49.0x49.5x48.9 | 70.0 | 28.86 | |

B.2.11 Compressive strengths of K-based geopolymer pastes at ambient temperature

| Series | Specimen No. | Size(mm) | Ultimate Load, KN | Compressive strength (MPa) | Average strength (MPa) |
|---|---|---|---|---|---|
| K-3 | 1 | 50.2x50.5x50.8 | 78.0 | 30.77 | 29.26 |
| | 2 | 50.4x50.2x50.7 | 72.0 | 28.46 | |
| | 3 | 50.2x50.0x50.6 | 71.0 | 28.28 | |
| | 4 | 50.3x50.5x50.2 | 80.0 | 31.50 | |
| | 5 | 50.0x50.2x50.5 | 68.5 | 27.30 | |
| | 6 | 50.1x49.8x50.0 | 48.5 | - | |

B.2.12 Compressive strengths of K-based geopolymer pastes at 200ºC temperature

| Series | Specimen No. | Size(mm) | Ultimate Load, KN | Compressive strength (MPa) | Average strength (MPa) |
|---|---|---|---|---|---|
| K-3 | 1 | 50.2x50.0x50.1 | 84.0 | 33.47 | 31.20 |
| | 2 | 50.2x49.5x50.2 | 35.5 | - | |
| | 3 | 50.0x50.0x50.8 | 80.0 | 32.0 | |
| | 4 | 50.6x50.0x50.5 | 91.0 | 35.97 | |
| | 5 | 50.4x50.2x50.8 | 70.5 | 27.86 | |
| | 6 | 50.1x50.5x50.2 | 67.5 | 26.67 | |

B.2.13 Compressive strengths of K-based geopolymer pastes at 400ºC temperature

| Series | Specimen No. | Size(mm) | Ultimate Load, KN | Compressive strength (MPa) | Average strength (MPa) |
|---|---|---|---|---|---|
| K-3 | 1 | 49.8x49.0x50.0 | 94.5 | 38.73 | 35.94 |
| | 2 | 50.1x49.5x49.6 | 50.0 | - | |
| | 3 | 50.5x49.2x50.2 | 99.0 | 39.84 | |
| | 4 | 49.6x50.0x50.0 | 91.0 | 36.70 | |
| | 5 | 49.9x49.6x50.1 | 90.0 | 36.36 | |
| | 6 | 49.8x50.1x49.9 | 70.0 | 28.05 | |

B.2.14 Compressive strengths of K-based geopolymer pastes at 600ºC temperature

| Series | Specimen No. | Size(mm) | Ultimate Load, KN | Compressive strength (MPa) | Average strength (MPa) |
|---|---|---|---|---|---|
| K-3 | 1 | 50.0x49.2x50.0 | 87.5 | 35.6 | 36.98 |
| | 2 | 49.6x49.8x50.0 | 79.0 | 32.0 | |
| | 3 | 49.9x49.3x49.8 | 90.0 | 36.58 | |
| | 4 | 49.8x49.5x49.9 | 102.5 | 41.60 | |
| | 5 | 49.8x50.0x49.8 | 99.0 | 39.75 | |
| | 6 | 49.0x50.2x50.3 | 89.5 | 36.38 | |

B.2.15 Compressive strengths of K-based geopolymer pastes at 800ºC temperature

| Series | Specimen No. | Size(mm) | Ultimate Load, KN | Compressive strength (MPa) | Average strength (MPa) |
|---|---|---|---|---|---|
| K-3 | 1 | 49.2x48.6x49.5 | 26.5 | - | 30.58 |
| | 2 | 48.9x49.0x49.0 | 61.5 | 25.67 | |
| | 3 | 48.6x48.8x49.9 | 66.0 | 27.82 | |
| | 4 | 48.9x48.8x49.0 | 79.4 | 33.27 | |
| | 5 | 48.7x48.8x49.5 | 73.0 | 30.72 | |
| | 6 | 48.8x48.0x49.1 | 83.0 | 35.43 | |

**B.3 Mass loss results of Na-based geopolymer paste after exposure to elevated temperatures.**

B.3.1 Mass loss results of Na-based geopolymer paste at 200ºC temperature.

| Series | Specimen No. | Wt. before exposure, gm | Wt. after exposure, gm | Mass loss, gm | Average mass loss, gm |
|---|---|---|---|---|---|
| Na-2 | 1 | 233.27 | 223.23 | 10.04 | 11.44 |
| | 2 | 236.49 | 224.25 | 12.24 | |
| | 3 | 237.32 | 227.12 | 10.20 | |
| | 4 | 235.01 | 223.03 | 11.98 | |
| | 5 | 227.47 | 216.48 | 10.99 | |
| | 6 | 240.76 | 227.56 | 13.20 | |

B.3.2 Mass loss results of Na-based geopolymer paste at 400ºC temperature.

| Series | Specimen No. | Wt. before exposure, gm | Wt. after exposure, gm | Mass loss, gm | Average mass loss, gm |
|---|---|---|---|---|---|
| Na-2 | 1 | 233.32 | 211.30 | 22.02 | 21.95 |
| | 2 | 235.29 | 214.85 | 20.44 | |
| | 3 | 234.65 | 212.24 | 22.41 | |
| | 4 | 235.49 | 213.44 | 22.25 | |
| | 5 | 234.58 | 212.59 | 22.00 | |
| | 6 | 234.20 | 211.63 | 22.57 | |

B.3.3 Mass loss results of Na-based geopolymer paste at 600ºC temperature.

| Series | Specimen No. | Wt. before exposure, gm | Wt. after exposure, gm | Mass loss, gm | Average mass loss, gm |
|---|---|---|---|---|---|
| Na-2 | 1 | 234.74 | 209.58 | 25.18 | 26.58 |
| | 2 | 237.56 | 210.10 | 27.46 | |
| | 3 | 238.30 | 210.19 | 28.11 | |
| | 4 | 233.10 | 209.12 | 23.98 | |
| | 5 | 234.45 | 209.31 | 25.14 | |
| | 6 | 239.90 | 210.28 | 29.62 | |

B.3.4 Mass loss results of Na-based geopolymer paste at 800ºC temperature.

| Series | Specimen No. | Wt. before exposure, gm | Wt. after exposure, gm | Mass loss, gm | Average mass loss, gm |
|---|---|---|---|---|---|
| Na-2 | 1 | 235.53 | 209.13 | 26.40 | 26.26 |
| | 2 | 242.48 | 215.28 | 27.20 | |
| | 3 | 235.79 | 204.83 | 25.96 | |
| | 4 | 236.04 | 209.63 | 26.41 | |
| | 5 | 236.24 | 210.60 | 25.64 | |
| | 6 | 240.04 | 214.41 | 25.63 | |

B.3.5 Mass loss results of Na-based geopolymer paste at 200ºC temperature.

| Series | Specimen No. | Wt. before exposure, gm | Wt. after exposure, gm | Mass loss, gm | Average mass loss, gm |
|---|---|---|---|---|---|
| Na-2.5 | 1 | 240.03 | 222.34 | 17.69 | 16.89 |
| | 2 | 242.73 | 226.65 | 16.08 | |
| | 3 | 241.12 | 224.81 | 16.31 | |
| | 4 | 242.72 | 224.59 | 18.13 | |
| | 5 | 239.14 | 221.80 | 17.30 | |
| | 6 | 244.49 | 228.49 | 16.00 | |

B.3.6 Mass loss results of Na-based geopolymer paste at 400ºC temperature.

| Series | Specimen No. | Wt. before exposure, gm | Wt. after exposure, gm | Mass loss, gm | Average mass loss, gm |
|---|---|---|---|---|---|
| Na-2.5 | 1 | 245.37 | 219.21 | 26.16 | 25.71 |
| | 2 | 237.39 | 212.71 | 24.68 | |
| | 3 | 242.57 | 215.62 | 26.95 | |
| | 4 | 242.52 | 217.17 | 25.35 | |
| | 5 | 236.16 | 210.24 | 25.92 | |
| | 6 | 240.97 | 215.74 | 28.23 | |

B.3.7 Mass loss results of Na-based geopolymer paste at 600ºC temperature.

| Series | Specimen No. | Wt. before exposure, gm | Wt. after exposure, gm | Mass loss, gm | Average mass loss, gm |
|---|---|---|---|---|---|
| Na-2.5 | 1 | 237.90 | 210.75 | 27.15 | 26.36 |
| | 2 | 238.96 | 217.38 | 26.58 | |
| | 3 | 241.66 | 215.46 | 26.20 | |
| | 4 | 240.79 | 213.71 | 27.08 | |
| | 5 | 237.11 | 211.08 | 26.03 | |
| | 6 | 233.84 | 208.70 | 25.14 | |

B.3.8 Mass loss results of Na-based geopolymer paste at 800ºC temperature.

| Series | Specimen No. | Wt. before exposure, gm | Wt. after exposure, gm | Mass loss, gm | Average mass loss, gm |
|---|---|---|---|---|---|
| Na-2.5 | 1 | 235.29 | 208.71 | 26.58 | 27.86 |
| | 2 | 240.08 | 212.45 | 27.63 | |
| | 3 | 238.80 | 211.11 | 27.69 | |
| | 4 | 242.38 | 213.38 | 29.00 | |
| | 5 | 237.69 | 209.49 | 28.20 | |
| | 6 | 235.05 | 207.00 | 28.05 | |

B.3.9 Mass loss results of Na-based geopolymer paste at 200ºC temperature.

| Series | Specimen No. | Wt. before exposure, gm | Wt. after exposure, gm | Mass loss, gm | Average mass loss, gm |
|---|---|---|---|---|---|
| Na-3 | 1 | 238.15 | 220.13 | 18.02 | 16.83 |
| | 2 | 238.02 | 221.47 | 16.55 | |
| | 3 | 236.47 | 220.10 | 16.37 | |
| | 4 | 234.60 | 217.45 | 17.15 | |
| | 5 | 244.43 | 227.64 | 16.79 | |
| | 6 | 236.12 | 220.00 | 16.12 | |

B.3.10 Mass loss results of Na-based geopolymer paste at 400ºC temperature.

| Series | Specimen No. | Wt. before exposure, gm | Wt. after exposure, gm | Mass loss, gm | Average mass loss, gm |
|---|---|---|---|---|---|
| Na-3 | 1 | 238.06 | 213.56 | 24.50 | 24.77 |
| | 2 | 239.74 | 214.33 | 25.44 | |
| | 3 | 241.88 | 216.94 | 24.94 | |
| | 4 | 239.64 | 213.41 | 26.23 | |
| | 5 | 234.70 | 211.21 | 23.49 | |
| | 6 | 238.96 | 214.94 | 24.02 | |

A.3.11 Mass loss results of Na-based geopolymer paste at 600ºC temperature.

| Series | Specimen No. | Wt. before exposure, gm | Wt. after exposure, gm | Mass loss, gm | Average mass loss, gm |
|---|---|---|---|---|---|
| Na-3 | 1 | 242.72 | 216.02 | 26.70 | 26.55 |
| | 2 | 231.85 | 206.50 | 25.35 | |
| | 3 | 241.27 | 213.41 | 27.86 | |
| | 4 | 241.50 | 214.86 | 26.64 | |
| | 5 | 236.35 | 210.32 | 26.03 | |
| | 6 | 237.07 | 210.36 | 26.71 | |

B.3.12 Mass loss results of Na-based geopolymer paste at 800ºC temperature.

| Series | Specimen No. | Wt. before exposure, gm | Wt. after exposure, gm | Mass loss, gm | Average mass loss, gm |
|---|---|---|---|---|---|
| Na-3 | 1 | 240.98 | 214.41 | 26.57 | 27.62 |
| | 2 | 241.27 | 213.54 | 27.73 | |
| | 3 | 244.75 | 215.93 | 28.82 | |
| | 4 | 243.72 | 215.15 | 28.57 | |
| | 5 | 242.61 | 214.16 | 28.45 | |
| | 6 | 234.33 | 208.71 | 25.62 | |

**B.4 Mass loss results of K-based geopolymer paste after exposure to elevated temperatures.**

B.4.1 Mass loss results of K-based geopolymer paste at 200ºC temperature.

| Series | Specimen No. | Wt. before exposure, gm | Wt. after exposure, gm | Mass loss, gm | Average mass loss, gm |
|---|---|---|---|---|---|
| K-2 | 1 | 230.64 | 214.08 | 16.53 | 13.5 |
| | 2 | 227.27 | 216.13 | 11.14 | |
| | 3 | 231.21 | 219.28 | 11.93 | |
| | 4 | 231.26 | 215.55 | 15.71 | |
| | 5 | 227.24 | 216.53 | 10.81 | |
| | 6 | 230.38 | 215.54 | 14.84 | |

B.4.2 Mass loss results of K-based geopolymer paste at 400ºC temperature.

| Series | Specimen No. | Wt. before exposure, gm | Wt. after exposure, gm | Mass loss, gm | Average mass loss, gm |
|---|---|---|---|---|---|
| K-2 | 1 | 231.26 | 211.05 | 20.21 | 20.37 |
| | 2 | 227.27 | 207.41 | 19.86 | |
| | 3 | 231.21 | 210.78 | 20.43 | |
| | 4 | 227.24 | 208.21 | 19.03 | |
| | 5 | 230.61 | 207.94 | 22.67 | |
| | 6 | 230.38 | 210.35 | 20.03 | |

B.4.3 Mass loss results of K-based geopolymer paste at 600ºC temperature.

| Series | Specimen No. | Wt. before exposure, gm | Wt. after exposure, gm | Mass loss, gm | Average mass loss, gm |
|---|---|---|---|---|---|
| K-2 | 1 | 239.75 | 213.79 | 25.96 | 24.00 |
| | 2 | 236.61 | 211.33 | 25.28 | |
| | 3 | 235.60 | 212.55 | 23.05 | |
| | 4 | 231.77 | 208.28 | 23.49 | |
| | 5 | 230.09 | 207.97 | 22.12 | |
| | 6 | 209.59 | 209.59 | 24.08 | |

B.4.4 Mass loss results of K-based geopolymer paste at 800ºC temperature.

| Series | Specimen No. | Wt. before exposure, gm | Wt. after exposure, gm | Mass loss, gm | Average mass loss, gm |
|---|---|---|---|---|---|
| K-2 | 1 | 232.50 | 209.43 | 23.07 | 23.61 |
| | 2 | 231.44 | 207.14 | 24.30 | |
| | 3 | 234.48 | 210.02 | 24.46 | |
| | 4 | 231.38 | 209.71 | 21.67 | |
| | 5 | 239.53 | 214.06 | 25.47 | |
| | 6 | 238.95 | 216.26 | 22.69 | |

B.4.5 Mass loss results of K-based geopolymer paste at 200ºC temperature.

| Series | Specimen No. | Wt. before exposure, gm | Wt. after exposure, gm | Mass loss, gm | Average mass loss, gm |
|---|---|---|---|---|---|
| K-2.5 | 1 | 234.61 | 220.66 | 13.95 | 13.02 |
| | 2 | 231.65 | 218.99 | 12.66 | |
| | 3 | 233.23 | 221.77 | 11.46 | |
| | 4 | 229.46 | 216.99 | 12.47 | |
| | 5 | 231.97 | 217.80 | 14.17 | |
| | 6 | 234.77 | 221.36 | 13.41 | |

B.4.6 Mass loss results of K-based geopolymer paste at 400ºC temperature.

| Series | Specimen No. | Wt. before exposure, gm | Wt. after exposure, gm | Mass loss, gm | Average mass loss, Gm |
|---|---|---|---|---|---|
| K-2.5 | 1 | 228.03 | 208.31 | 19.72 | 17.82 |
| | 2 | 220.75 | 203.41 | 17.34 | |
| | 3 | 224.85 | 209.34 | 15.51 | |
| | 4 | 226.96 | 209.52 | 17.44 | |
| | 5 | 225.27 | 206.96 | 18.31 | |
| | 6 | 227.04 | 208.44 | 18.60 | |

B.4.7 Mass loss results of K-based geopolymer paste at 600ºC temperature.

| Series | Specimen No. | Wt. before exposure, gm | Wt. after exposure, gm | Mass loss, gm | Average mass loss, gm |
|---|---|---|---|---|---|
| K-2.5 | 1 | 232.72 | 215.29 | 17.43 | 20.84 |
| | 2 | 236.46 | 213.54 | 22.90 | |
| | 3 | 234.55 | 210.37 | 24.18 | |
| | 4 | 230.12 | 212.33 | 17.79 | |
| | 5 | 233.55 | 211.21 | 22.34 | |
| | 6 | 232.50 | 212.05 | 20.45 | |

B.4.8 Mass loss results of K-based geopolymer paste at 800ºC temperature.

| Series | Specimen No. | Wt. before exposure, gm | Wt. after exposure, gm | Mass loss, gm | Average mass loss, gm |
|---|---|---|---|---|---|
| K-2.5 | 1 | 231.00 | 208.12 | 22.88 | 21.05 |
| | 2 | 228.81 | 209.00 | 19.81 | |
| | 3 | 226.47 | 211.28 | 15.19 | |
| | 4 | 230.79 | 209.56 | 21.23 | |
| | 5 | 231.14 | 211.72 | 19.42 | |
| | 6 | 233.30 | 211.38 | 21.92 | |

B.4.9 Mass loss results of K-based geopolymer paste at 200ºC temperature.

| Series | Specimen No. | Wt. before exposure, gm | Wt. after exposure, gm | Mass loss, gm | Average mass loss, gm |
|---|---|---|---|---|---|
| K-3 | 1 | 232.97 | 216.75 | 16.22 | 13.90 |
| | 2 | 227.29 | 212.85 | 14.44 | |
| | 3 | 230.43 | 217.63 | 12.80 | |
| | 4 | 225.70 | 211.96 | 13.74 | |
| | 5 | 226.56 | 214.08 | 12.48 | |
| | 6 | 232.97 | 219.27 | 13.70 | |

B.4.10 Mass loss results of K-based geopolymer paste at 400ºC temperature.

| Series | Specimen No. | Wt. before exposure, gm | Wt. after exposure, gm | Mass loss, gm | Average mass loss, gm |
|---|---|---|---|---|---|
| K-3 | 1 | 225.52 | 209.69 | 15.83 | 18.35 |
| | 2 | 223.71 | 206.82 | 17.12 | |
| | 3 | 231.94 | 212.19 | 19.75 | |
| | 4 | 231.45 | 211.53 | 19.92 | |
| | 5 | 231.73 | 212.52 | 19.21 | |
| | 6 | 231.86 | 213.62 | 18.24 | |

B.4.11 Mass loss results of K-based geopolymer paste at 600ºC temperature.

| Series | Specimen No. | Wt. before exposure, gm | Wt. after exposure, gm | Mass loss, gm | Average mass loss, Gm |
|---|---|---|---|---|---|
| K-3 | 1 | 224.39 | 206.34 | 17.65 | 17.43 |
| | 2 | 227.06 | 209.38 | 17.68 | |
| | 3 | 227.51 | 209.75 | 17.76 | |
| | 4 | 227.28 | 209.74 | 17.54 | |
| | 5 | 225.45 | 208.31 | 17.14 | |
| | 6 | 227.85 | 211.02 | 16.83 | |

B.4.12 Mass loss results of K-based geopolymer paste at 800ºC temperature.

| Series | Specimen No. | Wt. before exposure, gm | Wt. after exposure, gm | Mass loss, gm | Average mass loss, gm |
|---|---|---|---|---|---|
| K-3 | 1 | 232.62 | 208.49 | 24.13 | 22.80 |
| | 2 | 237.00 | 211.91 | 25.09 | |
| | 3 | 231.75 | 207.54 | 24.21 | |
| | 4 | 229.33 | 209.03 | 20.30 | |
| | 5 | 235.45 | 210.68 | 24.77 | |
| | 6 | 224.23 | 205.79 | 18.44 | |

**C. 1. Experimental program and mix proportions (mix 1)**

| **Mix 1** | | | |
|---|---|---|---|
| **Sample ID** | **$Na_2SiO_3$/NaOH** | **Activators/fly ash** | **Kiln Temperature** |
| Na-2-28 | 2 | 0.35 | Ambient |
| Na-2-200 | 2 | 0.35 | 200 |
| Na-2-400 | 2 | 0.35 | 400 |
| Na-2-600 | 2 | 0.35 | 600 |
| Na-2-800 | 2 | 0.35 | 800 |
| Na-2.5-28 | 2.5 | 0.35 | Ambient |
| Na-2.5-200 | 2.5 | 0.35 | 200 |
| Na-2.5-400 | 2.5 | 0.35 | 400 |
| Na-2.5-600 | 2.5 | 0.35 | 600 |
| Na-2.5-800 | 2.5 | 0.35 | 800 |
| Na-3-28 | 3 | 0.35 | Ambient |
| Na-3-200 | 3 | 0.35 | 200 |
| Na-3-400 | 3 | 0.35 | 400 |
| Na-3-600 | 3 | 0.35 | 600 |
| Na-3-800 | 3 | 0.35 | 800 |

**C. 2. Experimental program and mix proportions (mix 2)**

| **Mix 2** | | | |
|---|---|---|---|
| **Sample ID** | **$K_2SiO_3$/KOH** | **Activators/fly ash** | **Kiln Temperature** |
| K-2-28 | 2 | 0.35 | Ambient |
| K-2-200 | 2 | 0.35 | 200 |
| K-2-400 | 2 | 0.35 | 400 |
| K-2-600 | 2 | 0.35 | 600 |
| K-2-800 | 2 | 0.35 | 800 |
| K-2.5-28 | 2.5 | 0.35 | Ambient |
| K-2.5-200 | 2.5 | 0.35 | 200 |
| K-2.5-400 | 2.5 | 0.35 | 400 |
| K-2.5-600 | 2.5 | 0.35 | 600 |
| K-2.5-800 | 2.5 | 0.35 | 800 |
| K-3-28 | 3 | 0.35 | Ambient |
| K-3-200 | 3 | 0.35 | 200 |
| K-3-400 | 3 | 0.35 | 400 |
| K-3-600 | 3 | 0.35 | 600 |
| K-3-800 | 3 | 0.35 | 800 |

**D.3. Experimental program and mix proportions (mix 3)**

| **Mix 3** | | | | |
|---|---|---|---|---|
| **Sample ID** | **$K_2SiO_3$/KOH** | **Activators/(FA+NS)** | **Kiln Temperature** | **NS%** |
| KN-1-28 | 3 | 0.4 | Ambient | 1 |
| KN-1-200 | 3 | 0.4 | 200 | 1 |
| KN-1-400 | 3 | 0.4 | 400 | 1 |
| KN-1-600 | 3 | 0.4 | 600 | 1 |
| KN-1-800 | 3 | 0.4 | 800 | 1 |
| KN-2-28 | 3 | 0.4 | Ambient | 2 |
| KN-2-200 | 3 | 0.4 | 200 | 2 |
| KN-2-400 | 3 | 0.4 | 400 | 2 |
| KN-2-600 | 3 | 0.4 | 600 | 2 |
| KN-2-800 | 3 | 0.4 | 800 | 2 |
| KN-4-28 | 3 | 0.4 | Ambient | 4 |
| KN-4-200 | 3 | 0.4 | 200 | 4 |
| KN-4-400 | 3 | 0.4 | 400 | 4 |
| KN-4-600 | 3 | 0.4 | 600 | 4 |
| KN-4-800 | 3 | 0.4 | 800 | 4 |

## C.3. Experimental program and mix proportions (mix 4)

| **Mix 4** | | | | |
|---|---|---|---|---|
| **Sample ID** | **$K_2SiO_3$/KOH** | **Activators/(FA+FS)** | **Kiln Temperature** | **FS%** |
| KFS-3-28 | 3 | 0.4 | Ambient | 5 |
| KFS-3-200 | 3 | 0.4 | 200 | 5 |
| KFS-3-400 | 3 | 0.4 | 400 | 5 |
| KFS-3-600 | 3 | 0.4 | 600 | 5 |
| KFS-3-800 | 3 | 0.4 | 800 | 5 |
| KFS-2.5-28 | 3 | 0.4 | Ambient | 10 |
| KFS-2.5-200 | 3 | 0.4 | 200 | 10 |
| KFS-2.5-400 | 3 | 0.4 | 400 | 10 |
| KFS-2.5-600 | 3 | 0.4 | 600 | 10 |
| KFS-2.5-800 | 3 | 0.4 | 800 | 10 |
| KFS-3-28 | 3 | 0.4 | Ambient | 20 |
| KFS-3-200 | 3 | 0.4 | 200 | 20 |
| KFS-3-400 | 3 | 0.4 | 400 | 20 |
| KFS-3-600 | 3 | 0.4 | 600 | 20 |
| KFS-3-800 | 3 | 0.4 | 800 | 20 |

## C.4. Experimental program and mix proportions (mix 5)

| **Mix 5** | |
|---|---|

| **Sample ID** | **$K_2SiO_3$ /KOH** | **Activators/ (FA+NS)** | **Kiln Temperature** | **NS%** |
|---|---|---|---|---|
| Na-N-1-28 | 3 | 0.4 | Ambient | 1 |
| Na-N-1-200 | 3 | 0.4 | 200 | 1 |
| Na-1-400 | 3 | 0.4 | 400 | 1 |
| Na-N-1-600 | 3 | 0.4 | 600 | 1 |
| Na-N-1-800 | 3 | 0.4 | 800 | 1 |
| Na-N-2-28 | 3 | 0.4 | Ambient | 2 |
| Na-N-2-200 | 3 | 0.4 | 200 | 2 |
| Na-N-2-400 | 3 | 0.4 | 400 | 2 |
| Na-N-2-600 | 3 | 0.4 | 600 | 2 |
| Na-N-2-800 | 3 | 0.4 | 800 | 2 |
| Na-N-4-28 | 3 | 0.4 | Ambient | 4 |
| Na-N-4-200 | 3 | 0.4 | 200 | 4 |
| Na-N-4-400 | 3 | 0.4 | 400 | 4 |
| Na-N-4-600 | 3 | 0.4 | 600 | 4 |
| Na-N-4-800 | 3 | 0.4 | 800 | 4 |

### C.5. Experimental program and mix proportions (mix 6)

| **Mix 6** | | | | |
|---|---|---|---|---|
| Sample ID | $K_2SiO_3$/ KOH | Activators/( FA+FS) | Kiln Temperature | FS% |
| Na-FS-3-28 | 3 | 0.4 | Ambient | 5 |
| Na-FS-3-200 | 3 | 0.4 | 200 | 5 |
| Na-FS-3-400 | 3 | 0.4 | 400 | 5 |
| Na-FS-3-600 | 3 | 0.4 | 600 | 5 |
| Na-FS-3-800 | 3 | 0.4 | 800 | 5 |
| Na-FS-2.5-28 | 3 | 0.4 | Ambient | 10 |
| Na-FS-2.5-200 | 3 | 0.4 | 200 | 10 |
| Na-FS-2.5-400 | 3 | 0.4 | 400 | 10 |
| Na-FS-2.5-600 | 3 | 0.4 | 600 | 10 |
| Na-FS-2.5-800 | 3 | 0.4 | 800 | 10 |
| Na-FS-3-28 | 3 | 0.4 | Ambient | 20 |
| Na-FS-3-200 | 3 | 0.4 | 200 | 20 |
| Na-FS-3-400 | 3 | 0.4 | 400 | 20 |
| Na-FS-3-600 | 3 | 0.4 | 600 | 20 |
| Na-FS-3-800 | 3 | 0.4 | 800 | 20 |

### C.6. Experimental program and mix proportions (mix 7)

| **Mix 7** | | | | |
|---|---|---|---|---|
| Sample ID | $K_2SiO_3$/ KOH | Activators/ (FA+NS) | Kiln Temp. | Basalt fiber% |

| | | | | |
|---|---|---|---|---|
| KB-1-28 | 3 | 0.35 | Ambient | 1 |
| KB-1-200 | 3 | 0.35 | 200 | 1 |
| KB-1-400 | 3 | 0.35 | 400 | 1 |
| KB-1-600 | 3 | 0.35 | 600 | 1 |
| KB-1-800 | 3 | 0.35 | 800 | 1 |
| KB-2-28 | 3 | 0.35 | Ambient | 2 |
| KB-2-200 | 3 | 0.35 | 200 | 2 |
| KB-2-400 | 3 | 0.35 | 400 | 2 |
| KB-2-600 | 3 | 0.35 | 600 | 2 |
| KB-2-800 | 3 | 0.35 | 800 | 2 |
| KB-4-28 | 3 | 0.35 | Ambient | 4 |
| KB-4-200 | 3 | 0.35 | 200 | 4 |
| KB-4-400 | 3 | 0.35 | 400 | 4 |
| KB-4-600 | 3 | 0.35 | 600 | 4 |
| KB-4-800 | 3 | 0.35 | 800 | 4 |

## C.7. Experimental program and mix proportions (mix 8)

| Mix 8 | | | | |
|---|---|---|---|---|
| Sample ID | $K_2SiO_3$/KOH | Activators/ (FA+FS) | Kiln Temp. | Carbon fiber% |
| KC-3-28 | 3 | 0.35 | Ambient | 5 |
| KC-3-200 | 3 | 0.35 | 200 | 5 |
| KC-3-400 | 3 | 0.35 | 400 | 5 |
| KC-3-600 | 3 | 0.35 | 600 | 5 |
| KC-3-800 | 3 | 0.35 | 800 | 5 |
| KC-2.5-28 | 3 | 0.35 | Ambient | 10 |
| KC-2.5-200 | 3 | 0.35 | 200 | 10 |
| KC-2.5-400 | 3 | 0.35 | 400 | 10 |
| KC-2.5-600 | 3 | 0.35 | 600 | 10 |
| KC-2.5-800 | 3 | 0.35 | 800 | 10 |
| KC-3-28 | 3 | 0.35 | Ambient | 20 |
| KC-3-200 | 3 | 0.35 | 200 | 20 |
| KC-3-400 | 3 | 0.35 | 400 | 20 |
| KC-3-600 | 3 | 0.35 | 600 | 20 |
| KC-3-800 | 3 | 0.35 | 800 | 20 |

## C.8. Experimental program and mix proportions (mix 9)

| Mix 9 | | | |
|---|---|---|---|
| Sample ID | $Na_2SiO_3$/NaOH | Activators/fly ash | Kiln Temperature |
| Na-3-28 | 3 | 0.40 | Ambient |
| Na-3-200 | 3 | 0.40 | 200 |
| Na-3-400 | 3 | 0.40 | 400 |
| Na-3-600 | 3 | 0.40 | 600 |

| | | | |
|---|---|---|---|
| Na-3-800 | 3 | 0.40 | 800 |
| K-3-28 | 3 | 0.40 | Ambient |
| K-3-200 | 3 | 0.40 | 200 |
| K-3-400 | 3 | 0.40 | 400 |
| K-3-600 | 3 | 0.40 | 600 |
| K-3-800 | 3 | 0.40 | 800 |

**D-1. Research Flowchart**